The Influence of Oceanic Transform Boundaries on the Generation and Evolution of Oceanic Lithosphere

A thesis presented to the Faculty
of the State University of New York
at Albany
in partial fulfillment of the requirements
for the degree of
Master of Science

College of Science and Mathematics
Department of Geological Sciences

David G. Gallo
1984

The Influence of Oceanic Transform Boundaries on the Generation and Evolution of Oceanic Lithosphere

Abstract of

a thesis presented to the Faculty

of the State University of New York

at Albany

in partial fulfillment of the requirements

for the degree of

Master of Science

College of Science and Mathematics

Department of Geological Sciences

David G. Gallo

1984

ABSTRACT

The first-order geologic and morphologic relationships at, along and proximal to ridge-transform-ridge plate boundaries are used to construct an empirical and speculative tectonic model. The geometry of a ridge-transform intersection necessitates the juxtaposition of relatively cold, thick lithosphere against the truncated end of an accreting plate boundary. The cold face of lithosphere cools the adjacent wedge of asthenosphere rising beneath the axis of accretion and restricts the amount of partial melting thus attenuating the amount of basaltic melt segregated from the asthenosphere per unit time. The manifestation of this cold edge effect is a thinner oceanic crust. At depth, upper-mantle material is welded against the cold edge and creates a shear-couple that results in the progressive reorientation of tensile stresses as the ridge-transform intersection is approached. The model predicts that the geologic expressions of this cold edge effect will become more dramatic with increasing thickness of the truncating edge. Field data supporting this model were collected from the intersection of the East Pacific Rise with the Tamayo Transform Fault. The field program involved both a surface ship (R/V GILLISS) and a manned submersible (DSRV ALVIN).

Acknowledgments

The several years I spent as a student at SUNYA allowed me to be in the company of faculty, graduate students, and staff to whom I owe endless thanks. I thank Drs. Peter Benedict, John Dewey, Kevin Burke, Win Means, Steve Delong, Akhio Miyashiro, George Putman, and Dan Fornari for introducing me to the geology of the planet on which I live. Thanks go to Jeff Fox who is now and has always been my academic mentor and good friend. Special thanks go to Dr. William Kidd for tolerating me in the lecture hall, in thick Taconic woods and on the decks of rolling ships in tropical waters and in the cod-infested waters of Newfoundland. Much deserved thanks go to Diana Paton for saving me from administrative death on many occasions. Of my fellow graduates, Dave Rowley, Dick Moody, Rick Livaccari, and Bruce Idleman were truly my partners in crime. There is no way that I can begin to thank my close friend and colleague, Celal Sengor for all that he has done for me.

Finally, I thank my parents, Mr. and Mrs. Albert G. Gallo. They are solely responsible for convincing me to return to school and have lended endless support to my ventures. If not for my parents I would still be selling shoes.

Preface

The material presented in this thesis is divided into two chapters, each representing manuscripts that have been submitted and accepted for publication in scientific journals. In as much as both chapters represent research completed through my collaboration with various colleagues, I here state my role in these efforts and give credit to my coauthors.

The first chapter, Tectonics at the Intersection of the East Pacific Rise with the Tamayo Transform Boundary(in press, Marine Geophysical Research), presents the results of a manned submersible study(DSRV Alvin) carried out at the mouth of the Gulf of California during the Fall of 1979. I was a participating scientist and diver during the field portion of this program and was responsible for the compilation, synthesis, and presentation of the collected data set. In that regard, I acknowledge the special efforts of Drs. W.S.F. Kidd, J.A. Karson, and P.J. Fox. The remaining participating scientists and coauthors include Drs. K.C. Macdonald, K. Crane, P. Choukroune, M. Seguret, K. Kastens, and Mr. R.H. Moody.

The second chapter, A Tectonic Model for Ridge-Transform-Ridge Plate Boundaries: Implications for the Structure of Oceanic Lithosphere(in press, Tectonophysics), presents an empirical model based on field, experimental and theoretical considerations. This model has grown through years of testing and modification, and has reached the present stage only through close collaboration with my coauthor, Dr. P.J. Fox.

Table of Contents

Table of Contents (continued)

List of Figures

Chapter I

Chapter II

CHAPTER I

Tectonics at the Intersection of the East Pacific Rise with the Tamayo Transform Fault

1. Introduction

Investigations of the morphotectonic fabric developed proximal to ridge-transform intersections (Crane, 1976; Lonsdale, 1978; Searle, 1979; Macdonald et al., 1979; OTTER, 1983; Karson and Dick, 1983) indicate that the topographic trends in these regions are oblique to both the ridge axis and the transform fault. Two different mechanisms have been suggested to account for the presence of this obliquity. In one scheme, oblique topographic elements evolve as the product of a system of strike-slip or oblique-slip faults referred to as Riedels and anti-Riedels (Tchalenko, 1970; Riedel, 1929), or secondary shear structures (McKinstry, 1953; Chinnery, 1976) that are known to form within and along zones of shear. If these structures are responsible for the development of the oblique trending fabric found at ridge-transform intersections, then evidence for strike-slip displacement in those areas should be apparent. An alternative explanation suggests that the oblique topographic elements reflect faults with dominant dip-slip displacements, that form near the ridge-transform boundary where the shear couple produced by the transform distorts the regional stress field associated with the ridge-axis (Courtillot et al., 1974; Crane, 1976; Lonsdale, 1978; Gallo et al., 1980; Searle, 1979).

The resolution of conventional underway or deep-towed geophysical tools is not adequate to determine the sense of displacement across faults that characterize ridge-transform intersections and the focus of our ALVIN investigation was to use the high-resolution capabilities of a submersible to establish the tectonic character of a ridge-transform intersection and to

Scanner slave and pdf file editor's note:

The pages in the library shelf copy of the MS thesis text of Chapters I and II, including especially the figures, were made from photocopies of carbon copies, or multiple generation photocopies and, as can be seen from the samples of the first and last pages of those two chapters included in this file, are consequently quite difficult to read in most parts. The details of the figures and photos, in particular, are degraded; compare for example the diagram for Figure 10b of Chapter I (page 48 from the thesis) reproduced on the page following this note, and the identical, but much more readable figure (page 36 of this pdf file) in the following material derived from the published paper, of which the thesis Chapter I text was the submitted manuscript. The same explanation applies to the presentation of Chapter II in this pdf file version of the MS thesis. The text pagination table of contents given in the introductory matter applies to the original and has not been modified to fit, and therefore does not match, this pdf file version.

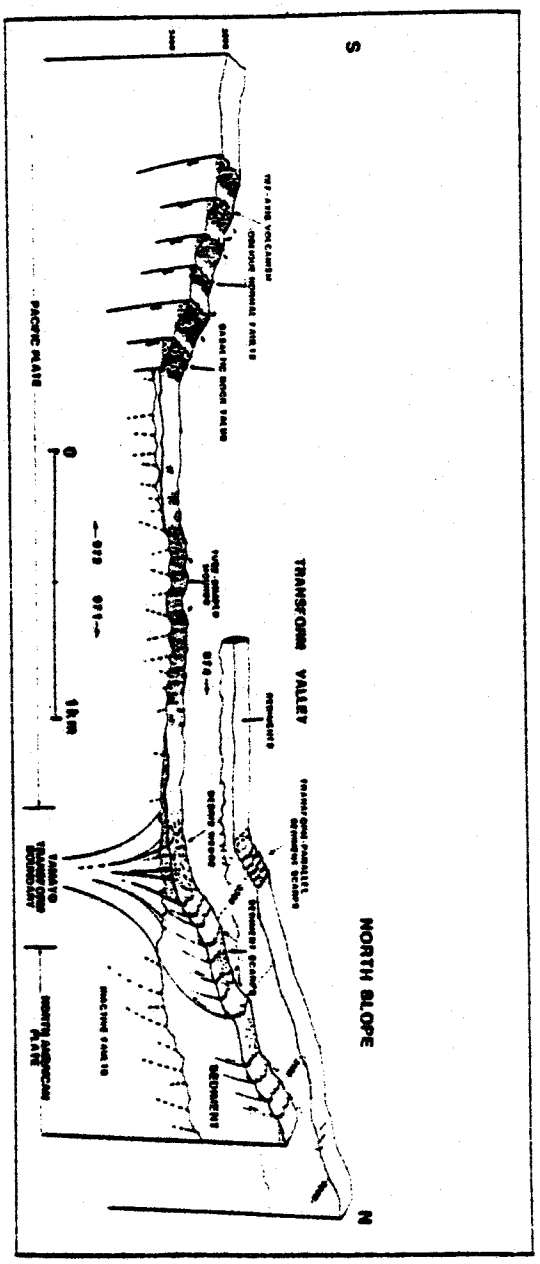

Figure 10b

TECTONICS AT THE INTERSECTION OF THE EAST PACIFIC RISE WITH TAMAYO TRANSFORM FAULT

1. Introduction

Investigations of the morphotectonic fabric developed proximal to ridge-transform intersections (Crane, 1976; Lonsdale, 1978; Searle, 1979; Macdonald *et al.*, 1979; OTTER, 1984; Karson and Dick, 1983) indicate that the topographic trends in these regions are oblique to both the ridge axis and the transform fault. Two different mechanisms have been suggested to account for the presence of this obliquity. In one scheme, oblique topographic elements evolve as the product of a system of strike-slip or oblique-slip faults referred to as Riedels and anti-Riedels (Tchalenko, 1970; Riedel, 1929), or secondary shear structures (McKinstry, 1953;

Chinnery, 1976) that are known to form within and along zones of shear. If these structures are responsible for the development of the oblique trending fabric found at ridge-transform intersections, then evidence for strike-slip displacement in those areas should be apparent. An alternative explanation suggests that the oblique topographic elements reflect faults with dominant dip-slip displacements, that form near the ridge-transform boundary where the shear couple produced by the transform distorts the regional stress field associated with the ridge-axis (Courtillot *et al.*,1974; Crane, 1976; Lonsdale, 1978; Gallo *et al.*, 1980; Searle, 1979; Macdonald *et al.*, 1979).

The resolution of conventional underway or deep-towed geophysical tools is not adequate to determine the sense of displacement across faults that characterize ridge-transform intersections and the focus of our ALVIN investigation was to use the high-resolution capabilities of a submersible to establish the tectonic character of a ridge-transform intersection and to document the effects of the Tamayo Transform boundary upon the structural and geochemical processes responsible for the generation of the oceanic lithosphere along the East Pacific Rise (EPR; Tamayo Scientific Team, 1980a, b, c). A complementary surface ship program using R/V GILLISS mapped (by using a conventional 12 kHz echo sounder) and systematically sampled (conventional dredging) the EPR axial volcanic terrain from the EPR/Tamayo intersection to a distance 40 km south of the Tamayo transform boundary. The surface ship program was designed to provide a geochemical test for the deep-seated thermal effects of the Tamayo Transform boundary upon the generation of oceanic lithosphere along this segment of the EPR. The results of the dredging program are mentioned briefly in this paper and are presented in detail in a separate publication (Bender *et al.*, 1984).

2. Regional Setting of the Tamayo Transform and General Tectonic Framework

The Tamayo Transform represents the southernmost strike-slip plate boundary segment withing the gulf of California (Larson *et al.*, 1968, 1972; Figure 1). It links the Gulf Rise with the East Pacific Rise (EPR), and roughly parallels the theoretical slip-line between the Pacific and North American plates. The Tamayo transform domain is 80 km long and 35 km wide, strikes WNW – ESE (120°), and is characterized by right-lateral relative motion of approximately 6.0 cm $yr.^{-1}$ A bathymetric map compiled by Kastens *et al.* (1979) indicates that the transform domain is comprised of 3 first-order morphotectonic elements: a northern trough, a southern trough and an intervening median ridge (Figure 2A). The southern trough is about 10 km wide, and 60 km long. The floor of the trough is flat and its margins are outlined by approximately the 2800 m isobath. A 100 to 400 m high elongate ridge defines a central lineament along the transform valley axis and runs the length of the transform. At its western end this median ridge is broad (8 km), and high, standing 400 m above the flanking troughs but towards the east it loses

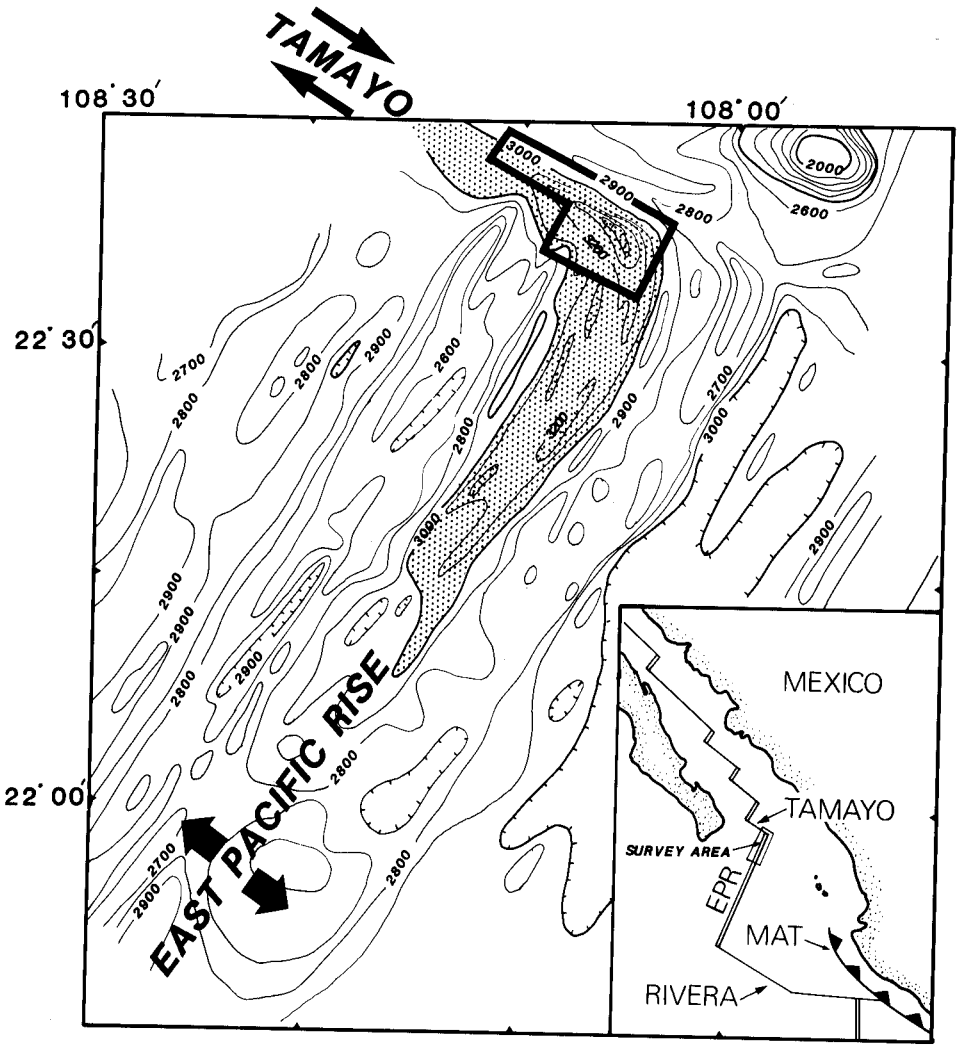

Fig. 1. Bathymetry of the East Pacific Rise (EPR) and the Tamayo Transform; regional location given in insert (MAT – Middle America Trench). Within about 30 km of the Tamayo Transform, the EPR axis gradually develops a well-defined rift valley (inner-valley floor shaded). Location of ALVIN dives at the EPR-Tamayo intersection shown by boxed area. Bathymetry compiled from data collected by R/V GILLISS, and this cruise (uncorrected meters).

definition and relief. The north trough is clearly defined by the 2900 m isobath, and is approximately 15 km wide. Seismic reflection data reveal that flat lying, undisturbed and acoustically reverberant sediments partially fill the north and south troughs with thicknesses ranging from 100 to 300 m (Kastens *et al.*, 1979). These data also show that diapir-like structures protrude into the sediment of both the northern and southern troughs. Several of the diapiric bodies deform reflectors

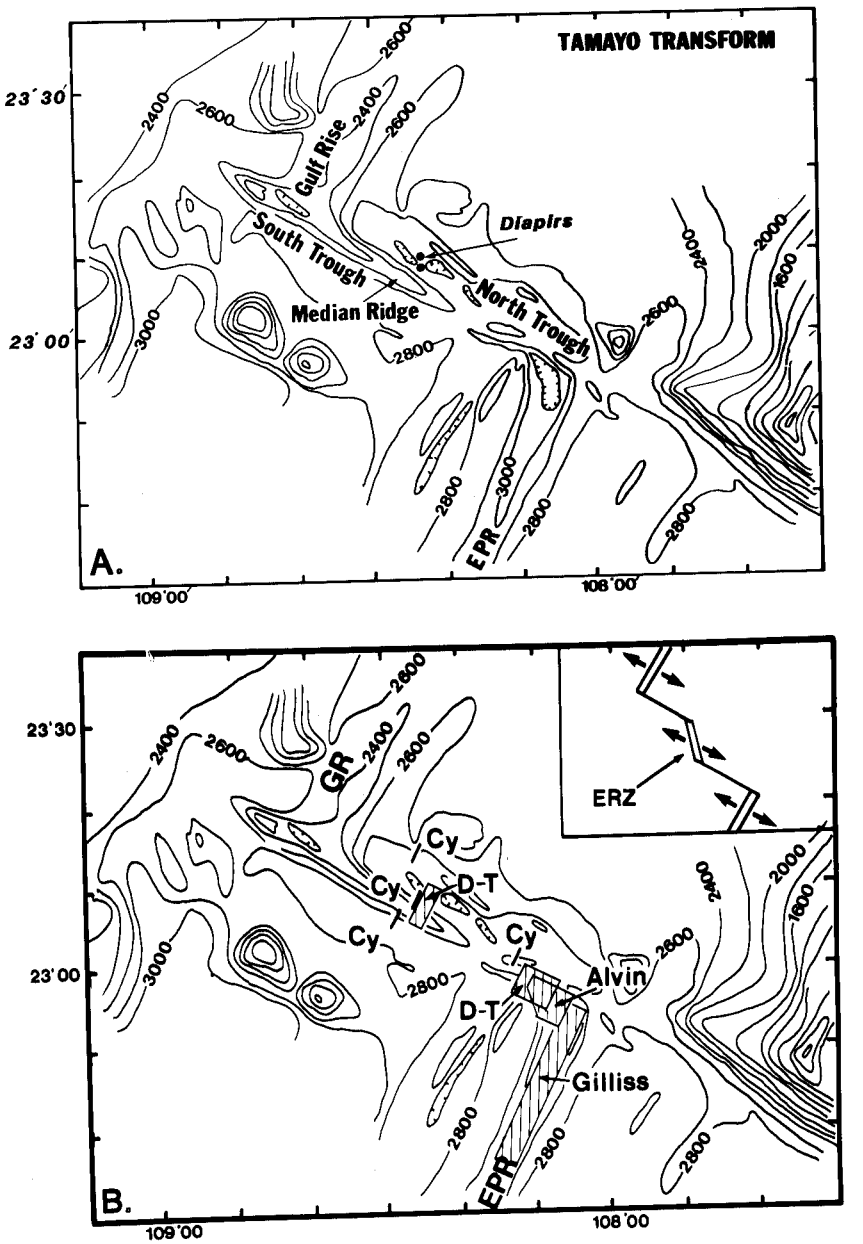

Fig. 2A. Morphotectonic province of the Tamayo Transform (after Kastens *et al.*, 1979). The Tamayo Transform is characterized by right- lateral strike-slip displacement of about 6cm/yr. Total transform offset is approximately 80 km. (B) Location of previous detailed geologic investigations of the Tamayo Transform boundary. GR – Gulf Rise; EPR – East Pacific Rise; CY – CYANA dives (CYAMEX and Pastouret, 1981); D–T – Deep Tow Study Areas (Macdonald *et al.*, 1979); ALVIN – ALVIN dive areas (this paper); and GILLISS – Dredging program (this paper, and Bender *et al.*, 1983). Also shown in insert is the kinematic interpretation of the Tamayo Transform showing two strike-slip segments linked by an extensional relay zone (ERZ; Macdonald *et al.*, 1979; CYAMEX and Pastouret, 1981).

at shallow sub-bottom depths by punching up through or bowing up the horizontal strata.

Surface ship bathymetric surveys (Lewis *et al.*, 1983; Lewis, 1979) and a deep-towed geophysical-package profile (Macdonald *et al.*, 1979) show that the morphotectonic character of the EPR axis changes gradually, over a distance of 50 km towards the transform, from a broad and subtly rifted topographic swell into a well-defined valley exhibiting classic Atlantic-type rift valley morphology (Figure 1). Seismic refraction studies by McClain and Lewis (1980) suggest that the thickness of the oceanic crust created along the EPR thins by 2 to 3 km as the Tamayo Transform is approached. Both of these observations are interpreted to reflect the thermal influence of the Tamayo Transform boundary upon the deep-seated processes responsible for the generation of oceanic lithosphere (Fox and Gallo, 1984).

Two areas of the Tamayo Transform have been studied in detail using a deep-towed geophysical package (Macdonald *et al.*, 1979; Figure 2B). The first survey area lies along a N–S line at the center of the transform. Along the transect, which crossed parts of both troughs and the median ridge, shallow reflectors are undisturbed and conformable to the sea floor except in the center of the northern trough where a diapir-like body punches through the sediment overburden uplifting a cap of acoustically reverberant sediments.

The second region investigated by Macdonald and others (1979) lies a few kilometers to the west of the Tamayo-EPR intersection (Figure 2B). The survey shows that the ridge-transform intersection is characterized by an elongate depression that extends westwards along a strike of WNW–ESE (115°). The floor of the depression is comprised of sparsely sedimented volcanic terrain proximal to the EPR but is covered by a sedimentary blanket farther to the west. The north side of the depression is bounded by a 300 to 400 m high, south facing slope which dips 10° to 20° towards the axis of the depression. The smooth regional gradient of the slope is disrupted by steep scarps with individual relief of a few tens of meters and with continuity along a strike of several hundreds of meters to a few kilometers. The southern flank of the depression is a 500 m high north facing ediface consisting of a series of steeply dipping scarps exhibiting trends both oblique (345°) and parallel to the strike of the East Pacific Rise axis (030°). Macdonald and others (1979) interpret the scarps that disrupt the northern slope of the depression to represent a narrow (< 1 km) principal transform displacement zone (PTDZ). The ridge-axis parallel and oblique structures that bound the depression to the south can be traced to within a few hundred meters of the PTDZ suggesting to Macdonald *et al.*, (1979) that the zone of decoupling between the extensional regime of the rise axis and the strike-slip environment of the transform is very narrow. The oblique trends were interpreted to be the product of a shear couple that forms at the EPR-Tamayo intersection.

Four dives by the French submersible CYANA were located within the Tamayo Transform (Figure 2B): one dive, positioned along the north side of the northern

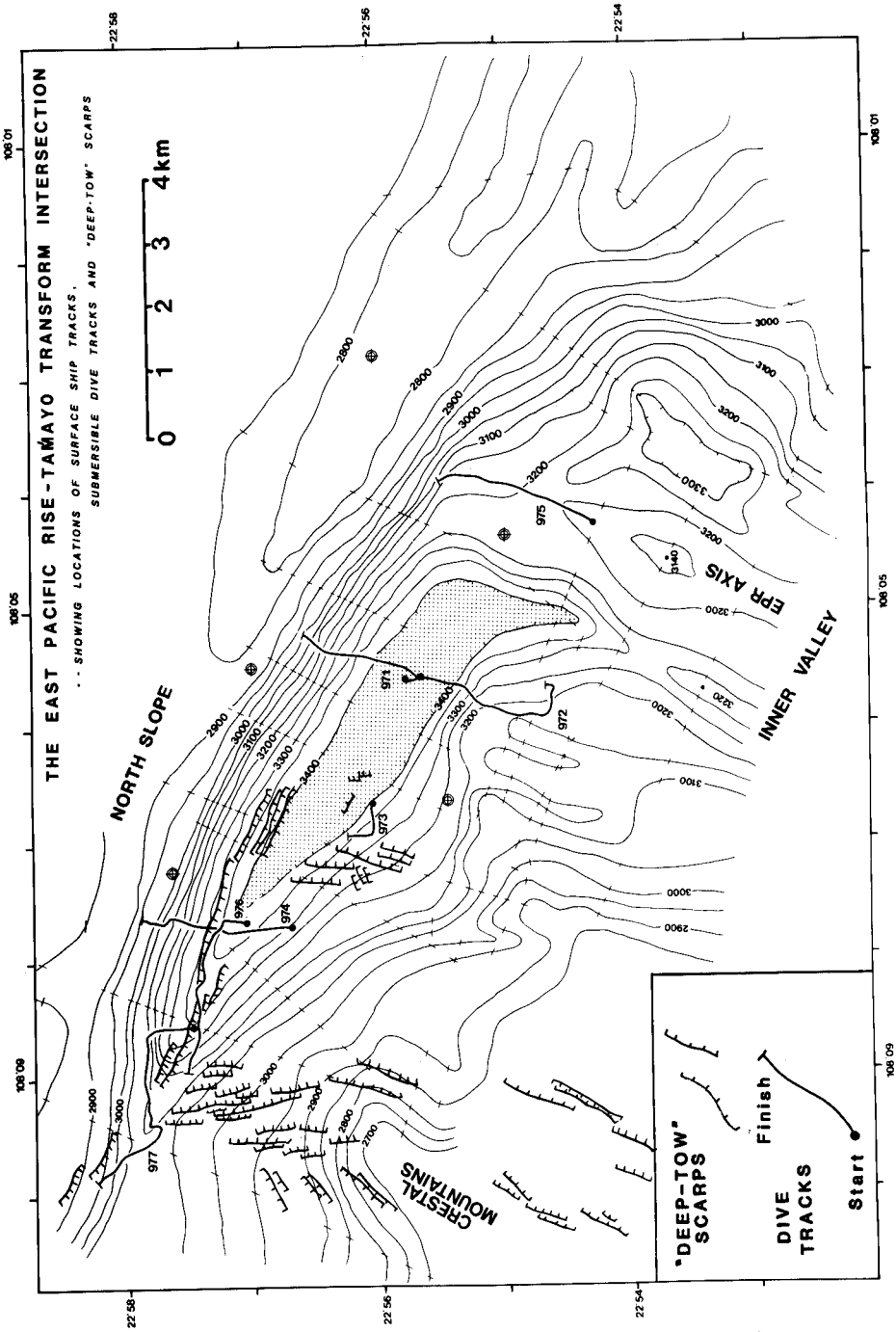

Fig. 3. Bathymetry of the EPR-Tamayo Intersection (location given by Figures 1, 2B) and position of ALVIN dive tracks (971–977). Deep-tow lineaments, interpreted to be fault scarps, are shown as lines with hachures in the downslope direction. Bathymetry by 12 kHz echo sounding from R/V LULU, this cruise. Note that only part of this area has deep-tow side-scan sonar coverage (see Macdonald *et al.*, 1979).

trough west of the diapir field surveyed by Macdonald *et al.*, (1979), crossed a narrow (< 500 m) zone of recently deformed sediment with structures striking 115°; two dives which traversed the median ridge documented that there is no evidence for recent tectonism in this region; one dive, located towards the eastern end of the median ridge, found a 500 m wide zone of recent tectonism defined by structural lineaments striking 120° (CYAMEX and Pastouret, 1981).

The combined results from surface-ship surveys, deep-towed geophysical investigations and submersible observations suggest that the PTDZ at various locations along the transform is relatively narrow (< 1 km) and that the zone of strike-slip motion is not continuous along strike down the length of the Tamayo transform but rather appears to be offset by an extensional relay zone characterized by presumed serpentinite diapirs (Macdonald *et al.*, 1979; CYAMEX and Pastouret, 1981; Figure 2B, Insert).

3. The Geology of the EPR-Tamayo Intersection: Sea Floor Observations

Seven dives with the DSRV ALVIN were completed at the eastern end of the Tamayo Transform boundary, proximal to its intersection with the axis of the EPR (Figures 2B, 3). Four dives (971, 972, 973, 975) were located in the immediate vicinity of the EPR/Tamayo intersection (Figures 3, 4, 5) and three dives (974, 976, 977) were positioned 6 to 10 km to the west along the intersection depression (Figures 3, 6, 7). These dives, in whole or in part, traversed the morphotectonic zones described for the intersection area by Macdonald *et al.*, (1979). These zones include the EPR rift valley floor (Dive 975), the EPR/Tamayo intersection deep (Dives 971, 972, 973), the western rift valley wall of the EPR (Dive 972), and the northern wall of the intersection depression (Dives 971, 974, 976, 977; Figure 3).

3.1. The rift valley floor

Visual observations from submersible ALVIN confirm that the rift valley floor, in the vicinity of the Tamayo Transform fault, is comprised of glass encrusted, lightly sediment-dusted volcanic terrain that has been only slightly disrupted by tectonic activity (fissuring and faulting; Figures 8A, B). The bathymetric map of this area (Figure 3; see also Figure 5 of Macdonald *et al.*, 1979) show that the axis of the EPR, just south of the Tamayo Transform boundary, is dominated by a 1–2 km wide topographic high, whose crest stands nearly 100 m above the surrounding rift valley floor. As this axial-high is traced northward, towards the Tamayo Transform boundary, it appears to taper gradually both in width and height. Visual observations of the northern end of this feature (Dive 975; Figures 3, 4, 5D) show that it is composed of numerous constructional volcanic mounds, haystacks, and steep (>60°) lava tube-covered edifices. The maximum relief of these features (mounds, ridges, etc.) is typically less than a few tens of meters and the mounds themselves are characterized by a predominance of fresh, completely

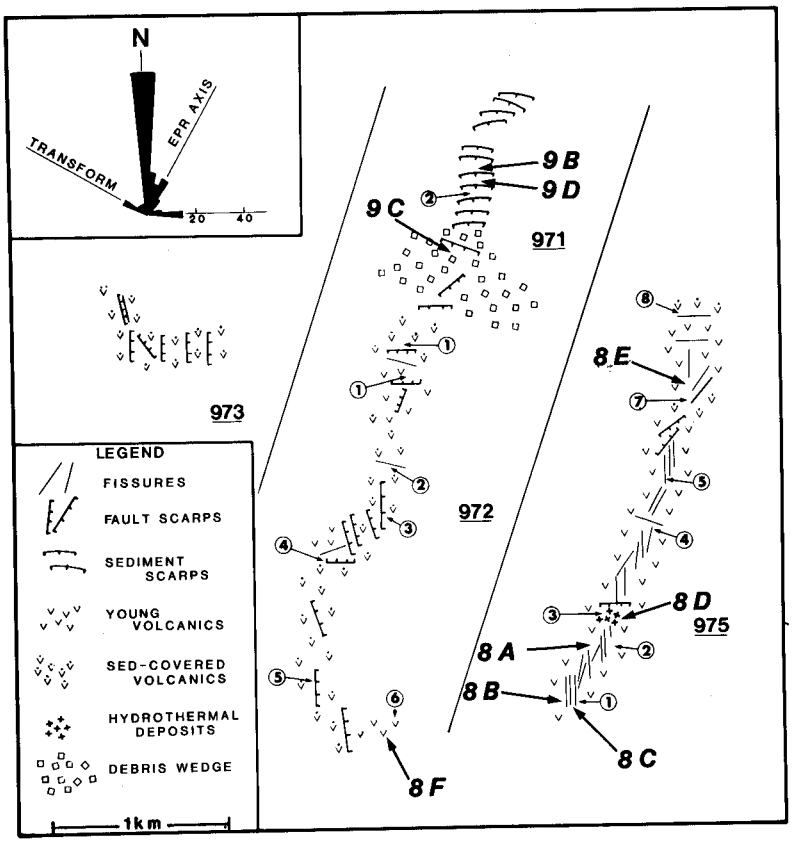

Fig. 4. Structural lineaments and geology of the EPR-Tamayo intersection (Dives 971, 972, 973, 975), locations given by Figure 3. Note that the dominant trend of brittle structures (faults, fissures) within the EPR volcanic basement is N–S (000°, see rose diagram insert) oblique by 30° to the regional EPR trend but scarps in sediment, not included in rose diagram (Dive 971–northern end) trend subparallel to the trend of the Tamayo Transform valley (120°). Circled numbers indicate sampling locations. Bold numbers indicate locations of photos given in Figures 8 and 9. See text for further discussion.

glassy pillow and tubular lavas. Extensive sheet or pounded flows were not observed on this dive but localized occurences are suggested by a broad, thin (2–3 cm) veneer of basalt that partially buries pillow forms (Figure 8C). The youthfulness of this volcanic terrain is shown not only by a paucity of pelagic sediment cover (> 2 cm) in this area of relatively high sedimentation rate, but also by the presence of delicate ornaments (e.g. glass buds) on pillows and thick, unpalagonitized glass rinds on pillow surfaces. Furthermore, at one location next to a fissure, a fluffy yellow-white amorphous chemical precipitate (iron-rich montmorillonite to nontronite, M. Mottl, personal communication) was observed partially blanketing very heavily manganese-coated pillows and is interpreted to be of low-temperature hydrothermal origin (Figure 8D). It is important to note that the number of fissures observed in this area (61) is much greater than the number of faults (5) indicating that horizontal extension, without vertical displacment

along fault scarps, is the primary deformational process acting here. Fissures range up to 4 m wide but most are about 1–2 m wide. Many of them expose sections through pillows with a chalky film of vein material on the broken surfaces. The dominant trend of the fissures and faults in this region is N–S (000°); oblique by 30° (counterclockwise) to the regional trend (030°) of the EPR axis (Figure 4 insert). None of the structures (faults/fissures) observed in this terrain are laterally continuous for more than about 50 m and none develop significant amounts of vertical relief (< 5 m). Typically, the base of fault scarps are characterized by sediment-free talus ramps, composed of abundant cobble-sized and larger pillow and tube fragments. The youthful appearance and extent of the talus indicate that mass-wasting processes tend to smooth any tectonically created relief soon after it is generated.

Curiously, as the axial volcanic high approaches the northern side of the intersection depression the relief and continuity of the high appear to diminish but the amplitude of the hummocky volcanic terrain (i.e. the relief of individual volcanic mounds, etc.) increases considerably and the average depth to basement decreases (Dive 975, Figure 5D). Tube-draped mounds and ridges in this area exhibit relief on the order of 50 m to 70 m and their flanks develop slopes that are locally steeper (40° to vertical) than those found along the first half of Dive 975 immediately to the south. In addition to the increased amplitude of individual volcanic-constructional elements, several other interesting contrasts emerge between the terrain seen during the first and second phase of Dive 975. Sharp breaks in slope, well developed sediment-free talus ramps (Fig 8E; > 10 m high), and scarp faces exposing freshly truncated pillows and tubes signify that faulting has been recent and that significant dip-slip displacement (10–30 m) has occurred along the faults in this area. As opposed to the predominance of fissuring over faulting seen during the first half of Dive 975, fissures were rarely seen during the second half. The few fissures that were observed have trends that are subparallel to that of the Tamayo Transform (120°; Figure, 4), significantly different from the N–S trend observed on the first part of Dive 975, and the dominant 030° structural trend along the EPR axis farther to the south.

3.2. Western rift valley wall

The only large throw (> 40 m) faults observed within or proximal to the EPR/Tamayo intersection area are a set of east-facing faults scarps traversed by Dive 972 (Figures 3, 4, 5B). These structures exist in lithosphere that is inferred to be approximately 100000 yr old and, based on our detailed bathymetric maps (Figures 1, 3) and on the Deep Tow bathymetric profile across the EPR (Macdonald *et al.*, 1979), are interpreted to represent the base of the EPR inner rift valley western wall. The bathymetric map (Figure 3) and dive profile (Figure 5B) suggest that this wall begins at about the 3400 m contour and shoals to about 3100 m. Dive 972 traversed up, along, and then partially down a portion of the western wall and documented that the observed 250 m relief is the product of

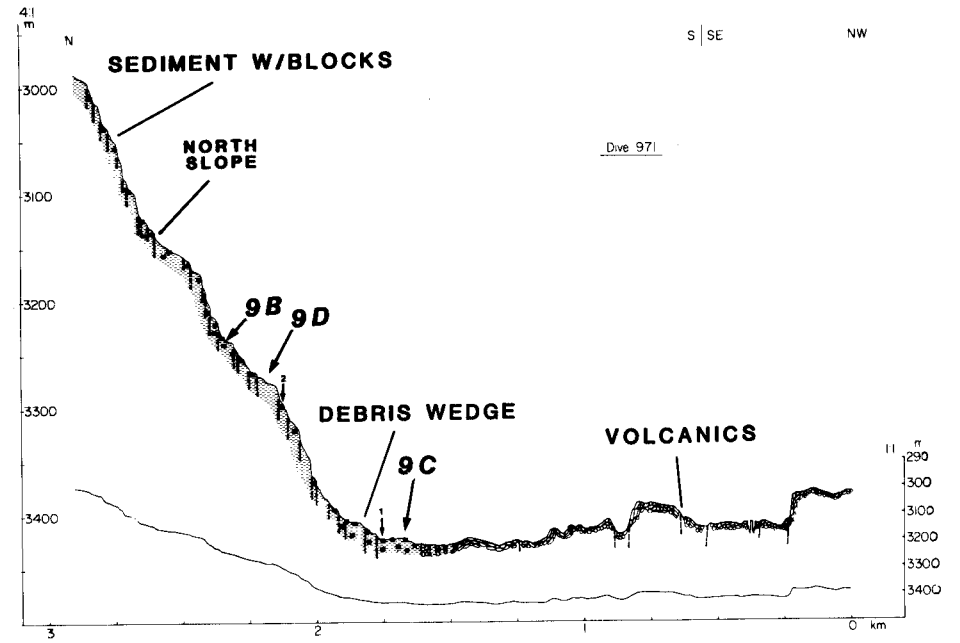

A.

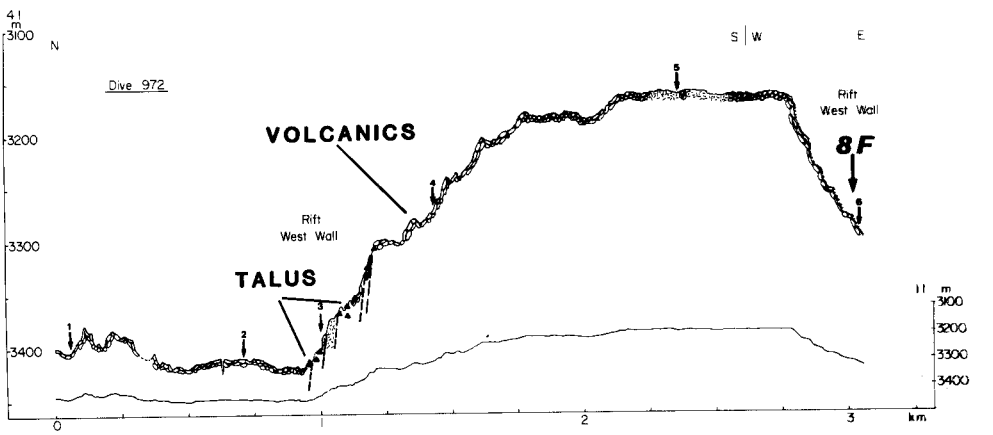

B.

several fault scarps which are laterally continuous for at least 1.5 km and have trends at the dive location of approximately 000°; that is, parallel with the local dominant fault and fissure trend of the EPR inner valley floor and significantly oblique to the regional trend of the EPR axis (030°; Figures 3, 4, 5B). Two of these faults expose truncated pillows and tubes and are characterized by sediment-free talus ramps that contain both massive and pillow basalt fragments. The larger throw faults at the base of the western wall also expose massive basalt sequences up to 50 m thick which, in places, show well-developed columnar jointing. These

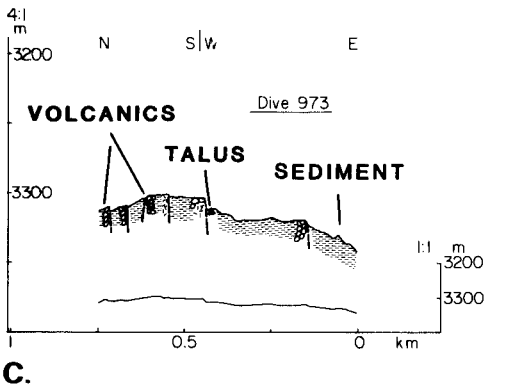

C.

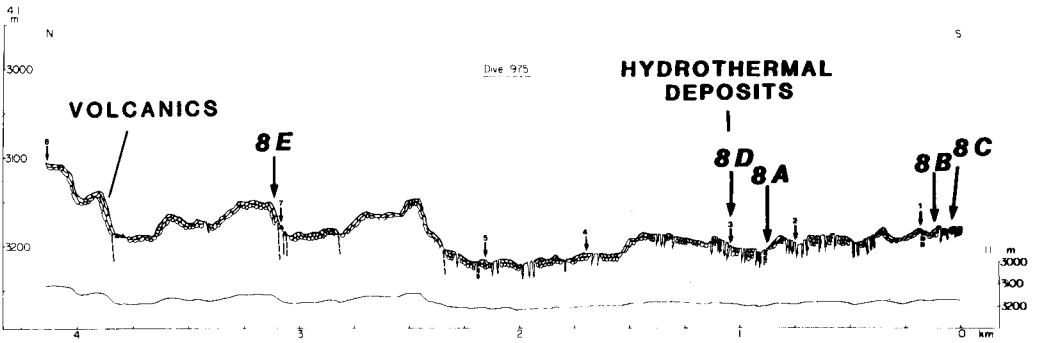

D.

Fig. 5A–D. Geologic profiles and sampling location numbers above profiles) along Dives 971, (A), 972 (B), 973 (C), 975 (D) respectively (locations shown by Figure 3). 4:1 and 1:1 profiles are given for each dive. Symbols used for geology are identified for each profile. Bold numbers indicate locations of photos given in Figures 8 and 9.

massive layers are interpreted to represent ponded flows and/or sills interlayered with the pillowed flows. Although it is clear that the large throw faults of the western wall reflect the onset of a regime in which tectonism dominates over the processes of volcanism, we found evidence showing that some volcanism has occurred at or near the top of the western rift valley escarpment, slightly off the axis of the EPR. In both upward and downward traverses of Dive 972, the steep uppermost portion of the western wall is draped with unbroken tubular lavas that appear to have been erupted from the top or from a location near the top of the wall (Figure 8F). This terrain of the upper part of the western wall is completely sediment-free and covered with glass-encrusted tabular lava forms, as shown by visual observations and samples recovered. West of these young pillows covering the upper part of the inner rift wall, the terrain is a gently undulating bench, exposing markedly more heavily sediment-covered (1–10 cm) pillows and sheet-type flows, including one small collapse pit.

3.3 The EPR-Tamayo intersection depression

Observations made during Dives 971 and 972 document that, with the exception of a thin (< 3 cm) veneer of hemipelagic sediment, a similar terrain to the EPR axial high exists three kilometers west of it along the floor of the intersection depression (Figures 3, 4, 5A, B). Based on a half-spreading rate of 30 mm yr^{-1} (Larson *et al.*, 1968), the volcanic terrain seen in this area should be approximately 100000 years older than that seen along the Dive 975 traverse; judging by the appearance of the lavas, the surface flows are much younger than this. As was observed during the second half of Dive 975, high-amplitude (> 20 m) volcanic mounds are present, and fissures are conspicuously scarce, although the few observed strike subparallel to the Tamayo Transform trend (120°).

Five kilometers west of the EPR axial volcanic high, the hummocky ridge-generated volcanic terrain of the intersection depression is overlain by a veneer of sediment several centimeters thick (Dive 973; Figures 3, 4, 5C). Based on the calculated 30 mm yr^{-1} half-rate of seafloor spreading, volcanic basement in this area is estimated to be on the order of 165000 years old. The sea floor observed in this region has subtle relief consisting of a gentle southeast-sloping sediment surface broken only by a few small (< 10 m high) N–S trending, east-facing scarps and ridges. The sediment cover is pock-marked by abundant worm-tracks, burrows and other indicators of active bioturbation. Dish-shaped depressions (< 1 m deep and usually < 50 cm in diameter) were observed and interpreted to be locations where unconsolidated sediment has drained, like sand in an hour-glass, either into voids within the underlying volcanic tunnel and tube systems, or into open fissures.

Although the oceanic crust seen along Dive 973 is 165000 yr older than that observed during Dive 975 and 65000 yr older than that observed during Dives 972 and 971, there is evidence to suggest that some structures observed in this area are tectonically active. In a few locations, several N–S scarplets (10–30 cm high, 10–15 m long) were seen within the sediment cover. The scarp-faces are near vertical and scarred by vertical striae suggestive of recent dip-slip motion. Masswasted debris is absent from the base of these scarps and indicates relatively recent formation. Also, near the end of Dive 973, a N–S trending graben-like structure was observed (5–7 m wide 2–3 m deep). The walls of this graben expose both truncated pillow and massive basalt. The sediment cover along the floor of the graben is littered with angular, sediment-free basalt fragments and boulders (0.5–1 m in diameter) suggesting some recent tectonic activity. However, the largest (~ 10 m high) N–S scarp seen on this dive showed sediment-blanketed manganese-veneered talus at its foot, demonstrating no recent activity along it.

At two locations along the intersection depression (Dives 976, 977; Figures 3, 6, 7B, 7C) topographic ridges of volcanic rock emerge from the > 1 m thick sediment cover that blankets the deepest portion of the depression. These basalt ridges trend NNW–SSE and WNW–ESE and are characterized by a gently dipping

west-facing slope and steep east-facing scarps that can be as high as 50 m (Dive 977, Figures 6, 7C). The steep scarps expose mostly manganese veneered angular basalt talus blocks and minor amounts of massive basalt outcrop (Figure 9A). Degraded pillow forms were observed at the tops of these scarps. The scanning sonar system (CTFM) of ALVIN shows that the largest of these features (Dive 977; Figures 6, 7C) is laterally continuous over a distance of at least 1.5 km and other ridges were traced along strike for distances of 500 m. All of the scarps seen in older terrain appear to be tectonically inactive; the talus piles are blanketed by sediment, the fragments are manganese veneered, and individual fragments of talus are in places welded together by manganese encrustation.

3.4. The northern side of the intersection depression

The northern boundary of the EPR/Tamayo intersection depression is defined by a steep, south-facing slope that rises abruptly above the elongate closed-contour depression creating between 300 to 600 m of relief (Figure 3). Four dives (971, 974, 976, 977; Figures 3, 4, 5, 6, 7) traveled either up, or up and along the slope in order to investigate its tectonic character and, in particular, to examine the 115° trending scarps that were thought to represent the location of the principal transform displacement zone (PTDZ; Macdonald *et al.*, 1979).

As the base of the northern slope is approached on Dive 971 (Figures 3, 4), the relief of the hummocky, EPR volcanic terrain becomes first gradually, and then rapidly, subdued by a progressively thickening wedge of sediment that has apparently been shed from localities on the south facing slope. The distal end of this wedge consists of fine-grained, muddy sediment that blankets the volcanics. The proximal part and the bulk of this sedimentary wedge is composed of blocks and clods of variably consolidated, muddy to arenaceous sediment that, in all cases, are seen to lie within a matrix of similar sediment (Figures 9B, 9C). At one location clam shells were seen mixed in with and partially buried by the sediment. This sediment wedge is about 400 m wide on Dive 971; the part consisting of exposed blocks occupies about 300 m of this total. No firm evidence of faults cutting the chaotic sedimentary wedge deposited at the base of the sediment slope was seen.

Observations from Dive 971 (Figure 5A) show that near its base, above the sediment wedge, the south-facing slope of the north flank of the intersection trough is comprised of numerous small amplitude (< 5 m), closely spaced (< 20 m) scarps in sedimentary material. These features are very steep (70° to 90°), dip towards the south, and are interpreted to be the surface manifestations of active fault scarps. Towards the west (Figures 6, 7; Dives 974, 976, 977) the character and general orientation of the scarps remains the same but the width of the zone containing well-defined scarps is much less even though the density of scarp distribution increases. All of the scarps seen along the sediment slope occur within poorly to well-consolidated sediments (Figure 9D), and in no case was igneous basement definitely recognized. At one location on Dive 971, however, ALVIN

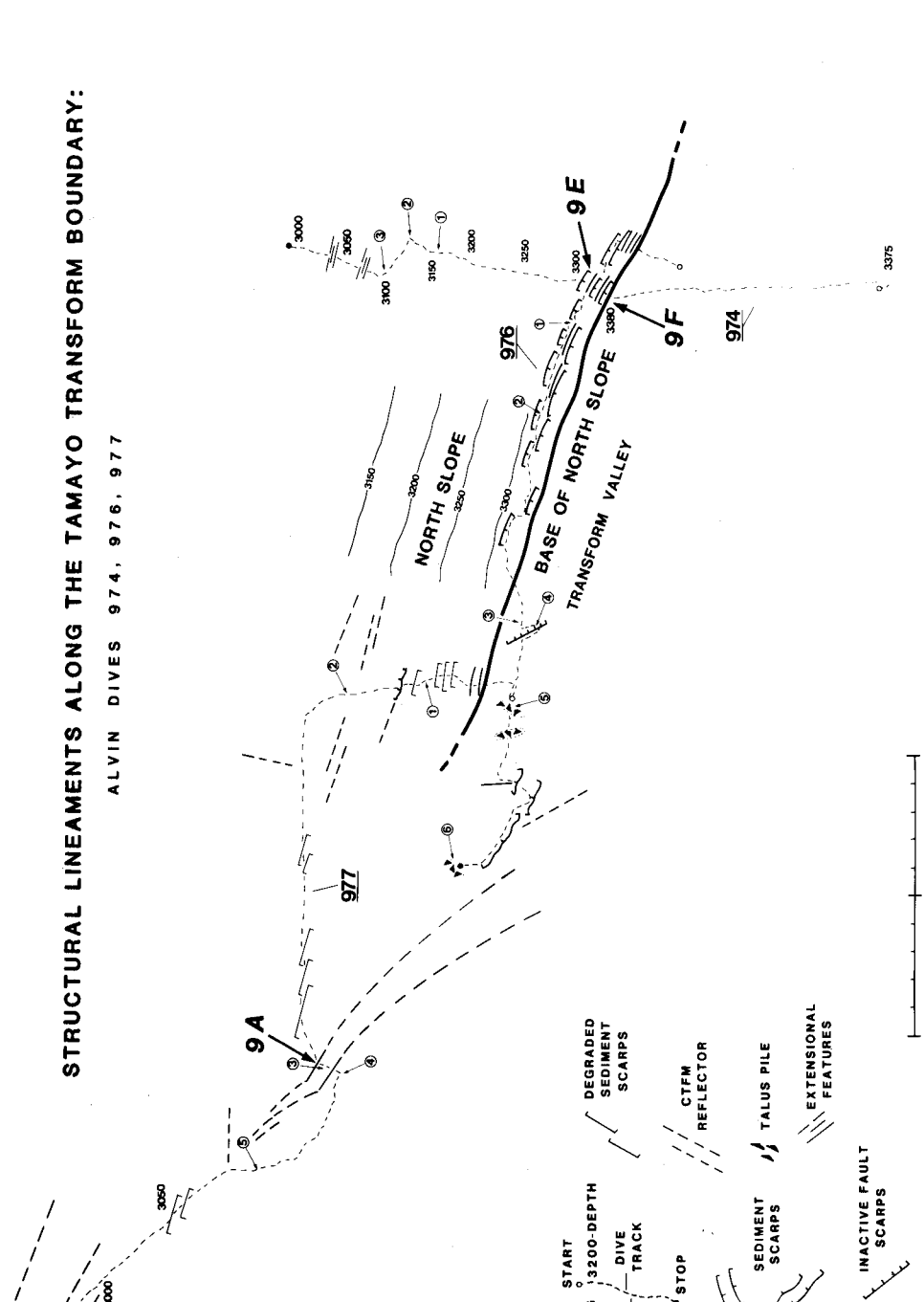

Fig. 6. Structural lineaments and geology along Dives 974, 976, 977 (location given in Figure 3). Inactive-fault scarps in volcanic basement trend obliquely while sediment scarps trend subparallel to the Tamayo Transform valley. Circled numbers indicate sampling locations. Bold numbers indicate locations of photos given in Figure 8 and 9.

bow camera photos show angular talus fragments and a possible source outcrop of volcanic rock as a small sill (~ 1 m thick) in the sediment. Apart from this example, no evidence of recent igenous activity was seen anywhere on the slope. In some instances the scarp faces expose laminations comprised of fine sands, silts and muds that are similar in appearance to the structures and relationships seen within the large disrupted blocks found on Dive 971 at the base of the sediment slope. Samples of this sediment were recovered from several localities along the slope and are composed of matrix-rich lithic and feldspathic sands that are finely laminated with lutites. The sands contain abundant angular quartz grains and contain lesser amounts of lithic particles, feldspar grains, and calcareous biogenic material. Analysis of the faunal assemblages indicate that the sediments are rich in Pleistocene to Quaternary benthic and pelagic assemblages, and that many of the benthic faunas are characteristic of relatively shallow water marine environments (shelf and upper slope), and therefore are suggestive of down slope displacement and resedimentation (personal communication: A. Boersma, W. Ruddiman, and M. Aubry). At some outcrops the scarps expose rubbly chaotic beds (~ 1 m thick) interlayered with the finely bedded arenites and lutites. The chaotic horizons observed in outcrop seem to be largely confined to the lower scarps. These chaotic beds are probably debris flows formed in the same way as those seen at the present base of the slope, re-exposed by tectonic activity.

The faces of scarps along the sediment slope typically show scalloped failure surfaces, and are corrugated by erosional rills and gullies along which the downslope movement of unconsolidated sediment occurs (Figures 9D, E, F). Along the base of individual sediment scarps, accumulations of talus are observed (Figure 9B) and consist of small sediment blocks and clods imbedded within a matrix of sedimentary material, partly hemipelagic, and similar in style to that of the more developed sedimentary wedge seen at the base of the sediment slope along Dive 971. Large detached slabs of manganese encrusted sediments (~ 4 m wide, < 2 m thick) are seen near the crest of some of the scarps along the sediment slope. All stages in the formation of these loose 'mega-blocks' are observed from nascent failure surfaces, represented by extensional gashes (see Figures 6, 7A; Dive 974) to individual sedimentary slabs found just downslope from their failure surfaces, to the large, mass wasted blocks found at the base of the sediment slope along Dive 971. Clearly, the sediment slope in this area is at least presently gravitationally unstable, and we infer that it is being tectonically disrupted.

Observations made during Dive 971 (Figures 4, 5A) show that the zone of active scarp degradation seen on the part of the slope crossed by that dive has a width, proximal to the ridge/transform intersection, of 1.5 km. Curiously, observations from Dives 974, 976, and 977 indicate that this zone, characterized by a series of steep, scalloped scarps, erosional gullies, and wedge-shaped debris deposits, becomes less prominent to the west (Figures 3, 6, 7). The total width of the disturbed terrain seen along Dive 974 was 250 m; along Dive 976, 150 m; and at the beginning of Dive 977, 100 m (Figures 6, 7). Farther to the west, in the middle

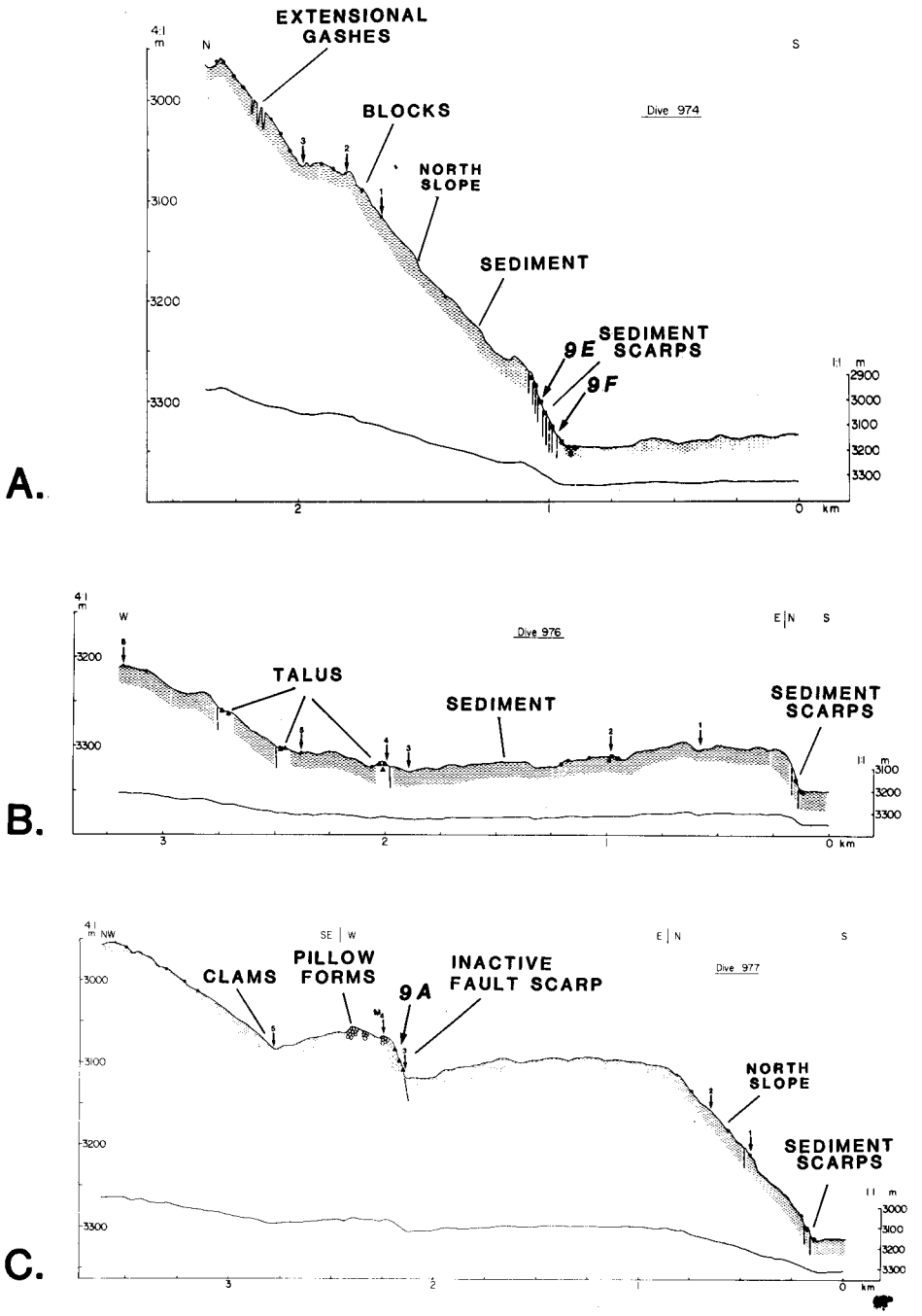

Fig. 7A–C. Geologic profiles and sampling locations (numbers above profiles) along Dives 974 (A), 976 (B), 977 (C) respectively (locations shown by Figure 3). 4:1 and 1:1 profiles are given for each dive. Symbols used for geology are identified for each profile. Bold numbers indicate locations of photos given in Figure 8 and 9.

and near the end of Dive 977 the zone of active mass wasting is not present at all along the base of the sediment slope. Instead, there are some smoothed-out, much degraded scarps (middle of Dive 977; Figure 7C) or none (near end of Dive 977). At the base of the north slope, near the end of Dive 977, a small, single area a couple of meters across was found in which a community of large clams existed. Most but not all of the creatures appeared to be dead; some had formed prominent trails in the mud bottom away from the area of greatest concentration. A small pit in the mud about 20 cm deep and 50 cm across next to the community contains what may be a small hydrothermal vent construction. The small size of the community suggests that the discharge was small and the moribund nature of the community suggests that the discharge is waning.

Dives 971 and 974 traveled perpendicular to the trend of the slope and the scarp trends, while Dive 976 and Dive 977 traveled, in part, parallel with the trend of the zone of active scarp degradation in order to examine individual scarps for continuity. Dive 976 (Figures 3, 7) traced a particular set of scarps for a distance of about 1.5 km along the transform valley and documented that these scarps are similar in location, trend and continuity to those defined by side-looking sonar data (Macdonald *et al.*, 1979). The scarp faces in this area are irregular, being disrupted and scalloped by local slope failure processes. Sediment scarp height within the more western area (Dives 974, 976, 977) is about the same as to that seen to the east along Dive 971 (~ 5 m), but the frequency of scarps in the zone in which they are developed in the western area seems to be greater (3–4 m) than that along 971, and nowhere are large, loose sedimentary slabs seen on slopes, nor are the sedimentary debris wedges at the base of scarps nearly as well developed (in areal extent or in size of blocks) as those seen towards the east opposite the EPR/Tamayo intersection (Dive 971). In fact, the lack of a significant debris wedge compared to the adjacent height and width of the zone of escarpments (see Figures 5A, 7A, 7B, 7C) on Dives 974, 976 and 977, and on Dive 971 is a key piece of evidence demonstrating that these are not the head scarps of rotational landslips. In the case of the three more western dives, the occurrence of these recent scarps at the base of the northern slope of the intersection depression requires that they cannot be landslide scarps and that they must be the surface expression of faults. The same argument applies to at least the lower scarps seen on Dive 971. Those seen higher on the slope during this dive cannot be so definitely identified as fault surface breaks on this criterion alone, although we think it is likely that they are, considering the overall geometry and distribution of the scarps and the debris derived from them (see Figures 5A, 7, 10b). A few small, north-facing scarps (~ 1 m high) were observed near the beginning of Dive 977 at the upper part of the zone of scarps and along the mid-section of Dive 976.

Above the zone of active scarp degradation described along Dives 974, 976, and 977, the south facing sediment covered slope is relatively undisturbed (Figures 3, 6, 7). Actively degrading sediment scarps of the size and style observed on the lower slopes are not seen, and the hemipelagic sediment-covered slope is only

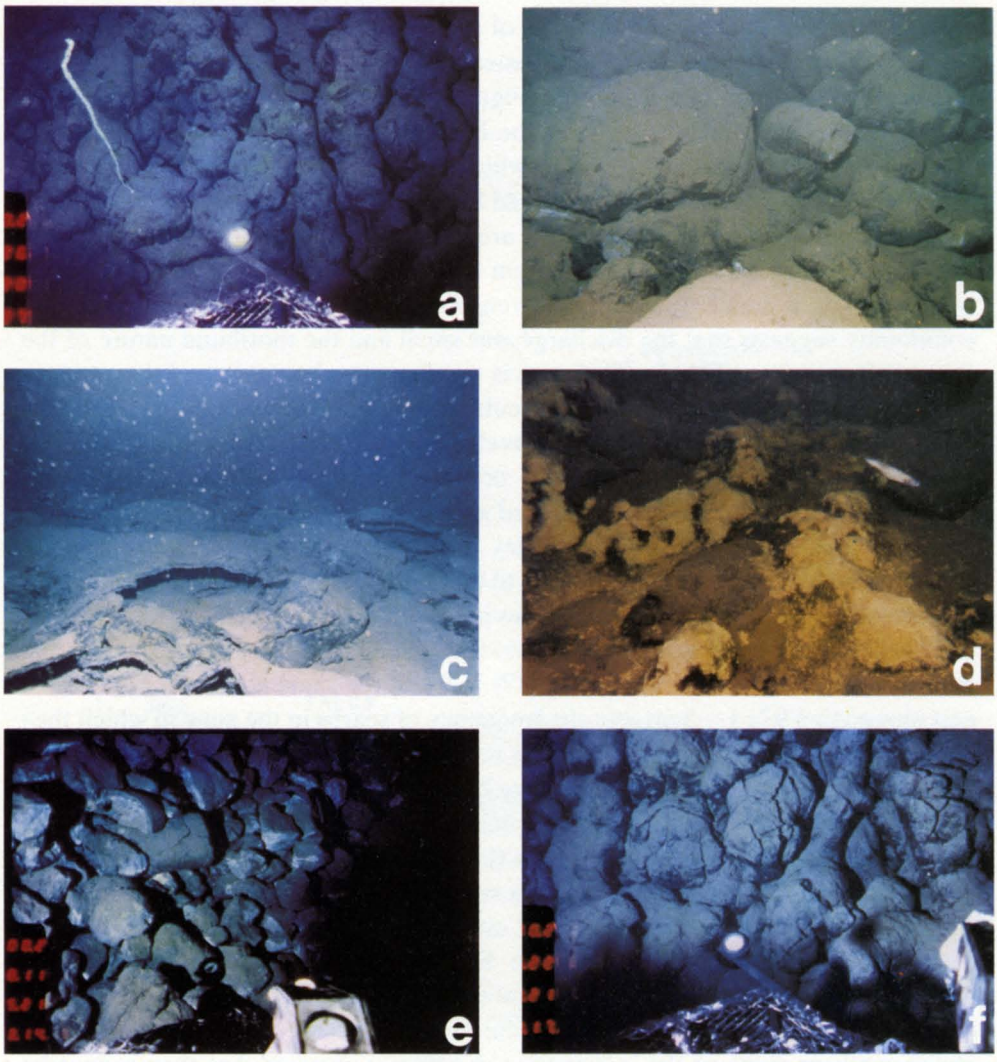

Fig. 8. Selected photographs of young volcanic terrain of the EPR. (A) Lightly sedimented pillows and tubular lava cylinders draping the flank of volcanic ridge located along EPR inner valley floor (Dive 975; time 17:54:20, depth 3188 m). (B) Lightly sedimented pillows and tubular lavas of the EPR inner-valley floor (Dive 975; time 17:19:09; depth 3179 m). (C) Thin (2–4 cm) veneer of flow overlying pillow forms (Dive 975; time 17:10:19; depth 3179 m). (D) Fluffy yellow-white precipitate interpreted to be of hydrothermal origin (Dive 975; time 18:10:03; depth 3203 m). (E) Fresh, sediment-free talus ramp at the base of a small (< 5 m) vertical offset fault scarp (Dive 975) indicative of recent tectonic activity and subsequent mass-wasting (Dive 975; time 21:13:14; depth 319 4m). (F) Relatively sediment-free, glass encrusted tubular and elongate pillow lavas seen high on the Western Rift valley wall suggesting a recent episode of off axis volcanism (Dive 972; time 21:53:17; depth 3325 m).

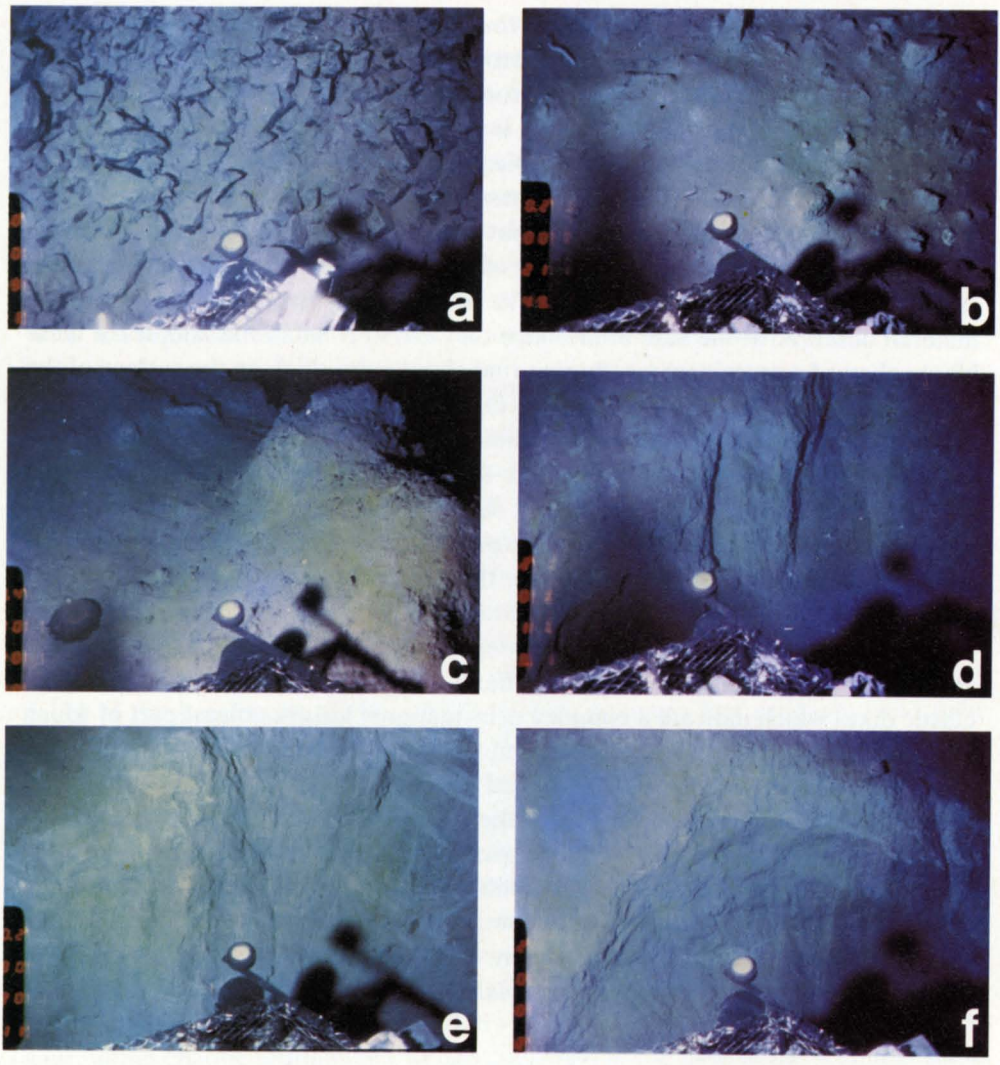

Fig. 9. Selected photographs of older volcanic terrain and north side of the intersection depression. (A) Talus ramp seen 9 km west of the EPR axis at the base of a N–S trending fault scarp. Managanese veneer and sediment cover suggests that this fault has been inactive for some time (Dive 972; time 19:12:21, depth 3082 m). (B) Debris wedge seen at the base of sediment scarps along the north side of the EPR-Tamayo intersection depression (Dive 971; time 21:54:49; depth 3260 m). (C) Larger (~ 1 m across) semi-consolidated sediment block in debris wedge at base of sediment scarps (Dive 971; time 20:29:10; depth 3435 m). (D) Scarps (< 2 m high) in semi-consolidated sediment showing corrugation of the scarp face. Scarp trend is approximately transform parallel (Dive 971; time 21:48:33; depth 3282 m). (E) Scarp face (< 2 m high) in semi-consolidated sediment showing erosional rills and lenses of lighter colored sedimentary material (Dive 974; time 20:35:11; depth 3315 m). (F) Scarp in semi-consolidated sediment showing 'scalloped' failure surface (Dive 974; time 20:31:22; depth 3323 m).

locally distorted by low amplitude, well-rounded sediment-covered benches which appear to be some type of inactive and eroded scarps in sediment. Although there is no evidence for recent faulting, throughout most or all of this area loose, sediment-veneered blocks are found scattered across and embedded in the hemipelagic blanket. The blocks are typically 10–50 cm in diameter and consist of either lithified sediments or weathered basalt. These blocks are widely spaced and some parts of the slope traversed do not show them; where they are seen, one might be observed in about 100 meters of traverse. Some of them are crumbling and disaggregating *in situ*, along cracks in the lithified rock, unlike the softer material observed at the base of the slope on Dive 971. All of the samples of these blocks showed a prominent weathering rind about 1 cm-thick on the surface of the block exposed to the water and next to cracks leading away from these surfaces. The extent of this weathering and the minimal hemipelagic coating on the blocks suggests that they have been exposed *in situ* for a significant time and that persistent winnowing of the hemipelagic material takes place along this part of the slope. The source area of these blocks, particularly those consisting of basalt, is presently unclear, although it is possible that fault scarp sources up-slope are not apparent due to a combination of tectonic and perhaps erosional degradation. Thin-section examination of a consolidated sedimentary block collected from this area, shows the presence of small microfaults ($\sim$ 1 cm offset) and associated small clastic dikes which indicate a complex deformational history at least part of which may have been of a surficial, soft sediment type. Another shows a complex network of cracks 1–2 mm wide filled with lithified micritic sediment, and has a surface on the base of the block showing low-relief 'slickensides-type' fabric defined by fibrous cryptocrystalline silica. This sample demonstrates derivation from a source where both brittle deformation and infiltration by initially soft sediment could occur. A few small incipient fissures, a few meters long and a centimeter or two wide, subparallel with the transform trend, were observed high on the slope on Dive 974 (Figure 7A). The significance of the isolated occurrence is not clear.

4. Discussion

4.1. The location of the principal transform displacement zone (PTDZ)

The trend, location and distribution of recently active scarps along the south facing sediment slope that bounds the north side of the EPR-Tamayo intersection depression suggest that this zone of instability reflects strike-slip deformation within the underlying volcanic basement and marks the location of the PTDZ. The orientation of the zone of scarp development and active mass wasting is roughly parallel with the regional trend of the Tamayo Transform (120°), the scarps represent the only sites of active transform-parallel deformation observed west of the EPR/Tamayo intersection area during our field program, and these structures, if extrapolated 20 km to the west along the transform valley, are coincident with a

deformed zone found by the submersible CYANA (CYAMEX and Pastouret, 1981). Although we documented abundant evidence for recent scarp development and slope modification, no field relationships were observed that demonstrate strike-slip displacements along the scarps. The structures observed along the sediment slope probably represent gravitationally induced erosional degradation of a free standing sediment wedge that is underlain by oceanic basement disrupted by strike-slip faulting.

It is interesting to note that when the along-strike perspective is considered, the character of the zone of slope instability changes markedly over a distance of 10 km. At the eastern end of our field area, opposite the EPR-tamayo intersection, the disturbed and disrupted terrain is over one kilometer wide. Towards the west the frequency of scarp development increases but the width of the disturbed zone is only about 100 m. We suggest that the apparent along strike change in the intensity of deformation is a function of the plate boundary geometry and kinematics of the transform. The turbidites and intercalated hemipelagic lutites sampled from scarps along the sediment slope were deposited on the floor of the Tamayo Transform at deposition centers located to the west within the northern trough. Subsequently, these deposits have been transported eastwards along the southern edge of the North American plate until they are exposed along the relatively deep closed-contour depression of the EPR-Tamayo intersection. As the sedimentary wedge moves from west to east along the intersection depression the depth to the floor of the depression increases, slope instability is enhanced because of continued transform tectonism, and deeper intervals of the sediment wedge are exposed as the relief of the slope increases (Figure 10A, B).

4.2. Structure and tectonic implications of the EPR-Tamayo intersection terrain

The orientation of fissures and small throw faults observed during the dive traverses (Dives 971, 972, 973, 975; Figure 4) located proximal to the EPR-Tamayo intersection clearly show that the most frequently observed structural trend is N–S (000°) and represents a structural fabric 30° oblique to the strike of the EPR axis (030°) and 60° oblique to the trend of the Tamayo Transform (120°). Farther to the west of the intersection, observations made during Dive 977 (Figure 6) document that structures located within a few kilometers of the PTDZ have orientations ranging from 350° to 000°. These structural data are all located within 5 km of the PTDZ and do not suggest a well-defined systematic change in orientation of structures with increasing proximity to the transform boundary. However, when these structural observations are integrated with the more regional perspective provided by deep-tow side-scan sonar data (Macdonald *et al.*, 1979; Figure 3) and regional bathymetry (Lewis *et al.*, 1983; Figure 3), there is a systematic change in the orientation of rise-axis parallel structures as the transform is approached and this pronounced change in orientation takes place about 5 km from the transform boundary. Previous investigations (Courtillot *et al.*, 1974;

Crane, 1976; Lonsdale, 1978; Searle, 1979; Macdonald *et al.*, 1979) of ridge-transform intersections have identified oblique trends but it remained to be established whether these structures represent faults that accommodate strike-slip displacements (Riedels, Anti-Riedels, secondary shear) or whether these structures are just oblique trending normal faults. The resolution of this ambiguity is crucial to an understanding of the tectonics of ridge-transform intersections. If the oblique faults largely accommodate strike-slip motion, then the intersection area encompassing the oblique structures is taken to represent a broad shear zone with strike-slip displacements distributed on numerous fractures. Continental analogues suggest that with time and continued displacement strike-slip motion would be focussed on a few faults which coalesce along strike to form a narrow shear zone (Tchalenko, 1970). Alternatively, if the oblique structures accommodate only or dominatly dip-slip displacements then these oblique trending normal faults simply reflect a distortion of the ridge axis extensional stress regime due to proximity to the strike-slip stress field generated along the transform boundary (Crane, 1976; Lonsdale, 1978; Searle, 1979; Macdonald *et al.*, 1979; Courtillot *et al.*, 1974).

Direct observation of these oblique structures during ALVIN traverses shows that the fissures do not accommodate large amounts of strike-slip displacements; the observations do not rule out a strike-slip component on these features much subordinate to the amount of extension. All fault-generated scarps observed on the dives in the extrusive terrain are degraded by varying degrees of mass wasting. It is therefore impossible to say with certainty (for example, by observing offset volcanic forms, or slickensides) that no strike-slip component of motion has occurred on these faults. However, the significant changes in orientation inferred for these faults along strike are more compatible with dominantly normal fault kinematics, as is their local parallelism with fissures (e.g. Dives 972, 975; Figures 4, 5). Furthermore, these faults are active at the ridge-transform boundary but are inactive (sediment-covered talus) to the west. Our dive observations support the notion that these oblique structures are the product of episodes of extension and that they do not accommodate significant amounts of strike-slip displacement and do not represent secondary shear within a broad zone of shear (Figure 10). This interpretation is consistent with models proposing that these structures result from the influence of a transform generated shear couple (Courtillot *et al.*, 1974; Crane, 1976; Lonsdale, 1978; Searle, 1979; Macdonald *et al.*, 1979; Gallo *et al.*, 1980).

It has recently been suggested that the oblique normal faults that are observed to disrupt the brittle volcanic skin of the oceanic crust is caused by a shear couple that forms at the ridge-transform intersection in the underlying upper mantle (Fox and Gallo, 1982; 1983). The juxtaposition of a cold edge of lithosphere against the truncated axis of an accreting plate boundary at a ridge-transform intersection cools the asthenosphere rising beneath the intersection and a mantle weld forms in the young lithosphere across the transform boundary. With continued sea floor spreading the weld deforms, creating a shear couple at the ridge-transform intersection which distorts the orientation of the axis of maximum tensile stress and

leads to the creation of normal faults and fissures with trends that are oblique to the overall direction of sea floor spreading.

The juxtaposition of a cold edge of lithosphere against an accreting plate boundary will also restrict the amount of partial melting which may occur in the rising asthenosphere at the ridge-transform intersection (Gallo and Fox, 1979; Stroup and Fox, 1981; Fox and Gallo, 1984). The production of smaller volumes of basaltic melt per unit time predicts that the crust should thin in the vicinity of ridge-transform intersections and that the underlying upper mantle should be heterogeneous. Seismic refraction studies (McClain and Lewis, 1980) indicate that the thickness of the oceanic crust thins by 2 to 3 km in the vicinity of the Tamayo Transform boundary. Furthermore, modeling of geochemical data from the analyses of basalts recovered in this project from along the axis of the EPR south of the Tamayo Transform demonstrate that the basalts created in close proximity to the Tamayo Transform boundary are the products of relatively small amounts of

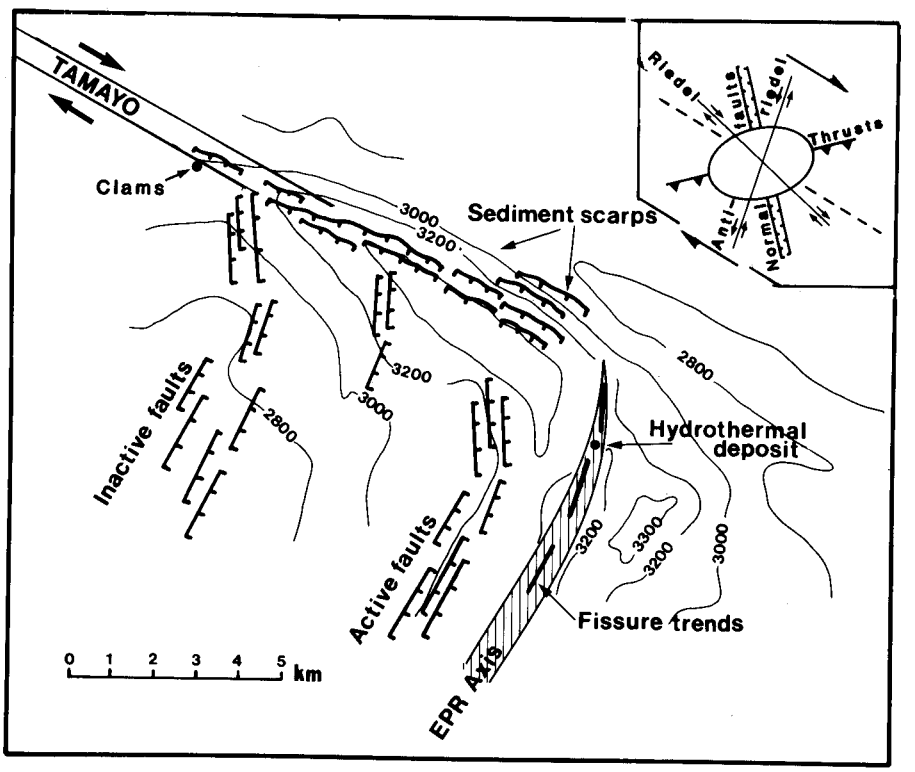

Fig. 10A. Schematic interpretation of the EPR-Tamayo intersection showing deflection of the EPR axis and fault and fissure trends as the Tamayo Transform is approached. Structures generated within a right-lateral shear couple are shown in insert (upper-right). Note that the volcanic terrain of the EPR axis protrudes across the Tamayo-EPR intersection depression. Sediment scarps on the north side of the EPR-Tamayo intersection are taken to represent strike-slip deformation in the underlying volcanic basement.

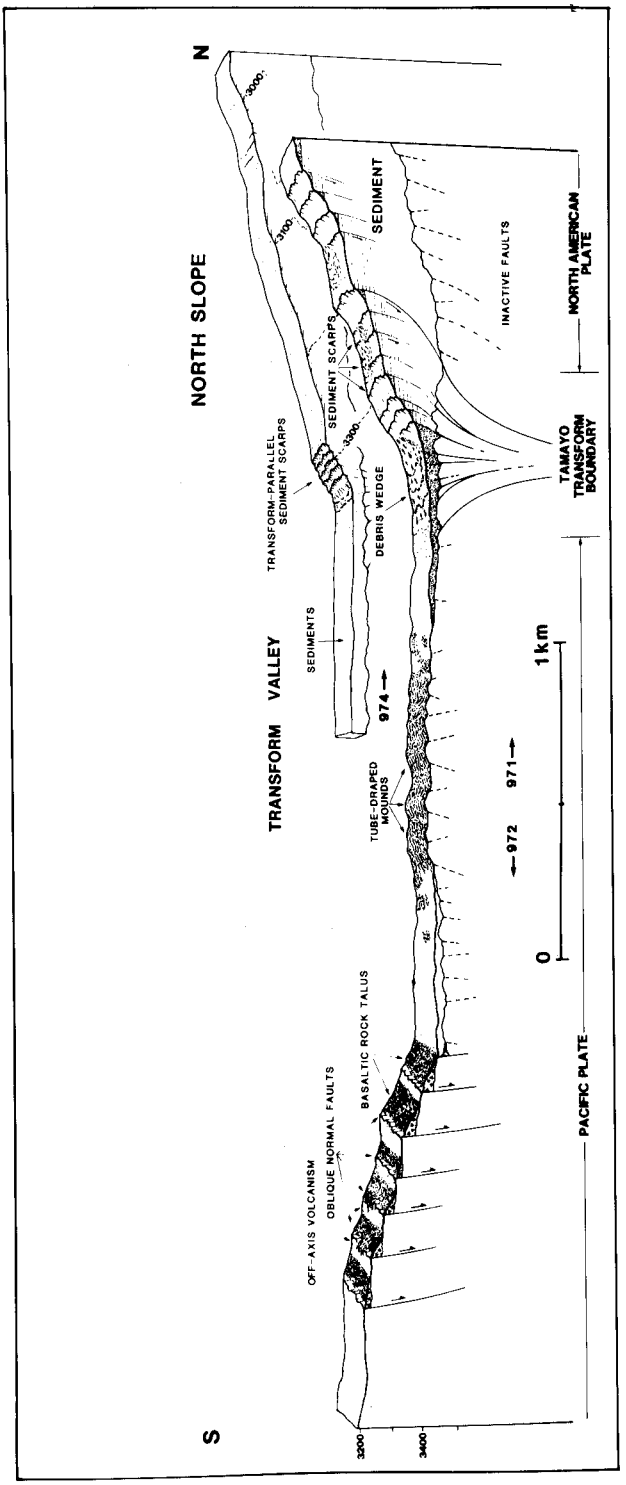

Fig. 10B. Schematic 3–D swath-profiles (compiled from Dives 971, 972, and 974) across the Tamayo Transform boundary showing observed relief, 'surface' geology and structure as well as interpretative basement geology.

partial melting; basalts sampled down the axis of the EPR away from the Tamayo Transform boundary indicate much higher degrees of partial melting (Bender *et al.*, 1981, 1984).

A further expression of the thermal effect of the transform can be seen in the progressive and systematic deepening of the axis of the East Pacific Rise as the transform boundary is approached over several tens of kilometers. This 700 m elevation difference may be due to a number of factors: the reduced thickness of the crust; a density gradient in the upper mantle caused by a descent of isotherms towards the transform and by a change in the composition of the upper mantle related to variable degrees of partial melting.

6. Concluding Remarks

The bathymetric and structural data collected during our 1979 investigation of the EPR-Tamayo intersection allows us to document some relationships that shed light on the processes that are responsible for shaping this type of tectonic terrain.

Rise axis constructional terrain can be traced down into and across the closed contour depression that defines the EPR-Tamayo intersection (Figure 10). Along the north side of the depression the volcanic basement disappears beneath a wedge of sedimentary talus that has been shed from actively eroding sediment scarps. These scarps are located along the lower portion of a 300 m to 600 m high sediment slope, they expose an interbedded assemblage of turbidites and hemipelagic lutites, and they define a narrow zone (100 to 1500 m) of active slope modification that can be traced along strike for a distance of 10 km. We suggest that this zone of active mass wasting and slope modification which trends 120°, approximately parallel to the North American plate-Pacific plate slip direction, marks the surficial location of the principal transform displacement zone (Figure 10). Strike-slip motion transports sediments of the north trough eastwards and exposes them on the northern flank of the intersection depression creating a gravitationally unstable edge of sediments that slump, fail and prograde out over the principal transform displacement zone. These deposits are in turn subjected to further tectonic erosion and mass wasting induced by strike-slip motion in the underlying volcanic basement.

Within about 5 km of the Tamayo Transform boundary, the dominant trend of faults and fissures created along the EPR is 000°; 60° oblique to the regional direction of sea floor spreading and 30° oblique to the axis of the EPR (Figure 10). All of the structures observed within the EPR/Tamayo ridge-transform intersection area are interpreted to accommodate primarily dip-slip motion. These data are consistent with models suggesting that oblique structures at ridge-transform intersections represent ridge-axis extensional regimes distorted by a shear couple (Courtillot *et at.*, 1974; Crane, 1976; Lonsdale, 1978; Searle, 1979; Gallo *et al.*, 1980) generated in the upper mantle beneath the ridge-transform intersection where newly formed lithosphere intermittenly welds to the cold edge of the transform boundary (Fox and Gallo, 1982, 1984).

Acknowledgements

We are indebted to the Masters, officers and crews of the research vessels LULU and GILLISS and especially to the pilots and technical support team of the Deep Sea Research Vessel ALVIN for their enthusiasm and dedication that kept the submersible operational making our science possible. We are grateful to J. F. Bender and C. H. Langmuir for providing insight to the petrologic character of the oceanic basalts generated proximal to transform boundaries and we thank them for a preprint of their paper. We thank D. J. Fornari and J. B. Stroup for constructive criticism of an early draft of this manuscript and K. Louden for his review of the final version. W. Ruddiman, A. Boursma, M. Aubry, and E. Pokras provided analyses of the faunal assemblages of the sediment samples and their help is gratefully acknowledged. This work was financially supported by the National Science Foundation under Grant Number OCE79-13144. WHOI cont. number 5488.

References

Bender, J. F., Hanson, J. N., and Langmuir, C. H.: 1981, 'Basalt Glasses from the East Pacific Rise-Tamayo Transform Intersection: Geochemical Evidence for Complex Magma Generation Processes', *Trans. Amer. Geophys. Union* **62**, 423.

Bender, J. F., Langmuir, C. H., and Hanson, J. N.: 1984, 'Petrogenesis of Basalts from the Tamayo Region, East Pacific Rise: Evidence that Partial Melting is Responsible for Systematic Variations in Glass Chemistry with Distance from a Transform Fault', *Jour. Petrol.* (in press).

Chinnery, M. A.: 1966, 'Secondary Faulting', *Can. Jour. Earth Science*, **3**, 163–174.

Courtillot, V., Tapponier, P., and Varet, J.: 1974, 'Surface Features Associated with Transform Faults: A Comparison Between Observed Examples and an Experimental Model', *Tectonophy*, **24**, 317–329.

Crane, K.: 1976, 'The Intersection of the Siquieros Transform Fault and the East Pacific Rise', *Mar. Geology* **21**, 25–46.

CYAMEX Scientific Team and Pastouret, L.: 1981, 'Submersible Structural Study of the Tamayo Transform Fault, East Pacific Rise at 23° N', *Mar. Geophys. Res.* **4**, 381–401.

Fox, P. J. and Gallo, D. G.: 1982, 'A Mantle Weld at Ridge Transform Intersections: Implications for the Development of Oblique Structures', *Trans. Amer. Geophys. Union* **63**, 446.

Fox, P. J. and Gallo, D. G.: 1984, 'A Tectonic Model for Ridge-Plate Boundaries: Implications for the Structure of Oceanic Lithosphere', *Tectonophysics* (in press).

Gallo, D. G. and Fox P. J.: 1979, 'The Influence of Transform Faults on the Generation of Oceanic Lithosphere', *Trans. Amer. Geophys. Union* **60**, 376.

Gallo, D. G., Rosencrantz, E. R., and Rowley, D. B.: 1980, 'Oblique Structures at Ridge-Transform Intersections: Implications for Ridge Dynamics and Pole Determinations', *Trans. An Geophys. Union* **61**, 358.

Karson, J. A. and Dick, H. J. B.: 1983, 'Tectonics of Ridge-Transform Intersections at the Kane Fracture Zone', *Mar. Geophys. Res.* **6**, 51–98.

Kastens, K. A., Macdonald, K. C., Becker, K., and Crane, K.: 1979, 'The Tamayo Transform Fault in the Mouth of the Gulf of California', *Mar. Geophys. Res.* **4**, 129–152.

Larson, R. L., Menard, H. W., and Smith, S. M.: 1968, 'Gulf of California: A Result of Ocean Floor Spreading and Transform Faulting', *Science* **161**, 781–784.

Larson, R. L.: 1972, 'Bathymetry, Magnetic Anomalies and Plate Tectonics History of the Mouth of the Gulf of California', *Geol. Soc. Am. Bull.* **83**, 3345–3360.

Lewis, B. T. R.: 1979, 'Periodicities in Volcanism and Longitudinal Magma Flow on the East Pacific Rise at 23° N', *Geophys. Res. Lett.* **6**, 753–756.

Lewis, B. T. R., Syndsman, W. E., McClain, J. S., Holmes, M. L., and Lister, C. R. B.: 1983, 'Site Survey

Results at the Mouth of the Gulf of California, Leg 65', *Deep Sea Drilling Project, Init. Repts. DSDP* **65**, 309–323.

Lonsdale, P.: 1978, 'Near-Bottom Reconnaisance of a Fast-Slipping Transform Fault Zone at the Pacific-Nacza Plate Boundary', *Jour. Geol.* **86**, 451–472.

Macdonald, K. C., Kastens, K., Spiess, F. M., and Miller, S. P.: 1979, 'Deep-Tow Studies of the Tamayo Transform Fault', *Mar. Geophys. Res.* **4**, 37–70.

McClain, J. S. and Lewis, B. T. R.: 1980, 'A Seismic Experiment at the Axis of the East Pacific Rise', *Mar. Geol.* **35**, 147–170.

McKinstry, H. E.: 1953, 'Shears of the Second Order', *Amer. Jour. Sci.* **251**, 401–414.

OTTER Scientific Team: 1984, 'The Geology of the Oceanographer Transform: The Ridge-Transform Intersection', *Mar. Geophys. Res.* **6**, 109–141 (this issue).

Riedel, W.: 1929, 'Zur Mechanic Geologischer Brucherscheinungen', *Zentralb. Mineral. Geol. Pal.* 1929B, 354–368.

Searle, R. C.: 1979: 'Side-Scan Sonar Studies of North Atlantic Fracture Zones', *J. Geol. Soc. London* **136**, 283–293.

Stroup, J. B. and Fox, P. J.: 1981, 'Geologic Investigations in the Cayman Trough: Evidence for Thin crust along the Mid-Cayman Rise', *J. Geol.* **89**, 395–420.

Tamayo Scientific Team: 1980a, 'Tectonics of a Ridge-Transform Intersection Zone: Tamayo-East Pacific Rise, Gulf of California, *EOS. Trans. Amer. Geophys. Union* **61(32)**, 574.

Tamayo Scientific Team: 1980b, 'Submarine Landsliding at the Eastern End of the Tamayo Transform Fault, Gulf of California', *EOS, Trans. Amer. Geophys. Union* **61(17)**, 359.

Tamayo Scientific Team: 1980c, 'East Pacific Rise-Tamayo Transform Fault Intersection', *Geol. Soc. Amer. Abstracts with Programs* **12(7)**, 461–462.

Tchalenko, J. S.: 1970, 'Similarities between Shear Zones of Different Magnitudes', *Geol. Soc. Am. Bull.* **81**, 1625–1640.

CHAPTER II

A Tectonic Model for Ridge-Transform-Ridge Plate Boundaries: Implications for the Structure of Oceanic Lithosphere

INTRODUCTION: RIDGE-TRANSFORM-RIDGE PLATE BOUNDARIES

First-Order Relationships: Compilations of reconnaissance bathymetric data of the oceans (e.g. Menard and Chase, 1970; physiographic map of Heezen and Tharp, 1977) and earthquake epicenter maps (e.g. Barazangi and Dorman, 1969) document that transform faults routinely offset the axis of the world-encircling Mid-Oceanic Ridge System. The distribution of transforms along the axis of the ridge, however, is not uniform. For example, along the axis of the slowly accreting Mid-Atlantic Ridge south of the Azores, transforms offset the axis every 50km to 100km (Fox et al., 1969; Johnson and Vogt, 1973; Collette et al., 1974; Phillips and Fleming, 1978) whereas along the rapidly accreting East Pacific Rise transforms occur infrequently and are located several hundreds of kilometers apart (Mammerickx and Smith, 1978). The offset lengths of these transforms range from several kilometers (i.e. Kurchatov Transform - Searle and Laughton, 1977) to well over 100 kilometers (i.e. Equatorial transforms - Heezen et al., 1964; van Andel et al., 1967) and the transform domain is composed of linear topography that is parallel with the strike of the transform fault. (The term transform domain is used here as a morphotectonic term to describe all the topographic elements that create the distinctive transform morphology; strike-slip tectonism takes place

Scanner slave and pdf file editor's note:

The pages in the library shelf copy of the MS thesis text of Chapters I and II, including especially the figures, were made from photocopies of carbon copies, or multiple generation photocopies and, as can be seen from the samples of the first and last pages of those two chapters included in this file, are consequently quite difficult to read in most parts. The details of the figures and photos, in particular, are degraded; compare for example the diagram for Figure 10b of Chapter I (page 48 from the thesis) reproduced on the page following this note, and the identical, but much more readable figure (page 36 of this pdf file) in the following material derived from the published paper, of which the thesis Chapter I text was the submitted manuscript. The same explanation applies to the presentation of Chapter II in this pdf file version of the MS thesis. The text pagination table of contents given in the introductory matter applies to the original and has not been modified to fit, and therefore does not match, this pdf file version.

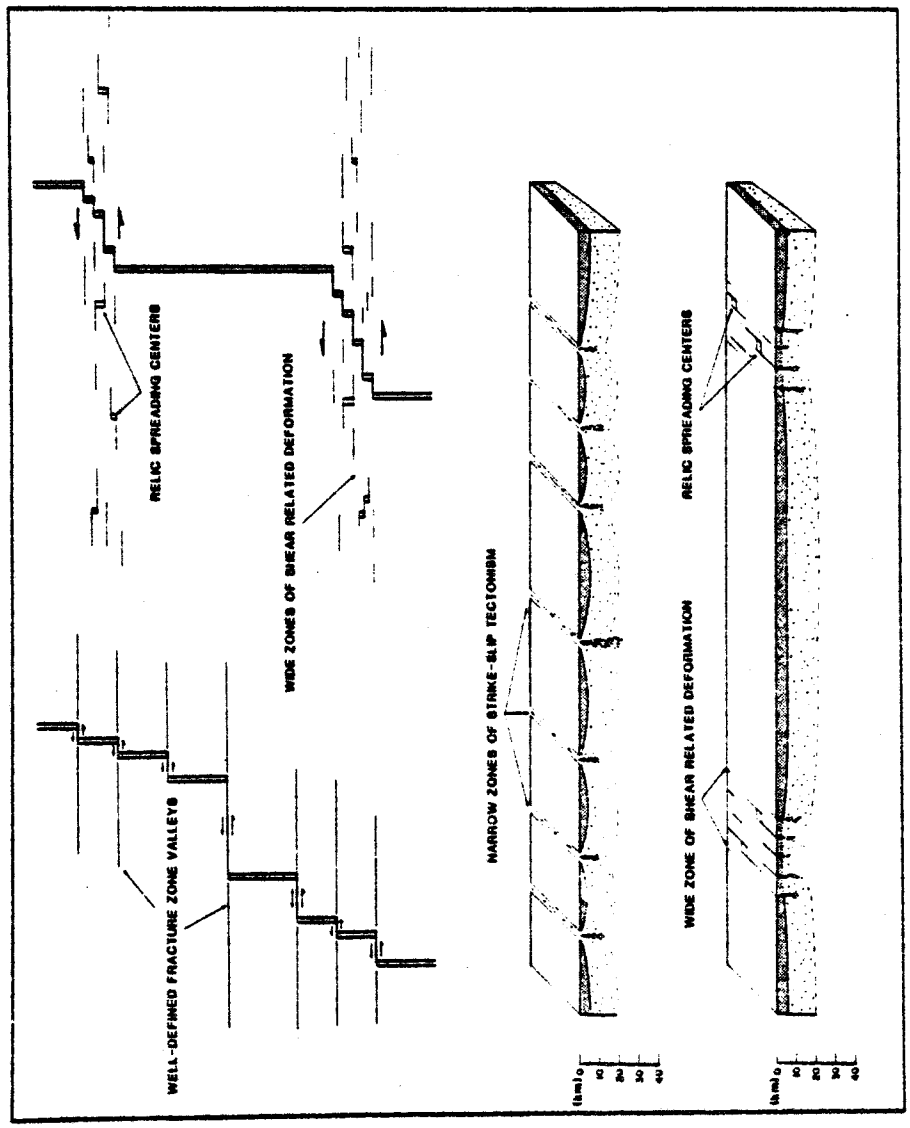
RELIC SPREADING CENTERS
WIDE ZONES OF SHEAR RELATED DEFORMATION
WELL-DEFINED FRACTURE ZONE VALLEYS
NARROW ZONES OF STRIKE-SLIP TECTONISM
RELIC SPREADING CENTERS
WIDE ZONE OF SHEAR RELATED DEFORMATION
(km)
0
10
20
30
40
(km)
0
10
20
30
40

Figure 10

INTRODUCTION: RIDGE–TRANSFORM–RIDGE PLATE BOUNDARIES

First-order relationships

Compilations of reconnaissance bathymetric data of the oceans (e.g. Menard and Chase, 1970; physiographic map of Heezen and Tharp, 1977) and earthquake epicenter maps (e.g. Barazangi and Dorman, 1969) document that transform faults routinely offset the axis of the world-encircling Mid-Oceanic Ridge System. The distribution of transforms along the axis of the ridge, however, is not uniform. For example, along the axis of the slowly accreting Mid-Atlantic Ridge south of the Azores, transforms offset the axis every 50 km to 100 km (Fox et al., 1969; Johnson and Vogt, 1973; Collette et al., 1974; Phillips and Fleming, 1978) whereas along the rapidly accreting East Pacific Rise transforms occur infrequently and are located several hundreds of kilometers apart (Mammerickx and Smith, 1978). The offset lengths of these transforms range from several kilometers (i.e. Kurchatov Transform —Searle and Laughton, 1977) to well over 100 km (i.e. Equatorial transforms— Heezen et al., 1964; Van Andel et al., 1967) and the transform domain is composed of linear topography that is parallel with the strike of the transform fault. (The term transform domain is used here as a morphotectonic term to describe all the topographic elements that create the distinctive transform morphology; strike-slip tectonism takes place within the domain but may be confined to a relatively narrow zone.) This distinctive transform topography can be traced away from the crest of the Mid-Oceanic Ridge across its flanks suggesting that the properties of oceanic lithosphere created within and proximal to a transform boundary contrast in some fundamental way with "normal" lithosphere.

Kinematic considerations mandate that strike-slip tectonism must be associated with transform boundaries (Wilson, 1965; Sykes, 1967). The total accretion rate of ridge segments varies from less than 2 cm/yr to approximately 18 cm/yr and, therefore, the slip-rate of transforms offsetting these ridge axes will vary accordingly. With slip rates varying by a factor of 10, the style, timing and intensity of deformation developed within and along the transform are likely to change in a progressive and systematic way as rates of slip range from low to high values (Fig. 1).

Geometric considerations of transforms coupled with the monotonic thickening of oceanic lithosphere with age (e.g. Parker and Oldenburg, 1973) indicate that a cold edge of lithosphere will be juxtaposed against the truncated axis of accretion at a ridge–transform intersection. The thickness of a truncating edge of lithosphere will

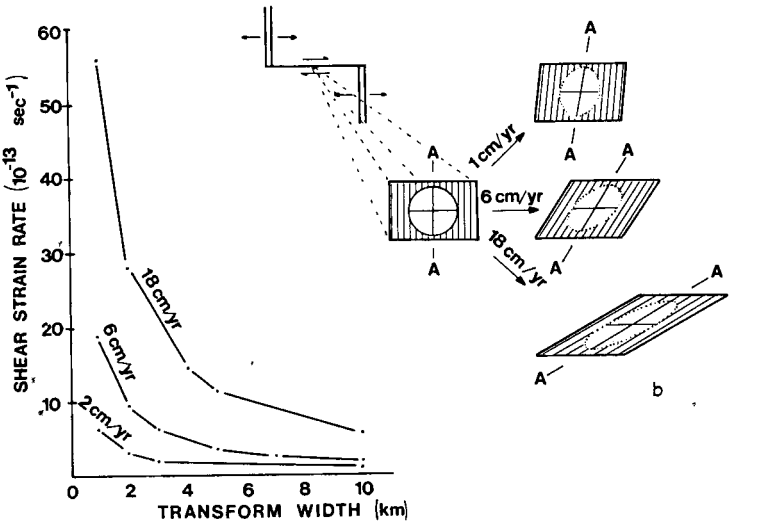

Fig. 1. a. Diagram depicting how shear strain rate changes as a function of the width over which shear displacement occurs for a range of transform slip-rates. Field studies suggest that shear displacements for oceanic transforms are confined to a narrow interval (2–4 km; e.g. Eittreim and Ewing, 1975; ARCYANA, 1975; Choukroune et al., 1978; CYAMEX and Pastouret, 1981; Castillo et al., 1982; OTTER, 1984). b. Schematic illustration showing relative shear deformation of a rectangle during the same time interval with different slip-rates. Numbers at right give percentage of extension along line $A-A$.

depend on its age which will vary as a function of the transform slip rate and the length of the transform offset. Ridge axis segments with low accretion rates (1–2 cm/yr) that are terminated by large-offset transforms (80–300 km) will be juxtaposed against evolved lithosphere that is several tens of kilometers thick but the contrast in the thickness of lithosphere across a ridge–transform intersection will decrease markedly as the rate of accretion increases.

It seems intuitively clear that, in the simplest case, the distinctive morphotectonic fabric of the transform domain must be a product of the complex interplay between strike-slip tectonism and the effects of juxtaposing a cold edge of lithosphere against an accreting plate boundary. The structural and petrologic manifestations of this tectonic process will be spatially variable because at one end of the spreading-rate spectrum there are ridge–transform–ridge (R–T–R) plate boundaries that are characterized by very low slip rates (< 2 cm/yr) and that have relatively thick edges of lithosphere (> 30 km) at the ridge–transform intersections. In contrast, at the other end of the spreading spectrum, the R–T–R boundaries are slipping at 18 cm/yr and relatively thin edges of lithosphere (< 15 km) are juxtaposed against a ridge axis at a transform boundary. We suggest that the morphology and the constitution of the oceanic lithosphere within the transform domain change in a systematic manner and that this variation can be related to changes in the kinematic and geometric parameters outlined above.

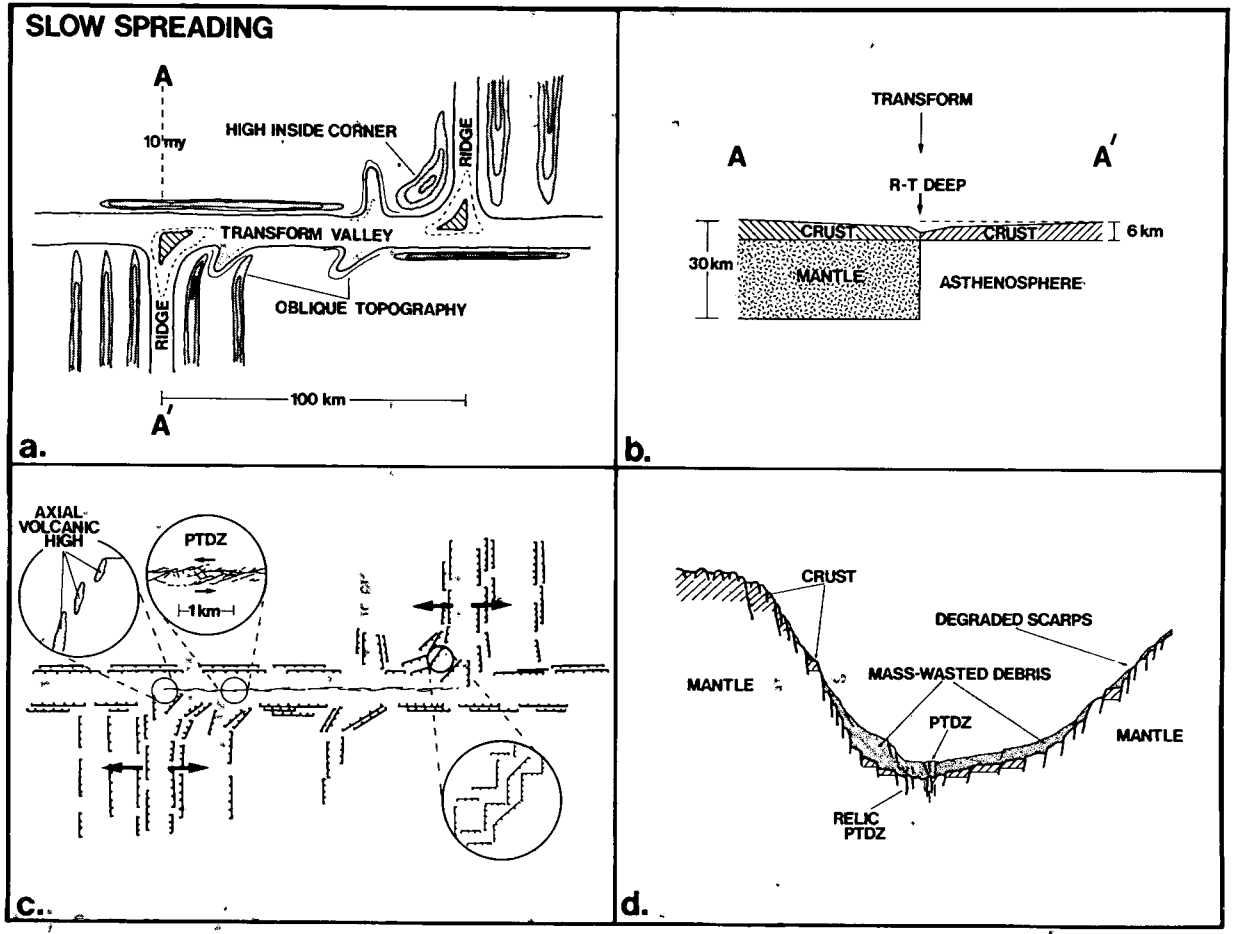
SLOW SPREADING
A
10 my
HIGH INSIDE CORNER
RIDGE
TRANSFORM VALLEY
OBLIQUE TOPOGRAPHY
RIDGE
100 km
A'
a.
TRANSFORM
A
A'
R-T DEEP
CRUST
CRUST
6 km
30 km
MANTLE
ASTHENOSPHERE
b.
AXIAL VOLCANIC HIGH
PTDZ
1 km
c.
CRUST
DEGRADED SCARPS
MANTLE
MASS-WASTED DEBRIS
PTDZ
MANTLE
RELIC PTDZ
d.

CHARACTERISTICS OF RIDGE–TRANSFORM–RIDGE PLATE BOUNDARIES

Slowing-slipping transforms

Bathymetric maps of slowly-slipping transform faults (full rate 1.5–5 cm/yr) with variable lengths (e.g. Heezen et al., 1964; Heezen and Tharp, 1965; Van Andel et al., 1967; Fox et al., 1969; Collette et al., 1974; Phillips and Fleming, 1978; Searle, 1981) demonstrate that these plate boundaries exhibit a similar morphotectonic fabric but the relief, scale and gradients of the terrain elements which characterize these tectonic domains vary systematically with changing length of transform offset: the larger the length of the transform the more dramatic the topography. All slowly-slipping transform faults are characterized by topographic lineaments that strike at a high angle to regional magnetic isochrons (Fig. 2a), and these topographic features, linear ridges and valleys, and aligned closed basins and conical peaks, fall within a transform domain; the scale of the topographic features and the width of the domain vary as a function of transform length. The most striking feature of a slowly-slipping transform domain is the broad, anomalously deep valley that is defined by inward-facing and opposing walls which rise up and away from an axis of maximum depth producing relief of 1000–5000 m. Small-offset (< 30 km) transforms like Transform A (Renard et al., 1975; Phillips and Fleming, 1978) and Kurchatov (Searle and Laughton, 1977) have relief of approximately 1500 meters contrasting markedly with the several thousands of meters of relief developed within the transform domain of large-offset (> 100 km) transforms like the Romanche (Heezen et al., 1964), Vema (Van Andel et al., 1971), Kane (Fox, 1972; Purdy et al., 1979) or Oceanographer (Fox et al., 1969; Schroeder, 1977; Fox et al., 1984).

The lower portions of the walls of slowly-slipping transforms are parallel with the regional transform fabric but at higher levels on the walls ridge-axis trends are often observed. Ridge-flank topography, made up of ridges and troughs, can be traced towards the transform over distances of tens of kilometers and as the transform is

---

Fig. 2. a. First order morphotectonic elements associated with slowly-slipping (< 6 cm/yr) ridge–transform–ridge (R–T–R) plate boundaries.

b. Schematic cross-section of the oceanic lithosphere proximal to a 100 km offset slowly-slipping ridge–transform intersection. Location of cross-section $A-A$ is given in Fig. 2a. Thickness of lithosphere is calculated as a function of age (e.g. Parker and Oldenburg, 1973); edge effect complexities are ignored.

c. Structural grain of slowly-slipping R–T–R plate boundary. Note that the ridge generated structures facing the transform become progressively more oblique with proximity to the transform over distances of 10–25 km (e.g. Searle and Laughton, 1977; Schroeder, 1977; Searle, 1979).

d. Schematic geologic cross-section across a slowly-slipping transform boundary based on submersible and high resolution bathymetric studies of North Atlantic transforms (OTTER, 1984; ARCYANA, 1975; Choukroune et al., 1978; VE = 4 : 1). Small throw, inward facing dip-slip faults create relief of transform valley; principal transform displacement zone (*PTDZ*) defined by a narrow belt of deformation centered about axis of maximum depth.

approached it is common, but not always the case, for the sea floor to deepen and for the orientation of the ridges and troughs to become oblique to the strike of the rise axis, swinging into the direction of strike-slip motion (Fig. 2a, c; Whitmarsh and Laughton, 1975, 1976; Searle and Laughton, 1977; Schroeder, 1977; Searle, 1979; 1981; Fox et al., 1984). At each ridge–transform intersection one flank of the ridge is accreted against the aseismic limb of a fracture zone never experiencing strike-slip related tectonism (the term fracture zone is used to include the transform and the aseismic limbs). Ridge-generated terrain in this environment is truncated abruptly by the aseismic limbs of the fracture zone, and the sea floor generally deepens, but there is little or no change in trend of the ridge axis parallel terrain as the fracture zone is approached (Fig. 2a, c; Searle and Laughton, 1977; Searle, 1979, 1981). Within some fracture zones long, linear ridges, trending parallel with the regional trend of the fracture zone, rise above the surrounding sea floor to create discontinuous ribbons of anomalously shallow topography; these ridges are thought to be composed predominantly of serpentinized ultramafic rocks and have probably evolved by diapirism of serpentizined blocks (Bonatti, 1976, 1978; Fox et al., 1976; Bonatti and Hamlyn, 1978; Bonatti and Chermak, 1981; Francis, 1981; OTTER, 1983).

The valley walls of slowly-slipping transforms develop regional gradients of 20°–30°, have relief on the order of a few to several thousand meters (e.g. Heezen and Tharp, 1965; Fox et al., 1969) and expose basalts, gabbros, ultramafics and their metamorphic equivalents (e.g. Miyashiro et al., 1969; Bonatti et al., 1970; Melson and Thompson, 1971). The relief of the transform valley is, however, not produced by a few, large-throw faults which provide tectonic windows into the foundation of the oceanic crust (ARCYANA, 1975; Francheteau et al., 1976; Fox et al., 1980) but rather these regionally steep slopes are the product of a very large number of inward-facing escarpments with relief of a few hundred meters or less that integrate spatially to create a deep valley (Detrick et al., 1973; ARCYANA, 1975; Francheteau et al., 1976; Choukroune et al., 1978; Searle, 1979, 1981; OTTER, 1980, 1984; D. Needham, unpublished SEA BEAM data). Deep-sea submersible investigations of the 3000 m high north and south walls of the Oceanographer Transform have found that the axis and the lower flanks of the transform valley are choked with an admixture of pelagic debris and talus creating steep (10°–30°) slopes that dip towards the axis (Fig. 2d; OTTER, 1980, 1984). At higher elevations on the walls, near-vertical, laterally discontinuous scarps expose predominantly gabbroic or ultramafic rocks, and have relief of several meters to a few hundred meters. These inward-facing outcrops have been badly incised and modified by mass-wasting; the scarps have orientations that are variable ranging from transform parallel to ridge-axis parallel (OTTER, 1984). The scarps are linked by steeply-dipping (20°–40°), semi-consolidated wedges of sediment creating a blanket that laps up, in an undisturbed fashion, against and around rock outcroppings.

Apart from the occasional rock fall and minor differential subsidence (Delong et

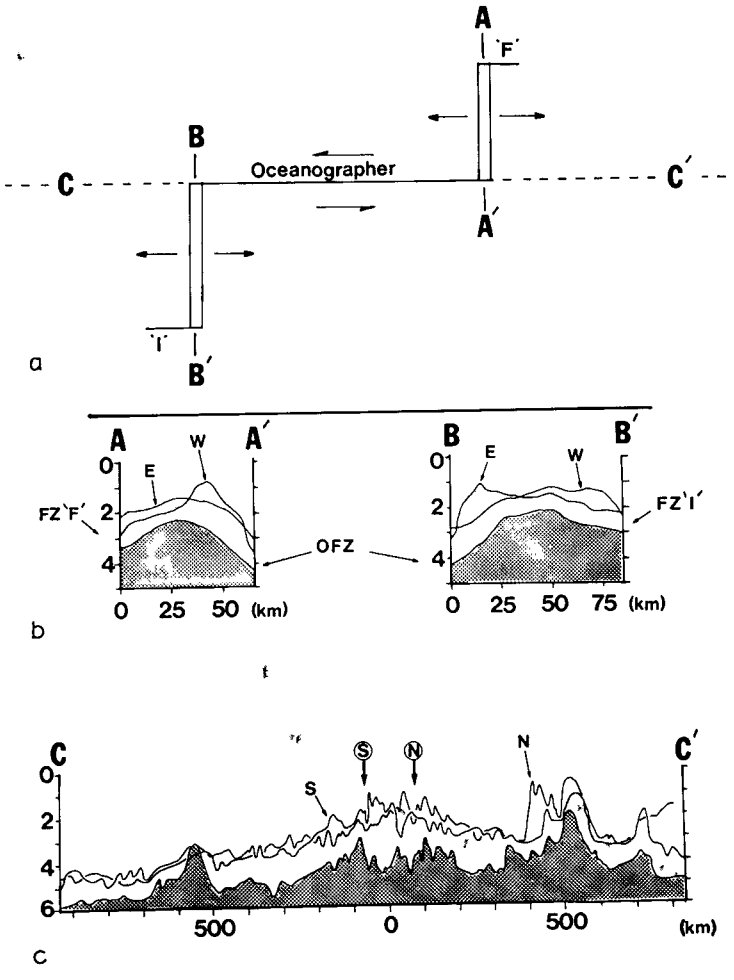

Fig. 3. a. Ridge–transform plate geometry shown for the Mid-Atlantic Ridge at 35°N including the Oceanographer, F and I transforms. Locations of cross-sections shown below are indicated by $A-A'$, $B-B'$ and $C-C'$.

b. Topographic cross-sections down the ridge axis segments to the north and south of Oceanographer. Shaded areas indicate depth to the floor of the rift valley along strike; E and W denote depths to crestal mountains on eastern and western side of ridge. Note that the change in depth toward the bounding transforms is greatest toward the large-offset (128 km) Oceanographer and less towards the shorter offset (< 30 km) transforms (Schroeder, 1977; Fox et al., 1984).

c. Profile $C-C'$ indicates maximum depth to basement along axis of the Oceanographer Fracture Zone (shaded). Lines N and S indicate depths to the crest of the bounding fracture zone walls (N for North and S for South); N and S (circled) give the location of the northern and southern ridge–transform intersections. Apart from two seamount complexes located approximately 500 km away from the ridge–transform intersections, the aseismic limbs of the fracture zone deepen with increasing age and the floor of the fracture zone is always deeper than flanking sea-floor.

al., 1977, 1979) slowly-slipping transform valley walls appear to be devoid of tectonic activity. Direct evidence for recent tectonic activity within both Transform A and the Oceanographer Transform, including recent near-vertical fault traces and fresh rubble, is confined to a narrow zone only a few hundred meters to a few kilometers wide that is centered about the axis of maximum depth (Fig. 2c; ARCYANA, 1975; Choukroune et al., 1978; OTTER, 1984). This narrow belt of complex and rapidly evolving terrain, disrupted by an anastomsing network of faults, is assumed to mark the location of the principal transform displacement zone (PTDZ) and represents the shallow level manifestations of strike-slip tectonism (Fig. 2c, Choukroune et al., 1978; OTTER, 1984).

Mapping of ridge segments proximal to slowly-slipping transform boundaries shows that over distances of 20–40 km the rift-valley floor slopes towards the closed-contour deep of the ridge–transform intersection with regional gradients of 1°–2° and elevation changes of 500–1500 m (Fig. 3; Needham and Francheteau, 1974; Macdonald and Luyendyk, 1977; Ramberg and van Andel, 1977; Schroeder, 1977; Phillips and Fleming, 1978; Fox et al., 1984). The larger the transform offset, the greater the change in the along-strike relief of the rift valley floor (Fig. 3). Furthermore, as the transform boundary is approached, the strike of the rift valley wall that is truncated by the transform becomes oblique with respect to the orientation of the rift valley (Fig. 2a, c), whereas the trend of the opposing rift wall parallels the strike of the rift valley and is unchanged with increasing proximity to the aseismic limb of the fracture zone (Whitmarsh and Laughton, 1975, 1976; Schroeder, 1977; Phillips and Fleming, 1978; Searle, 1979; Karson and Dick, 1983; OTTER, 1983a; K. Macdonald and P. Fox, unpublished Deep Tow data—Vema Transform).

Deep-towed camera and submersible investigations of the relationships developed at the eastern intersection of the Oceanographer Transform with the MAR indicate that the morphology of the rift valley is shaped by a distinctive fault pattern and by vigorous mass wasting of basement outcroppings (OTTER, 1983). Along the floor of the rift valley, over a distance of 10–20 km, the orientation of faults, fissures and volcanic ridges becomes increasingly more complex with proximity to the transform. Although the ridge-axis parallel orientations are still apparent, transform parallel structures and structures oblique to both the ridge and transform are recognized. The oblique structures are concentrated on the transform side of the rift floor and become more oblique with respect to the ridge axis as the transform boundary is approached mimicking the morphologic grain shown on surface-ship derived bathymetric maps (Fig. 2a, c). The structural fabric of the rift floor is rapidly modified, and obscured by degradation of bedrock exposures as the products of mass wasting, talus wedges and debris fans fill depressions, abut rock escarpments and smooth the terrain.

As parcels of crust and associated sediment leave the rift floor to create the distinctive inward facing steps of the rift valley walls the polarized structural fabric

developed on the rift floor is preserved. The morphology of the rift flank that is terminated by the aseismic limb of the fracture zone is the product of inward facing scarps that approximately parallel the ridge axis along with broad, sedimented slopes that dip steeply (10°–40°) towards the rift axis (Karson and Dick, 1983; OTTER, 1983). The morphology of the opposite wall, the transform side of the accreting plate boundary, is made up of a series of inward facing escarpments, exhibiting a range of orientations, that is linked by steeply dipping sediment slopes. Oblique trending escarpments as well as E–W and N–S striking scarps intersect to create the overall oblique trend of the rift wall (Fig. 2c). Irrespective of orientation, however, no evidence for strike-slip displacement is observed on the escarpments and evidence for normal (dip-slip) displacement is ubiquitous regardless of scarp orientation (Karson and Dick, 1983; OTTER, 1984).

Geophysical evidence indicates that the velocity structure and distribution of mass of the oceanic crust and upper mantle within the slowly-slipping fracture zone domain contrast with the properties of "normal" oceanic lithosphere. Gravity data indicate that large mass anomalies are often associated with fracture zones (Cochran, 1973; Robb and Kane, 1975; Sibuet and Veyrat-Peiney, 1980; Louden and Forsyth, 1982). These data have been interpreted in contrasting ways. In one instance, mass anomalies are thought to reflect the existence of upper mantle rocks at relatively shallow crustal levels (Cochran, 1973; Robb and Kane, 1975) but, in another model, mass anomalies are not required if mantle density is allowed to change with age across the fracture zone (Sibuet and Veyrat-Peiney, 1980). The fundamental unconstrained nature of gravity data makes it difficult to arrive at a unique solution but it seems clear that the mass distribution in and around fracture zones is heterogeneous disrupting the gravity anomaly pattern characteristic of "normal" oceanic lithosphere (Louden and Forsyth, 1982).

Seismic refraction experiments along the large offset fracture zones (Kane—Detrick and Purdy, 1980; Cormier et al., 1983; Oceanographer—Sinha, 1981; Sinha and Louden, 1981, 1983; and Vema—Detrick et al., 1982) reveal anomalous crustal structure. The Kane fracture zone is characterized by crustal thicknesses of only 2–3 km and the crust exhibits low compressional wave velocities. Proximal to the Oceanographer fracture zone refraction data indicate that the crust thins towards the fracture zone, and within the fracture zone there is evidence for very thin crust with anomalously low velocities (Sinha and Louden, 1983). The thickness of the oceanic crust within the Vema fracture zone is not anomalously thin but the compressional wave velocities observed for the crustal arrivals are anomalously low suggesting that the seismically defined crust is comprised predominantly of sheared and hydrated upper mantle rocks (Detrick et al., 1982). A seismic refraction experiment designed to investigate the velocity structure of a small offset (15 km) fracture zone suggests that anomalously high velocities (7.3–7.6 km/s) are found at shallow crustal levels (< 2 km) along the fracture zone (White and Matthews, 1980).

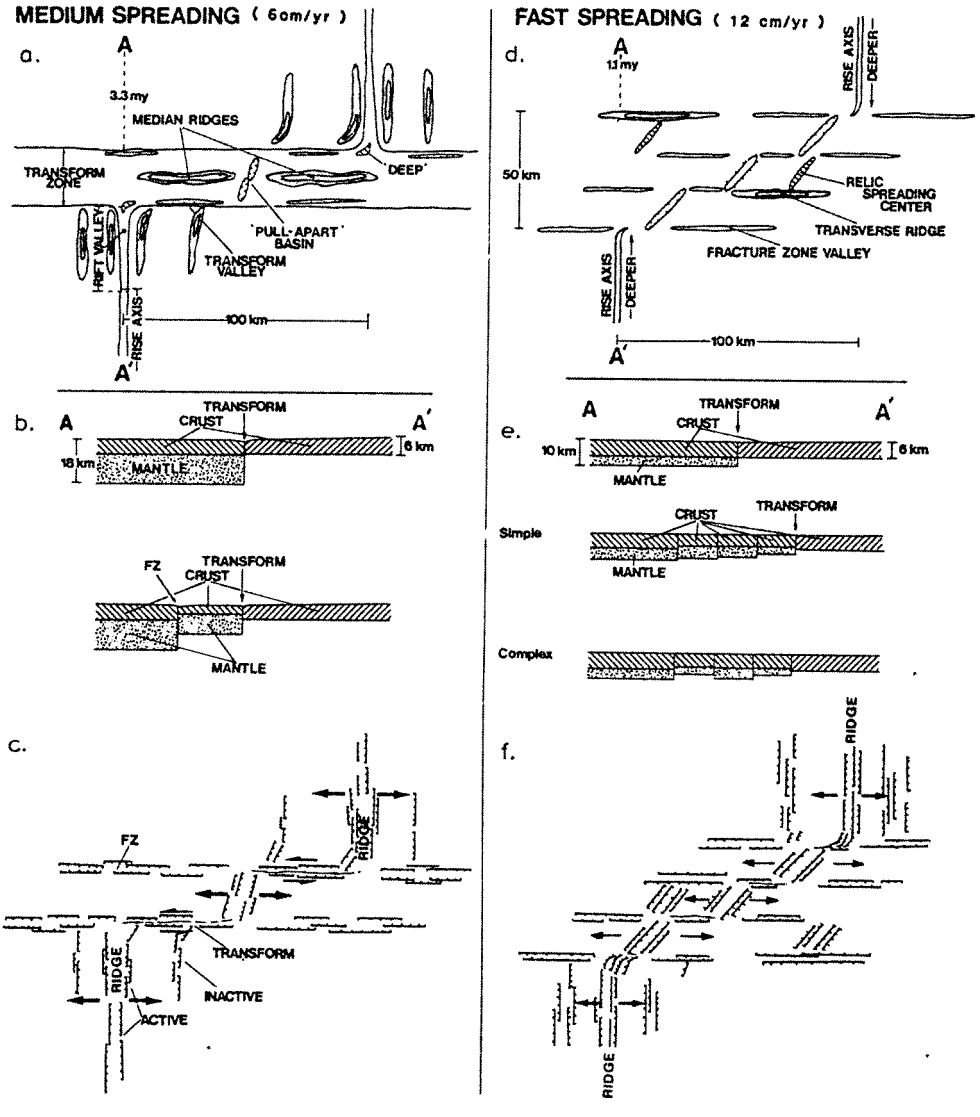

Fig. 4. a. First-order morphotectonic elements associated with a medium slip-rate (6–12 cm/yr) ridge–transform–ridge plate boundary.

b. Schematic cross-section of the oceanic lithosphere proximal to a medium slip-rate ridge–transform intersection. Location of cross-section $A-A'$ is given in Fig. 4a. Two possible cross-section geometries are shown: one depicts the simplest case where the transform is defined by a single shear zone (this geometry not shown in 4a); the other is a more complex geometry that would evolve if sea floor within the transform domain is created along a short extensional relay zone (reference Fig. 4a and 4c). Thickness of lithosphere is calculated as a function of age (e.g. Parker and Oldenburg, 1973); edge effect complexities are ignored.

c. Structural grain of a medium slip-rate R–T–R plate boundary. Ridge axis swings sharply into

Medium slip-rate transforms

The regional, morphotectonic fabric of medium slip-rate transforms (6–12 cm/yr) and adjoining ridge segments have not been as well investigated as their slowly-slipping counterparts. Recconnaissance studies, however, of the Tamayo (Kastens et al., 1979), Rivera (Reid, 1976; Prothero and Reid, 1982), Inca (Embley et al., 1984), Orozco (Trehu, 1982) and Siqueiros (Crane, 1976) transforms demonstrate that the transform domains of these plate boundaries exhibit many of the same morphotectonic relationships as their slowly-slipping counterparts, but the scale of the features is diminished and in some ways the tectonic pattern appears to be more complex when viewed along strike of the transform. The depth to the ridge axis increases towards the transform and the axis of the ridge sometimes terminates in a small, closed-contour nodal basin at the ridge–transform intersection (Fig. 4a; Macdonald et al., 1979; Tamayo Tectonic Team, 1983) but, in contrast to slowly-slipping ridge-transform intersections, the change in relief along the ridge axis is only a few hundred meters and the nodal basin is small (Fig. 4a). In the case of the Tamayo Transform, which is only slipping at 6 cm/yr, the morphology of the axis of the East Pacific Rise, over a distance of 30 km, evolves from a broad, gently-rifted swell into a shallow rift valley as the Tamayo Transform is approached (McClain and Lewis, 1980; Macdonald et al., 1979). The same structural fabric and relationships that are characteristic of slowly slipping R–T intersections are found to be associated with the medium slip rate R–T intersections (compare Fig. 2c with Fig. 4c; Tamayo Tectonic Team, 1983). The development of well defined rift valley morphology, however, is not recognized at faster-slipping ridge–transform intersections (> 8 cm/yr full rate; K. Macdonald and P. Fox, unpublished SEA BEAM data). Furthermore, at these faster slipping ridge–transform intersections structures on both sides of the ridge axis develop oblique trends progressively as the transform

---

transform over a distance of several kilometers; principal transform displacement zone is characterized by two shear zones linked by an extensional relay zone.

d. First-order morphotectonic elements associated with a fast-slipping (12–18 cm/yr) ridge–transform–ridge plate boundary.

e. Schematic cross-section of the oceanic lithosphere proximal to a fast-slipping ridge–transform intersection. Location of cross-section $A-A'$ is given in Fig. 4d. Three plate geometries are shown: the first assumes that the transform is defined by a single shear zone that links the two offset ridge axes (this geometry is not shown in Fig. 4d); the second assumes that the transform is characterized by a shear zone with a complex but stable geometry made up of strike-slip strands linked by right stepping extensional relay zones; the third assumes that the shear zone geometry of strike-slip strands and extensional relay zones is not stable in time and therefore the thickness of the lithosphere across the transform zone is variable.

f. Structural grain of a fast-slipping R–T–R plate boundary. Ridge axis swings very sharply into transform over a distance of several kilometers; principal transform displacement zone is characterized by several shear zones linked by extensional relay zones.

boundary is approached but only over distances ranging from several kilometers to 10 km; the larger the transform offset and/or the greater the slip-rate, the more apparent the development of oblique trends (Fig. 4f; Crane, 1976; K. Macdonald and P. Fox, unpublished SEA BEAM data for Rivera, Orozco, Clipperton and Siqueiros transforms). Deep-tow and submersible investigations at the Tamayo–East Pacific Rise intersection indicate that the oblique trending faults found at the ridge–transform intersection accommodate only dip-slip motion and that the transition from accretion related tectonics to strike-slip dominated processes is very narrow (< a few km; Macdonald et al., 1979; Tamayo Tectonic Team, 1983). At the present time we have no constraints on the motion of the oblique faults found at faster slipping ridge–transform intersections.

The transform domain of a medium slip-rate transform is often 20–30 km wide and is comprised of elongate ridges and troughs that strike at a high angle to the ridge axis and that develop relief, in general, of a few hundred to a thousand meters (Fig. 4a). These ridges and troughs are discontinuous and are sometimes interrupted by anomalously deep (3–4 km) basins and scarps striking at an angle oblique to the trend of the transform (e.g. Tamayo—Macdonald et al., 1979; Kastens et al., 1979; Orozco—Trehu, 1982). Submersible investigations at the Tamayo Transform document that evidence for recent tectonism within the transform domain is confined to a very narrow belt less than a kilometer wide and this interval is taken to represent the principal transform displacement zone (CYAMEX and Pastouret, 1981; Tamayo Tectonic Team, 1983). This zone is offset along strike, however, appearing to be displaced by an extensional relay zone or pull-apart basin that is located along the center of the transform (Fig. 4c). It is in this area that piercement structures (diapirs) are seen to protrude up and, in one case, through, the sedimentary fill of the transform (Macdonald et al., 1979). In addition, extensional relay zones have been predicted to exist within the Rivera (Prothero and Reid, 1982) and Orozco (Trehu, 1982; K. Macdonald and P. Fox, unpublished SEA BEAM data) transforms based on a distinctive pattern defined by earthquake epicenters and topography.

The Clipperton Transform (12 cm/yr slip rate), which offsets the East Pacific Rise 80 km in a right-lateral sense (in contrast to the other major transforms of the East Pacific Rise which all offset the axis in a left-lateral sense), is the one transform that does not exhibit a morphotectonic pattern suggestive of strike-slip zones linked by an extensional relay zone. Although the transform domain is typically wide (20 km) along most of its length, recently acquired SEA BEAM and SEA MARC I side scan data (P. Fox, K. Macdonald and W. Ryan, unpublished data) indicate that the truncated rise axis tips have propagated towards each other narrowing the transform domain. SEA MARC I data also define a narrow (< 1 km) belt of disturbed terrain disrupted by discontinuous and anastomosing transform parallel faults that can be traced in a direct line from one ridge tip to another.

With the exception of the deep basins that are oblique to the grain of the transform, the relief of medium slip-rate transforms is generally only several

hundred meters to approximately one thousand meters and *in situ* investigations of this terrain indicate that small-throw faults (< 100 m) integrate spatially to create steep regional slopes (Macdonald et al., 1979; CYAMEX and Pastouret, 1981; Tamayo Tectonic Team, 1983; Embley et al., 1984). Fine-grained extrusive basaltic rocks are recovered in abundance from these slopes (e.g. Batiza et al., 1977; Fornari et al., 1983; Tamayo Tectonic Team, 1983) suggesting that the processes associated with the development of medium slip-rate transforms do not lead to the routine exposure of deep-seated rocks (e.g. gabbroic and ultra-mafic rocks). In one instance, however, gabbros, serpentinized ultramafic rocks and mafic breccias have been recovered from fracture zone escarpments that offset the Galapagos Rise (Nishimori and Anderson, 1973). Seismic refraction experiments show that the oceanic crust associated with the Tamayo Transform (McClain and Lewis, 1980) and Orozco (Trehu, 1982; Ouchi et al., 1982) is 1–3 km thinner than normal oceanic crust, but these results do not indicate the extreme crustal thinning thought to be typical of slowly-slipping transforms (Detrick and Purdy, 1980; Fox et al., 1980; Stroup and Fox, 1981).

Fast-slipping transforms

The morphology and salient tectonic elements of fast-slipping transforms (12–18 cm/yr) have been poorly known until very recently. Compilations of reconnaissance data (Mammerickx and Smith, 1978; Lonsdale, 1978; Kureth and Rea, 1981; Rea, 1981) reveal that several large-offset transforms (Quebrada–Gofar System between 3°30′S and 4°40′S; Wilkes at 9°S; Garret at 12°S) are found to disrupt the axis of the East Pacific Rise along the Nazca–Pacific plate boundary, the fastest accreting ridge segment in the world. These transforms are composed of wide zones of discontinuous ridges and troughs that generally develop several hundred to a few thousand meters of relief (Figs. 4d, f). The Quebrada–Gofar transform system offsets the ridge axis a total of 390 km and can be best described as a 150 km-wide shear zone that is made up of a large number of short transforms that are linked together by short, oblique trending, extensional relay zones (Fig. 4d, Lonsdale, 1978; Searle and Francis, 1982; Searle, 1983). The Wilkes Transform offsets the rise axis 200 km and defines a 100 km wide interval of complexly arranged ridges and troughs; Kureth and Rea (1981) present a tectonic model based on bathymetric and magnetic data proposing that the transform domain is characterized by two shear zones linked by an extensional relay zone.

A Deep Tow survey of a 15 km^2 portion of the Quebrada Transform near its eastern intersection with the EPR axis defines a single narrow (< 200 m) principal transform displacement zone lying along the north side of a 7 km wide transform trough (Lonsdale, 1978). The east–west trending grain of the transform trough is disrupted by structures that are 45° oblique to the transform and are interpreted to represent normal faults (Lonsdale, 1978). A reconnaissance map of the intersection

east of the Deep-tow survey shows that the axis of the rise crest bends sharply into the transform over a distance of a several kilometers and slopes into the transform trough (Lonsdale, 1978).

The morphology of the Garret Transform, the fastest-slipping large-offset (130 km) transform in the world, was essentially unmapped until recently when a reconnaissance SEA BEAM survey (P. Lonsdale, pers. commun., 1982) followed by a detailed SEA BEAM investigation (P. Fox, unpublished data) showed that the Garret is characterized by a 20–30 km wide transform domain made up of several short strike-slip segments that are linked by oblique-trending ridges interpreted to be extensional relay zones. These results as well as SEA BEAM crossings (P. Lonsdale, pers. commun., 1982) and GLORIA data (Searle, 1983) from the Wilkes and Quebrada–Gofar transforms suggest that fast-slipping transforms have a distinctive and diagnostic morphotectonic character, defined as a broad region of complex topography composed of swaths of transform-parallel ridges and troughs that are bounded by short oblique ridges and basins (Figs. 4d, f).

GEOLOGIC MODEL

The morphotectonic character exhibited by ridge–transform–ridge plate boundaries varies in a systematic way: the relief and scale of the terrain associated with the transform domain becomes better defined as the thickness of the truncating edge of lithosphere at the ridge–transform boundary increases (compare Figs. 2b, 4b, e). For example, at the eastern ridge–transform intersection of the Oceanographer Transform, lithosphere that is approximately 35 km thick is juxtaposed against the ridge axis (Fig. 5); in this tectonic environment, the depth to the nodal basin approaches 5000 m and the relief developed at the intersection approaches 4000 m. The Tamayo Transform, on the other hand, juxtaposes lithosphere that is only 15 km thick against the axis of the East Pacific Rise and, in this tectonic environment, the nodal basin is only 3400 m deep and the relief developed at the intersection is about 1000 m (Fig. 5). Well constrained bathymetric data do not exist for many ridge–transform intersections and, in the absence of these data, we have plotted the maximum depth measured at a number of ridge–transform intersections against the estimated thickness of lithosphere at that intersection (Fig. 6). The correlation is striking and supports our working hypothesis that the processes responsible for the formation and evolution of oceanic lithosphere proximal to ridge–transform plate boundaries are sensitive to the plate-thickness geometry (Fox et al., 1981).

Based on theoretical considerations that investigate the thermal conditions governing the accretion and evolution of oceanic lithosphere, investigators have proposed that slowly accreting plate boundaries (1–2 cm/yr full rate) are approaching a lower limit below which sea-floor spreading (i.e. the emplacement of basaltic melts at shallow crustal levels) can no longer take place (Sleep, 1975; Kusznir and Bott, 1976). Bottinga and Allègre (1978) have suggested that the slower advection

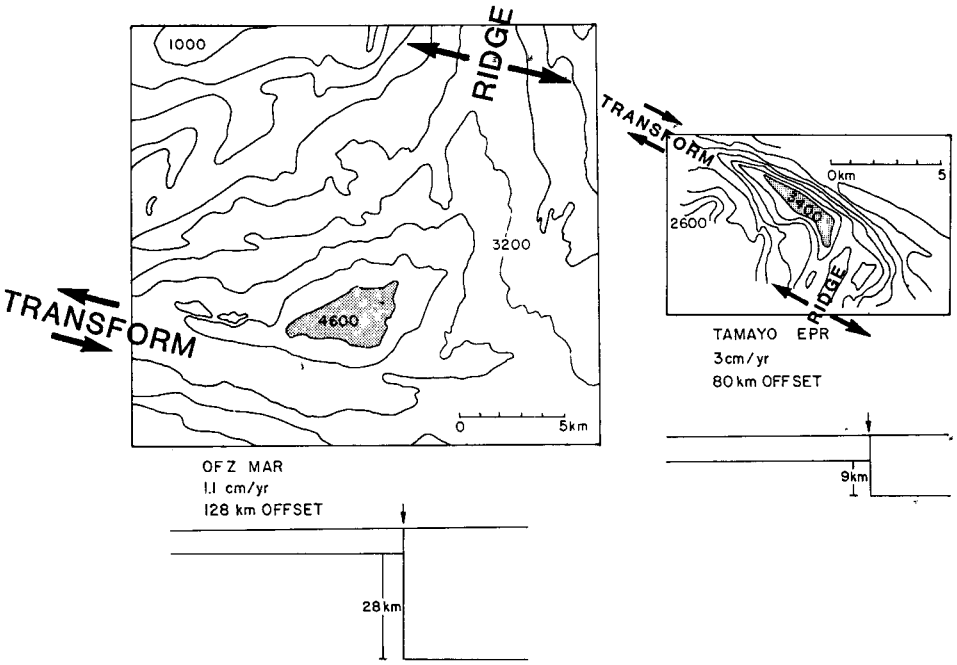

Fig. 5. Bathymetric comparison of two ridge–transform intersections (same scale) characterized by contrasting thicknesses of truncating lithosphere at the transform boundary. Oceanographer transform shown at left; Tanayo transform shown at right. Although the morphotectonic character of the two ridge–transform intersections is the same, the scale and relief of the topographic elements is much greater for the Oceanographer than for the Tamayo. Depth in meters.

beneath slowly spreading ridges results in lower temperatures and, as a result, less partial melt migrates to the surface to form oceanic crust. A compilation of seismic refraction data for segments of the Mid-Oceanic Ridge that exhibit different accretion rates suggests a correlation between total crustal thickness and spreading rate, with slower rates of spreading leading to the development of thinner crust (Reid and Jackson, 1981; Jackson et al., 1982). The results of these investigations are all consistent with the notion that at slow rates of accretion the processes leading to the generation and emplacement of basaltic melts are modified because of the cooler thermal environment governing the generation of oceanic lithosphere.

It seems intuitively reasonable to infer that the thermal environment beneath an accreting plate boundary will become even colder as a ridge–transform plate boundary is approached and a thick truncating edge of lithosphere, of variable thickness, is juxtaposed against an axis of accretion. We suggest that the result is the emplacement of oceanic lithosphere that contrasts markedly with lithosphere accreted at some distance from a ridge–transform intersection. The distance over which the properties of the oceanic lithosphere change with respect to a fracture zone will

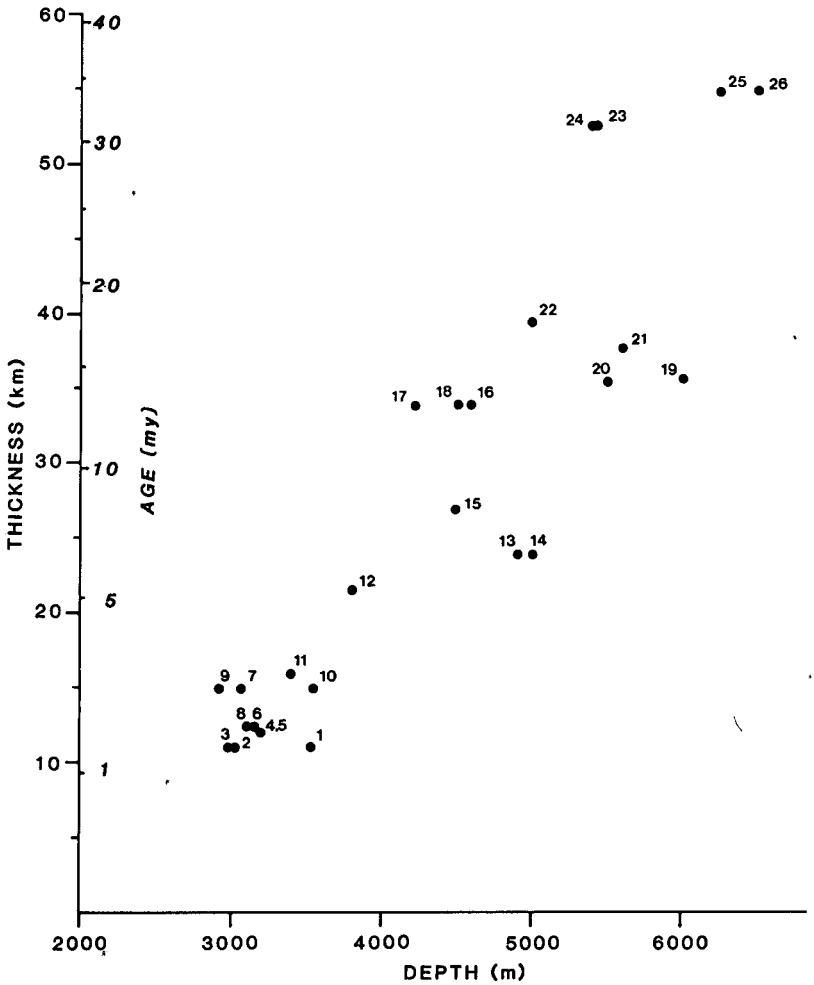

Fig. 6. Thickness of truncating lithosphere ($Z(t) = 9.4t^{1/2}$; Z = thickness in km and t = age in m.y.—Parker and Oldenburg, 1973) at various ridge–transform intersections plotted against the maximum depth observed at ridge–transform nodal deeps. Note the systematic increase in depth with increasing age of the truncating edge of lithosphere. Each dot defines a ridge–transform intersection, number by each dot keys these data to a list of locations and sources: *1*—eastern intersection of the 33°N Transform on the MAR (Naval Oceanographic Office, unpublished data, C. Smoot, pers. commun., 1982); *2*, *3*—Transform C (Phillips and Fleming, 1978); *4*, *5*-Kuchatov Transform (Searle and Laughton, 1977); *6*, *7*—Transform A (Phillips and Fleming, 1978); *8*, *9*—Transform B (Phillips and Fleming, 1978); *10*—Tamayo-EPR intersection (Tamayo Tectonic Team, 1983); *11*—Transform F (Phillips and Fleming, 1978); *12*—Blanco Transform eastern intersection with Gorda Ridge (Office of Naval Research unpublished data; C. Fox, pers. commun., 1982); *13*, *14*—Atlantis Transform on the MAR (Naval Oceanographic Office, unpublished data; C. Smoot, pers. commun., 1982); *15*—13°N Transform (Collette et al., 1974); *16*, *17*—Oceanographer Transform (Fox et al., 1969, Schroeder, 1977); *18*—Hayes Transform western intersection (Naval Research Lab, unpublished data; H. Fleming, pers. commun., 1980); *19*, *20*—Kane Transform (Fox, 1982; Purdy et al., 1978; Karson and Dick, 1983); *21*—Spitzbergen Transform

depend on the interplay of two factors: thickness of the edge of lithosphere that was juxtaposed against an axis of accretion at the time of formation and the thermal structure of the ridge segment in question (i.e. high accretion rate vs. a slow accretion rate). The cold edge of lithosphere that faces the axis of accretion across the transform lowers the temperature in the wedge of asthenosphere rising beneath the axis of accretion proximal to the plate boundary perturbing the processes of accretion.

Sleep and Biehler (1970) argued that the deep intersection depressions are the surface manifestation of viscous head loss experienced by the rising wedge of asthenosphere ascending beneath slowly-accreting plate boundaries immediately proximal to ridge–transform intersections. After emplacement this lost head is recovered as the depressed crust rises isostatically as it ages. Indeed, bathymetric data of well-mapped intersections (FAMOUS area—Phillips and Fleming, 1978; Oceanographer Transform—Fox et al., 1969; Schroeder, 1977; Kane Transform—Fox, 1972; Detrick and Purdy, 1980; Vema Transform–Needham, unpublished data; R. Prince, unpublished data) show that these nodal basins are short-lived and depths to basement initially decrease with distance from the depresion. An along-strike profile down the axis of the Oceanographer Fracture Zone illustrates how basement depths shallow rapidly away from these nodal basins (Fig. 3, profile *C*). Other deep basins are recognized along the transform axis of the Oceanographer Transform and these probably reflect expressions of vertical tectonism caused by aspects of strike-slip deformation (extensional and compressional relay zones) and/or differential hydration of blocks resulting in variable sepentinization of ultramafic rocks (Fox et al., 1976; Fox et al., 1984). The sides of the nodal basins flanking the aseismic limbs of the Oceanographer fracture zone reach a sill depth a few tens of kilometers from the ridge–transform depression and then the basement of the fracture zone floor deepens continuously with increasing age (Fig. 3, profile *C*). Independent of age, however, the depth to the axis of the fracture zone is always deeper than the adjacent oceanic lithosphere of equivalent age suggesting that some process, other than the isostatic considerations of viscous head loss, is operative along the transform.

Whitmarsh and Laughton (1976) suggested that fracture zone valleys associated with slowly-accreting plate boundaries are caused by a perturbation of volcanic processes proximal to the ridge–transform intersection due to the inhibiting effect of shear stresses focussed at the intersection and the reduced size of the magma chamber caused by the opposing edge of lithosphere. The recovery of gabbroic rocks

---

eastern intersection (Naval Research Lab., unpublished data; P. Vogt, pers. commun., 1983); *22*—15°N Transform (Collette et al., 1974); *23*, *24*—Vema Transform (unpublished SEA BEAM data; H. Needham, pers. commun., 1980); *24*—Oriente Transform–Cayman Ridge intersection (CAYTROUGH, 1979); *25*—Swan Transform–Cayman Ridge intersection (CAYTROUGH, 1979).

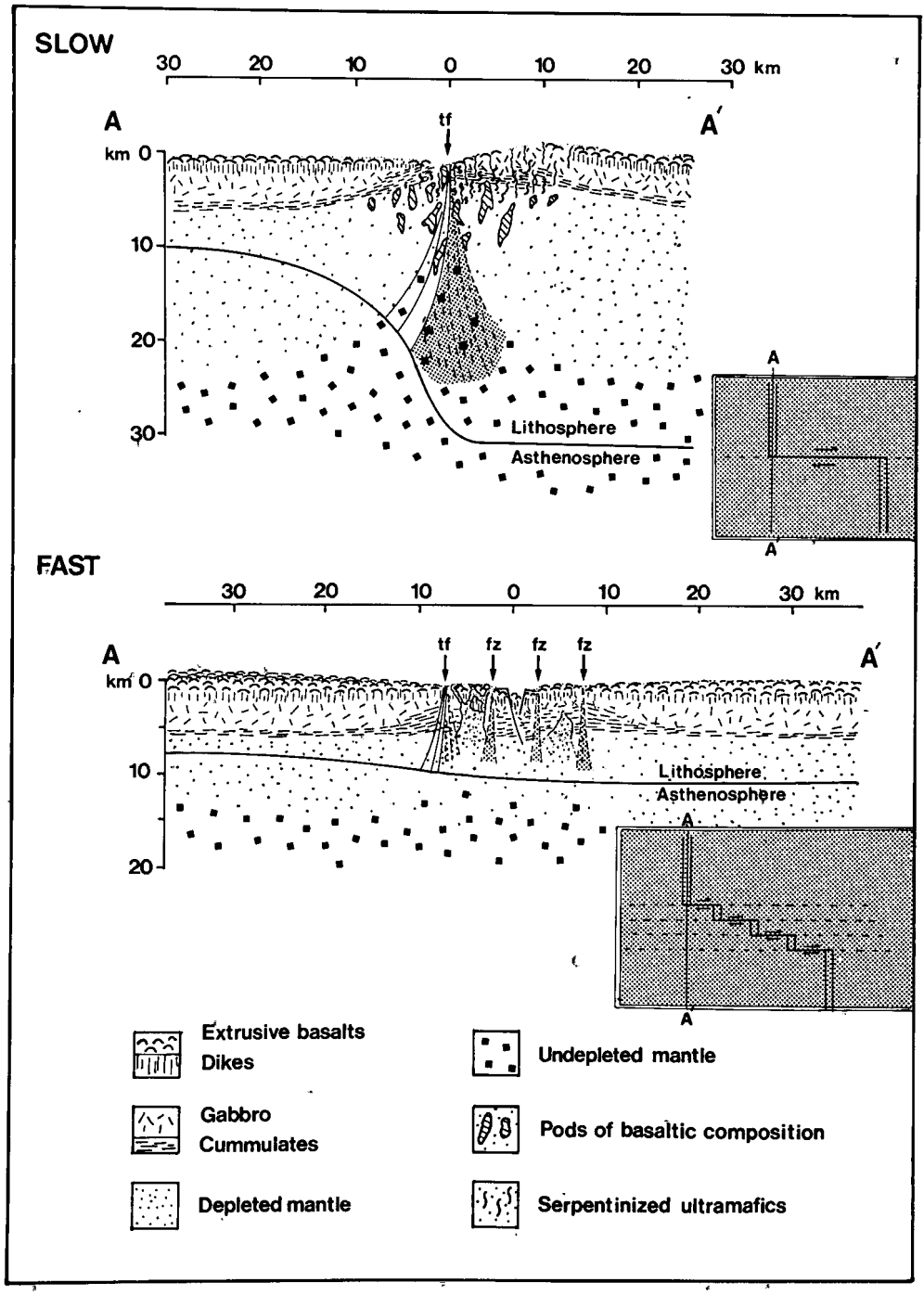

Fig. 7. Generalized geologic model of the structure of oceanic lithosphere at and proximal to a 100 km offset slowly-slipping (2 cm/yr) ridge–transform intersection (top) and a 100 km offset fast-slipping (18

from localities high on the walls of transform valleys along the Mid-Atlantic Ridge suggested to Francheteau et al. (1976) that the shallow intrusive and extrusive carapace (seismic Layer 2) of the oceanic crust is anomalously thin proximal to transforms and they proposed that this characteristic reflects a diminished volcanic budget caused by the thick, cold plate on one side of the intersection. Seismic refraction investigations of the Kane Transform (Detrick and Purdy, 1980) and the documentation by submersible sampling that oceanic crust is very thin along rift valley segments proximal to cold, thick transform edges (CAYTROUGH, 1979; Stroup and Fox, 1981; Karson and Dick, 1983) and along the bounding walls of fracture zones (Oceanographer Transform; OTTER, 1980, 1981, 1984) led to the formulation of more generalized models predicting that the occurrence of thin crust is a diagnostic and characteristic property of slowly-slipping ridge–transform–ridge intersections (Fox, 1978; Gallo and Fox, 1979; Detrick and Purdy, 1980; Fox et al., 1980; Stroup and Fox, 1981). The thickness of the oceanic crust is dependent upon the volume of basaltic melt that is segregated at depth from the asthenosphere and delivered to shallow level magma chambers. Proximal to the thick, cold wall of transform boundaries, lateral conductive heat flow reduces the ambient temperature and disrupts the upward migration of the hot upwelling asthenosphere diminishing the volume of basaltic melt generated and impairing the ability of the melt that is segregated to reach the surface. As a result, the total magmatic budget supplied to shallow level magma chambers decreases as the transform boundary is approached and the crust thins correspondingly (Fig. 7). At very large transforms, the edge effect may be so profound that the emplacement of basaltic magma at shallow levels is discontinuous with periods of accretion being punctuated by the emplacement of solely peridotites laced with stringers of basaltic rocks.

As the overlying crust thins towards the transform edge, the thickness of the underlying lithosphere will increase as newly formed lithosphere is plated against the base of the cold transform wall (Fig. 7). This thickening wedge of lithosphere will be very heterogeneous because some fraction of the melt produced during partial melting will never successfully pass through the upper mantle and contribute to the development of the crust but will be trapped within the upper mantle creating pods of rock with basaltic composition (Fig. 7). The magnitude of the cold-edge effect at ridge–transform intersections will vary as a function of the thickness of the lithosphere at the ridge axis termination; the effect will be profound at large-offset,

---

cm/yr) ridge–transform intersection (bottom). The models predict that the crust will thin and the underlying lithosphere will thicken as the ridge–transform boundary is approached. Lateral heterogeneities in composition, layering and mass distribution are predicted for both cases but will be dramatic at a slowly-slipping boundary where the cold edge of the transform is large. However, given the relatively thin edges of lithosphere characterizing fast-slipping transforms, a relatively wide and complex shear zone evolves developing complex structural and compositional relationships. See text for a more complete explanation.

slowly-slipping transforms (Fig. 7a) and will be increasingly less important as the thickness of the truncating cold edge diminishes (Fig. 7b). This model predicts that as a fracture zone is approached along an isochron, the crust and underlying mantle will become increasingly more heterogeneous in terms of lithology and distribution of mass; the degree of heterogeneity and the distance over which the heterogeneity is recognized along an isochron will depend on the plate-edge geometry that characterized the ridge–transform intersection at the time of lithosphere generation. The great relief associated with those ridge–transform intersections that juxtapose relatively thick edges of lithosphere against an accreting plate boundary (i.e. slowly-slipping transforms) reflects an isostatic response to the marked changes in the mass distribution within the oceanic lithosphere caused by thinning oceanic crust and the changing composition of the upper mantle due to a decrease in partial melting. These lateral variations in mass distribution are likely to result in a change in isostasy for the lithosphere. Furthermore, the thin crust proximal to transforms will allow seawater to penetrate into the underlying upper mantle and hydrate ultramafic rocks; serpentinite diapirs will be created leading to vertical tectonism and the creation of the large serpentinite ridges that are so often the hallmark of slowly-slipping, large-offset fracture zones (Aumento and Loubat, 1971; Bonatti, 1976; 1978; Bonatti and Honnorez, 1976; Francis, 1981). Serpentinization of mafic and ultramafic rocks will further complicate and contribute to the crustal and subcrustal heterogeneity predicted for ridge–transform–ridge plate boundaries in general and slowly-slipping ones in particular. Given this complex geologic environment, it is not surprising that gravity data suggest that the mass anomalies associated with fracture zone troughs are variable and not systematic (Louden and Forsyth, 1982). Seismic refraction experiments within and proximal to the transform domain typically record anomalously low mantle velocities (> 7.6–7.9 km/s; Detrick and Purdy, 1980; McClain and Lewis, 1980; Ouchi et al., 1982; White, 1983) and we suggest that these low values reflect the contamination of the upper mantle with pods and veins of rocks with basaltic compositions that have been trapped at depth (A. Nicolas, pers. commun., 1983, reports finding basaltic rocks impregnating peridotites in ophiolite terrains interpreted to be preserved remnants of transform faults).

Investigators have suggested that the oblique trends observed proximal to ridge–transform intersections reflect a change in the state of stress along the accreting plate boundary caused by a shear couple at the ridge–transform boundary (Crane, 1976; Lonsdale, 1978; Searle, 1979, 1981). We have documented that the oblique faults in this environment do not accommodate significant amounts of strike-slip motion (OTTER, 1983; Tamayo Scientific Team, 1983; Karson and Dick, 1983) and, therefore, these oblique trends are not analagous to the shear structures that are known to develop in continental shear zones and clay box experiments during the initial stages of deformation (e.g. Tchalenko, 1970; Tchalenko and Ambraseys, 1972; Wilcox et al., 1973; Courtillot et al., 1974).

We propose that the thick wedge of lithosphere that forms beneath the axis of

accretion proximal to the transform boundary creates a weld with the cold, thick lithosphere at the ridge–transform interface (Fig. 8). Part of the weld links newly formed lithosphere across the aseismic limb of the fracture zone and has little effect on intersection tectonics because the sense and magnitude of the relative motion

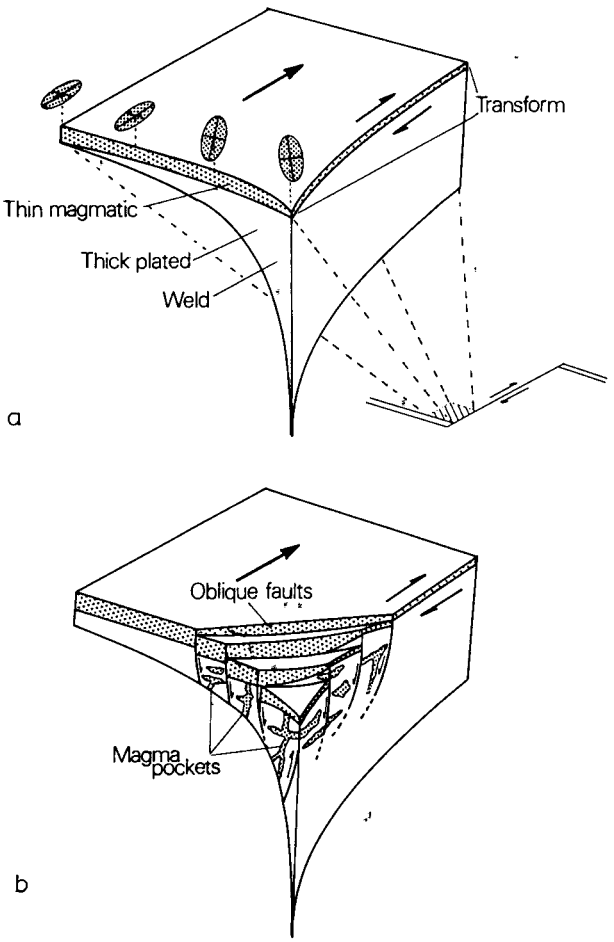

Fig. 8. a. Schematic model outlining the change in the thickness of the oceanic lithosphere as a ridge–transform plate boundary is approached; the magmatic component (crust) thins and the underlying mantle thickens. The newly formed mantle welds against the cold truncating edge of the transform creating a shear couple. Ellipses along the ridge axis show progressive reorientation of the direction of maximum tensile stress due to the shear couple generated during deformation of a mantle weld.
b. Geological consequences due to deformation of the mantle weld: proximal to the ridge–transform intersection normal faults form that strike oblique to the direction of plate motion (obliquity of the faults depend on the strength of the weld and the strain rate); batches of melt are trapped in the mantle proximal to the cold truncating edge (melt entrapment is dependent on the thickness of the cold transform edge).

across this boundary is the same. The weld, however, that bonds the newly formed lithosphere with cold lithosphere across the transform portion of the fracture zone creates a shear couple in the underlying lithosphere resulting in the progressive reorientation of the maximum tensile stress from normal to the ridge axis, at some distance from the ridge transform intersection, to an oblique angle near the boundary (Fig. 8; Gallo et al., 1980; Fox and Gallo, 1982). The brittle carapace of oceanic crust that is created proximal to the R–T intersection will not be an effective stress guide because of its disrupted and fragmented nature but, in response to strain in the underlying mantle weld, the basaltic carapace will deform accordingly with the development of oblique, dip-slip faults. The shear couple will be an intermittent phenomenon in that the mantle weld will be continually broken as the strain induced by transform related strike-slip motion exceeds the strength of the upper mantle rocks. For some period of time after the rupture of the mantle weld the orientation of the maximum tensile stress will be normal to the ridge axis. This temporal variation in the behavior of the mantle weld explains why, proximal to ridge–transform intersections, we observe dip-slip faults and fissures that exhibit a range of orientations (Fig. 2c; Tamayo Tectonic Team, 1983; OTTER, 1983).

The distance over which the transform-generated shear couple affects the tectonics of the accreting plate boundary will depend on the size of the mantle weld which in turn will vary as a function of the thickness of the truncating edge of the lithosphere at the transform boundary (Fig. 9). The number of well-mapped intersections is small but the distance over which oblique structures are recognized along the ridge axis seems to increase as the truncating edge of lithosphere becomes thicker: in the FAMOUS area or at the Tamayo Transform the thickness of the lithosphere at the ridge–transform intersection is only 10–15 km and oblique bathymetric and structural trends along the transform side of the rift valley are recognized over distances of only a few kilometers (Transform A—Detrick et al., 1973; Renard et al., 1975; Tamayo Transform—Tamayo Tectonic Team, 1983) whereas oblique structures develop over much greater distances (20–30 km) along rift wall segments terminated by a thick edge of lithosphere (> 30 km) like the Oceanographer (Schroeder, 1977; Fox et al., 1984) or Vema (K. Macdonald and P. Fox, unpublished Deep-Tow data) Transforms.

Another predicted manifestation of the development of anomalously thick lithosphere proximal to ridge–transform intersections is that at shallow levels these thick edges of lithosphere facing each other across the transform fault will tend to confine the deformation associated with the relative motion to a narrow, highly-strained principal transform displacement zone. Direct observations along Transform A (ARCYANA, 1975; Choukroune et al., 1978) and the Oceanographer Transform (OTTER, 1984), and a Deep-Tow study of a 60 km-long segment of the Vema Transform (Castillo et al., 1982) document that surficial evidence for recent deformation within the transform domain is located along a very narrow (< 2 km) linear belt that is centered about the axis of maximum basement depth. The Vema

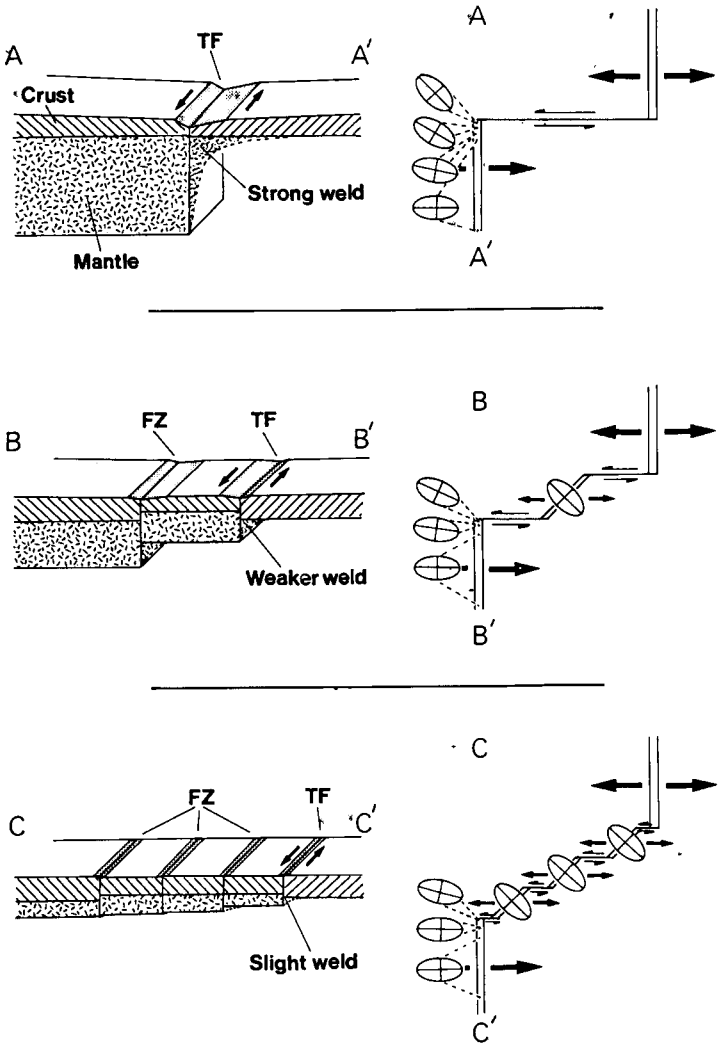

Fig. 9. Schematic models of the lithosphere at three ridge–transform intersections illustrating how contrasting thicknesses in these transform edges effect the tectonics of slowly-slipping (2 cm/yr; *A*), moderate slip-rate (6 cm/yr; *B*) and fast slip-rate (15 cm/yr; *C*) R–T–R plate boundaries (same total offset length for all three examples; ~100 km).

Transform is filled with over two kilometers of a flat bedded, laterally continuous, acoustically reverberant assemblage of Pliocene to Recent turbidites (Eittreim and Ewing, 1975; Supko and Perch-Nielsen, 1977). Seismic reflection profiles across the transform valley indicate that the acoustic stratigraphy is undisturbed across its width except for a narrow (< 2 km) zone that cuts vertically through the assemblage intersecting the basement along the axis of the transform valley. At the surface this

discordant zone is defined by disrupted reflectors, and is coincident with the 60 km-long disturbed zone mapped by Deep-Tow and can be traced as a continuous feature linking the two ridge–transform intersections (Eittreim and Ewing, 1975; D. Needham, unpublished data). We interpret these data to indicate that the strains associated with transform tectonism along the Vema Transform have remained fixed for as long (a few million years) as the turbidites have been deposited along the valley. Submersible traverses up the walls of the Oceanographer Transform (OTTER, 1984) find no evidence to suggest that strike-slip faulting has been important in shaping this terrain. Although more work must be done to establish the location and behavior of principal transform displacement zones in time and space, the fragmentary record is consistent with the notion that, except for major changes in the pole of relative motion, the thick edges of lithosphere associated with large-offset transform faults confine the PTDZ to a narrow zone centered along the plate edges.

The geologic model outlined in the preceding paragraphs is based largely on our understanding of slowly-slipping ridge–transform–ridge plate boundaries. The geologic constraints on the properties of medium and fast slip-rate transforms and the adjoining ridge segments are not as numerous thereby making it difficult to generalize with confidence, but a few first-order morphotectonic themes emerge and these can be tested against predictions of our model. As the slip-rate of a transform increases, the thickness of a truncating edge of lithosphere will decrease rapidly per unit length of transform when compared with a more slowly-slipping transform (compare Fig. 2b with Figs. 4b, 4e). Therefore, except for exceptionally long offset transforms, ridge segments displaced by medium and fast slip-rate transforms will be bounded at the transform intersection by relatively thin lithosphere (Figs. 4b, 4e). As a consequence, the edge effect of the cold wall on the thermal structure of the adjoining asthenosphere–lithosphere will not be as radical; the migration of basaltic melts and fractionated products to shallow levels will not be substantially inhibited (Fig. 7); the wedge of newly-formed lithosphere plated against the cold edge will not be large; and the significance of the shear-couple formed by intermittently welding the plated lithosphere to the cold edge will be reduced (Fig. 9b). As a result, the distribution of mass proximal to the transform is not as laterally heterogeneous as it is in the lithosphere created adjacent to a slowly-slipping ridge-transform plate boundary and, consequently, the relief of rapidly slipping transforms will become increasingly subdued with increasing rates of accretion. Furthermore, the relatively weak mantle weld predicted to characterize medium slip-rate intersections implies that the shear couple formed in the upper mantle will be restricted to the intersection with oblique structures forming only in close proximity to the transform boundary (Fig. 9).

Given the higher strain rates and the small age contrast in the lithosphere across a medium slip-rate transform it seems intuitively reasonable to assume that in this tectonic environment the location and geometry of the plate boundary would be unstable. Along this "soft" plate boundary the principal transform displacement

zone may remain fixed for relatively short periods of time (10^3 to 10^5 yrs. before it migrates to a new location. As a result, the geometry of the strike-slip zone is constantly changing with extensional or compressional relay zones forming to accommodate the strike-slip motion (Fig. 9). An extensional relay zone, depending on how long it remains active, could evolve from an anomalously deep, small rifted basin to a zone of serpentinized upper mantle diapirs and then to a zone of accretion (processes of accretion likely to be abnormal given the tectonic setting); a compressional relay zone would lead to the creation of ridges and shallow crustal flakes by thrust faulting. Indeed, based on various lines of evidence extensional relay zones have been evoked to explain the present-day tectonic settings of the Tamayo (Macdonald et al., 1979; CYAMEX and Pastouret, 1981), Rivera (Reid, 1976; Prothero and Reid, 1982) and Orozco (Trehu, 1982) transforms. Furthermore, if the PTDZ migrates within a broad, 10–30 km wide transform domain, the location of the ridge–transform intersections will not be stable under some conditions and the accretionary ridge tip may propagate into or retreat from the transform domain. It has been suggested that the morphology and magnetic pattern at the Cobb propagator–transform intersection located along the Juan de Fuca–Pacific plate boundary can be best explained by ridge–transform intersections that migrate back and forth (J. Delaney, pers. commun., 1982). The morphology of the Clipperton plate boundary and the present-day location of the truncated rise tips and linking PTDZ suggest that this plate geometry has not been stable and the rise tips have migrated into the transform domain modifying the pre-existing geometry (strike-slip strands linked by a short relay zone; K. Macdonald and P. Fox, unpublished data).

Given the very high slip-rates governing fast-accreting ridge–transform–ridge plate boundaries, the thickness contrast in lithosphere across a transform (i.e. 100 km offset length) will be very small (several kilometers; Fig. 4e) and the strain rates will be very high (Fig. 1). At these fastest-slipping plate boundaries the effect of the truncating edge of lithosphere on accretionary processes proximal to the intersection will be minimized and, as a consequence, the changes in accretionary processes (i.e. effect on partial melting, structure of the upper mantle and strength/size of the mantle weld) that we predict to be a product of this boundary will be subtle and will be apparent only in close proximity to the intersections (Fig. 7). The transform domain, however, will be wide and the tectonic geometry within the domain will be complex because the strains associated with a fast-slipping ridge–transform–ridge plate boundary will not be constrained by thick edges of lithosphere but will be free to migrate across the edges of thin lithosphere that bound the offset rise axis creating a broad zone of shear (Fig. 7; Rea, 1981). The shear zone appears to be characterized by short, strike-slip fault strands that are linked by oblique trending extensional relay zones (Fig. 9; Searle and Francis, 1982; Searle, 1983; P. Lonsdale, pers. commun., 1982; P. Fox, unpublished data). It is unlikely that the processes of accretion that take place along these short extensional relay zones will lead to the development of normal oceanic crust and upper mantle; rather accretion is likely to

be discontinuous with crustal sections thinned tectonically by extension and perhaps intruded by diapirs of serpentinized ultramafic rocks (Fig. 7). It is interesting to note that gabbroic and ultramafic rocks have been recovered from a small, anomalously deep, closed-contour basin (4500 m) within the transform domain of the Garret transform (Bideau et al., 1983). We suggest that these rocks have been recovered from terrain that is the product of discontinuous accretion and that has been thinned by extension. Since there are no accurate high-resolution maps at a regional scale of fast-slipping fracture zones, we do not have an accurate description of the time-integrated morphotectonic fabric and, therefore, we cannot use the topography to infer how the strike-slip, relay-zone geometry has behaved in time. We suspect, however, that the geometry will be temporally unstable in this tectonic environment characterized by high strain-rates and thin lithosphere and the time integrated product of this tectonic regime will create a swath of disrupted and anomalous oceanic lithosphere with variable properties and internal characteristics (Fig. 7).

DISCUSSION

In the preceding section we used the first-order geologic and morphologic relationships at, along and proximal to ridge–transform–ridge plate boundaries to construct an empirical and speculative tectonic model. We suggest that the distinctive but variable morphotectonic fabric and crustal structure of the transform domain are the product of a tectonic continuum that ranges from very slow rates of strain associated with very thick edges of lithosphere (slowly-slipping ridge–transform–ridge plate boundaries) to extremely high rates of strain associated with very thin edges of lithosphere (fast-slipping ridge–transform–ridge plate boundaries). The central theme of the model is that the cold edge of lithosphere juxtaposed against the truncated end of an accreting plate boundary perturbs the processes of accretion leading to the production of anomalous lithosphere.

This model implies that the cold edge of a ridge–transform plate boundary should condition the petrology of basalts created proximal to these boundaries. In order to determine the petrologic consequences, a suite of glassy basalts was collected at sixteen localities over a distance of 50 km down the axis of the East Pacific Rise south of the Tamayo Transform (Tamayo Tectonic Team, 1983). Twenty-nine samples of basalt glass were analyzed by Bender et al. (1984) for major and trace elements including the rare-earth suite and they found that there are systematic differences between samples collected in close proximity to the transform and those samples collected at distances greater than 20 km from the transform. Detailed modeling of these data by Bender et al. (1984) suggests that this geochemical signal can be explained both by lower extents of melting and more variable, but generally greater, extents of crystal fractionation near the transform because of the cooler thermal environment. They propose that the residual mantle beneath a transform will be less refractory and that small scale heterogeneities in the mantle will be more

frequently observed near transform faults because of autometasomatism, smaller degrees of partial melting and possibly greater extents of crystal fractionation. These same investigators are presently modeling geochemical data for basalt collections located proximal to other ridge–transform intersections and these results suggest that basalts close to a transform are generally derived by lower extents of partial melting compared to basalts far from the transform along the same ridge segment (Langmuir and Bender, 1984).

In terms of overall structure and composition, the geologic character of oceanic lithosphere is largely conditioned by the processes that govern the generation and emplacement of the predominantly mafic and ultramafic rocks along the Mid-Oceanic Ridge system in both time and space. Along any given ridge axis segment there will certainly be important, but as yet unresolved, temporal and spatial changes in the processes of plate accretion that will lead to non-trivial changes in oceanic lithosphere. These variations, however, are of second-order significance when compared to the changes in the structure and composition of oceanic lithosphere predicted to occur as the fracture zone is approached. Our model suggests, moreover, that there will be some important differences between the geology of lithosphere created along a slowly accreting plate boundary versus lithosphere created along rapidly accreting plate boundary.

Slowly accreting plate boundaries (< 4 cm/yr) are typically characterized by the frequent occurrence of variably-sized transform faults that offset the ridge axis every 30–80 km (see GEBCO map series for North and South Atlantic). Although the relative length of the transform may change with time due to phases of asymmetric spreading, the ridge–transform geometry is remarkably stable in time surviving numerous changes of the pole of relative motion (Schouten and White, 1980; Schouten and Klitgord, 1982). Given the validity of our model and the temporal stability of slowly-slipping ridge–transform–ridge plate boundaries, it means that ribbons of anomalous lithosphere can be traced, rib-like, from the ridge axis across the ocean basin to the margins (Fig. 10a). Each ribbon of anomalous lithosphere will be composed, in first-order terms, of two parts. There will be a relatively narrow band of highly-strained terrain, only a few kilometers wide, made-up of blocks of thin oceanic crust and partially serpentinized ultramafic rock (for example, see Karson and Dewey, 1978; Prinzhoffer and Nicolas, 1980; Karson, 1982; and Karson, 1983 for a discussion, based on ophiolite studies, of the complexities thought to characterize this interval) representing the paleo-principal transform displacement zone. At shallow levels (zone of brittle deformation) this high-strain zone is generally narrow because the strike-slip tectonism of the transform is constrained to a relatively narrow crush zone by the relatively thick edges of opposing lithosphere that face each other across the transform fault. It is interesting to note, however, that for small-offset (< 20 km) slowly-slipping ridge–transport–ridge plate boundaries, the thickness of the lithosphere may be thin enough (< 15 km) to permit the development of complex plate-boundary geometries in response to

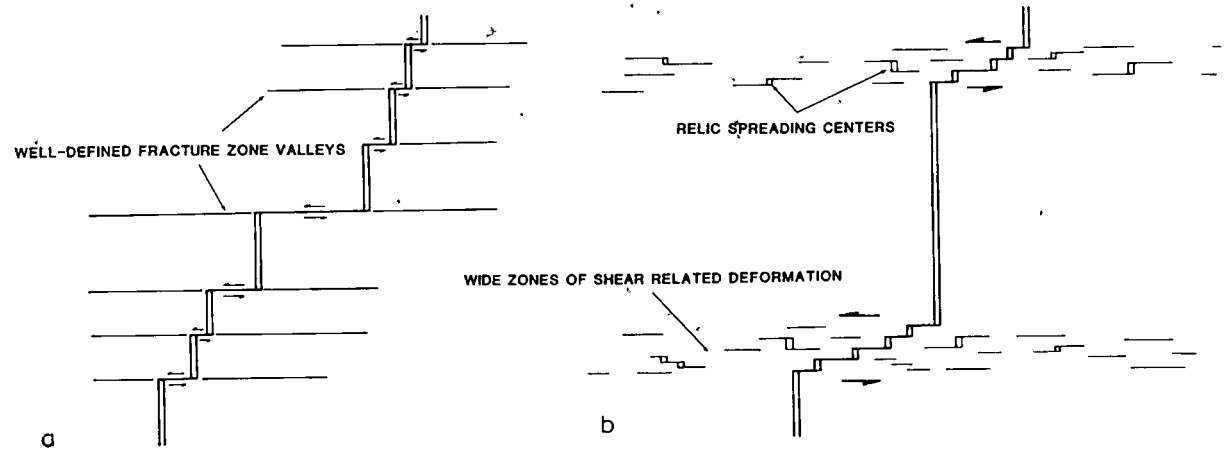
WELL-DEFINED FRACTURE ZONE VALLEYS
a
RELIC SPREADING CENTERS
WIDE ZONES OF SHEAR RELATED DEFORMATION
b

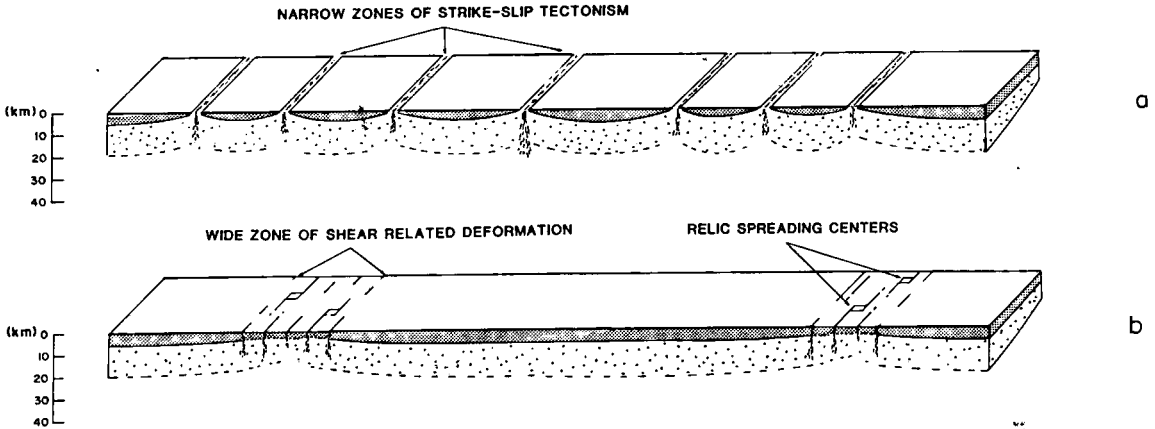
NARROW ZONES OF STRIKE-SLIP TECTONISM
(km) 0
10
20
30
40
a
WIDE ZONE OF SHEAR RELATED DEFORMATION
RELIC SPREADING CENTERS
(km) 0
10
20
30
40
b

minor adjustments in relative motion. The maps of the FAMOUS area (Phillips and Fleming, 1978) reveal a confused ridge axis-transform geometry showing overlapping ridge axes and discontinuous transform trends which have been interpreted to reflect an unstable geometry involving the migration of transform fault zones with small offsets (< 20 km) and the change in length of intervening echelon ridge segments (Ramberg et al., 1977; Schouten et al., 1980). Independent of plate edge thickness considerations, times of major changes in the pole of relative motion are likely to induce reorganization of the ridge–transform geometry and, depending on the tectonic adjustments, the zone of strike-slip tectonism will widen appreciably (Menard and Atwater, 1968, 1969; Dewey, 1975). Flanking the paleo-principal transform displacement zone will be a wide (10–30 km) band of anomalous oceanic lithosphere that will become increasingly more heterogeneous with proximity to the fracture zone (Figs. 7, 10a). The width of these ribbons of anomalous lithosphere will depend on how cold the accretionary environment was at the time of lithosphere formation which in turn will be primarily a function of the thickness of the truncating edge of lithosphere at the ridge–transform intersection. The frequent occurrence of ridge–transform intersections along slowly accreting plate boundaries (< 4 cm/yr full rate), the temporal stability of this plate tectonic geometry, and the predicted manifestations of the cold-edge effect at ridge–transform intersections (Fig. 7) mean that the time integrated product of accretion will lead to a very heterogeneous oceanic lithosphere (Fig. 10a). It is no surprise that at six localities within the North Atlantic, chosen on the basis of standard marine geological and geophysical data to be removed from fracture zones, the Deep Sea Drilling Project has recovered gabbroic and ultramafic rocks at shallow crustal levels (< 200 m; Ryan et al., 1973; Aumento et al., 1977; Melson et al., 1978; Leg 82 Scientific Party, 1982).

At rates of accretion greater than 6 cm/yr the number of transforms that offset the axis of accretion diminish markedly and occur every several hundred kilometers or more along the ridge axis (Mammerickx and Smith, 1978). These transforms are

Fig. 10. Schematic diagrams contrasting the different kinds of oceanic lithosphere that are likely to be created along a slowly accreting plate boundary with many transforms (a) and a rapidly accreting plate boundary with a few widely spaced transforms (b). The numerous, relatively thick edges of lithosphere found at slowly-slipping ridge–transform–ridge intersections disrupts the accretion process leading to the creation of heterogeneous lithosphere at a regional scale. The relatively thick edges of lithosphere, however, constrain the strike-slip tectonism to a relatively narrow interval within the heterogeneous swaths of oceanic lithosphere. Along rapidly accreting plate boundaries (> 6 cm/yr) large offset transforms are widely spaced. The accretionary processes are not radically perturbed at ridge–transform–ridge intersections because the contrast in the thickness of the lithosphere at the intersection is not large. Therefore, the changes in the properties of the oceanic lithosphere are not profound as the boundary is approached. The thin edges of lithosphere along fast-slipping transforms allow wide shear zones with unstable geometries to develop creating swaths of disrupted lithosphere (see text for details).

generally long-lived surviving changes in the pole of relative motion (Mammerickx and Klitgord, 1982; Klitgord and Mammerickx, 1982) and have offset magnitudes of approximately 100 km or more. The extensions of these relatively fast-slipping transforms can be traced across the Pacific Basin, but the swath width of fracture zone terrain is variable along strike (Mammerickx and Smith, 1978) suggesting that the ridge–transform geometry is temporally unstable. There is, however, little or no evidence for long-lived, short-offset transforms (< 50 km) and, given the very thin edges of lithosphere involved at a fast-slipping short-offset transform, this geometry is not likely to be stable for long periods of time because the short transforms will be abandoned as the offset accreting plate boundaries propagate across the shear zone into relatively thin lithosphere and link up (Macdonald and Fox, 1983). In time one limb of the overlapping spreading center will be isolated, the transform plate boundary will be abandoned and the new accreting geometry will describe a gentle sinuous bend.

The oceanic lithosphere within and proximal to the widely-spaced but long-lived fracture zones that offset fast accreting plate boundaries will exhibit geological relationships that distinguish this terrain from its tectonic counterpart found along slowly accreting plate boundaries (Fig. 10b). The more robust thermal regime that characterizes a fast accreting plate boundary (Sleep, 1975; Kusznir and Bott, 1976) coupled with the relatively small contrast in the thickness of lithosphere across a transform boundary means that the cold edge effect will diminish with increasing spreading rate and the lithosphere will not exhibit profound heterogeneity as the transform is approached (Fig. 7). The strain history of the rock bodies within the principal transform displacement zone will be more temporally and spatially complex than a slowly-slipping transform because the high rates of strain that characterize fast-slipping transforms (Fig. 1) will not be as constrained by the relatively thin edges of opposing lithosphere and, in response to relatively small changes in the pole of relatively motion, the shear zone along a transform will be free to migrate over a wide interval (10–20 km; Figs. 9, 10b). Depending on the sense of transform offset relative to a given alteration in relative motion, a transform would experience a component of extension or compression (Menard and Atwater, 1968, 1969; Dewey, 1975). A component of extension would facilitate the development of a wide shear zone with several strike-slip strands linked by extensional relay zones whereas a component of compression would tend to collapse the shear zone. As discussed in the preceding section, all the transforms south of the Gulf of California that offset the rise axis in a left-lateral sense (Tamayo, Rivera, Orozco, Siqueiros, Quebrada, Gofar, Wilkes and Garret) are characterized by wide shear zones with short strike-slip strands linked by extensional relay zones. The one transform that offsets the rise in a right-lateral sense, the Clipperton Transform, is presently characterized by a narrow zone of shear. Whether this distinction is fortuitous or indicative of very recent changes in the poles of relative motion (Gallo and Fox, 1981; Searle, 1983) remains to be established but it seems clear that the thin edges of fast-slipping

transforms will accommodate adjustments to small changes in plate kinematics relatively easily. Furthermore, the geometry within these fast-slipping shear zones is likely to be continually adjusting and changing and the time-integrated product of this evolving tectonic behavior will be the creation of oceanic lithosphere that is complex in terms of composition and structure. Accretionary processes within a 10–20 km wide shear zone will be disrupted by the unstable behavior of the shear zone; strike-slip faults will bound rock bodies of contrasting age; extensional relay zones can lead to tectonic thinning, hydration and uplift of the crust, or the development of a small zone of accretion. On the other hand compressional relay zones will create ridges through crustal thickening and under thrusting (Figs. 7, 10b).

The variation in the thickness of the truncating edge of lithosphere at a ridge–transform intersection will not only control the thickness of the oceanic crust but will also condition the structure of the oceanic crust and upper mantle. Bender and Langmuir have recently argued, based on geochemical data, that at ridge–transform intersections not only are smaller volumes of melt produced but those melts experience greater degrees of fractionation in shallow level reservoirs proximal to the transform termination (Bender et al., 1984; Langmuir et al., 1984). A similar conclusion was reached by Fornari et al. (1983) after collecting highly fractionated basalts from terrain proximal to the Inca Transform along the Galapagos Ridge. Enhanced fractionation suggests the accumulation of thicker sequences of cumulate ultramafics and/or olivine rich gabbros. Based on field mapping in the Bay of Islands, Newfoundland, Karson has defined the relationships that are developed along the contact between the Coastal Complex and the Bay of Island ophiolite (Karson and Dewey, 1978; Karson, 1982). Karson suggests that the relationships developed along this contact are the product of a relatively fast-slipping ridge–transform intersection and shows that as the contact is approached ultramafic cumulates (cumulate dunites, and megalenses of wehrlite and gabbro) thicken and lap up against the highly strained rocks of the transform boundary. This relatively shallow level expression of the cold transform edge would be perhaps most dramatic at faster slipping ridge–transform intersections where the volume of partial melt remains relatively high and magmatic processes are relatively continuous. The development of a thicker basal cumulate member should develop at a slowly slipping ridge–transform intersection but this assemblage will not be as well developed because of the smaller volume of melt produced and the very discontinuous nature of accretion in this environment.

Our discussion has largely focused on the structural differences predicted to exist between ridge–transform intersections with contrasting tectonic characteristics (i.e. slip-rate and truncating edge thickness). Superimposed against these tectonic variables are temporal variations in accretionary processes that can create pronounced changes in crustal structure. Recently it has become clear that the migration of basaltic melts into shallow level reservoirs and the extrusion of these products onto the sea floor is an episodic process with magmatic pulses migrating in time along a

ridge axis segment (e.g., Macdonald and Fox, 1983). This temporal variability of ridge axis accretion has important implications for crustal structure in general and, in terms of this discussion, ridge–transform intersections in particular. As the magmatic pulses near a given ridge–transform intersection wax and wane the thickness of the magmatic component and the constitution of the crust and the upper mantle will vary in complex ways. Consequently, when the the crustal structure of a fracture zone is viewed along strike the magmatic component should thicken and thin creating a lumpy profile.

CONCLUDING REMARKS

The preceding discussion has summarized the morphologic, geologic and geophysical characteristics of ridge–transform–ridge plate boundaries. Based on these data we suggest that the distinctive morphotectonic character exhibited by these plate boundaries is the surficial expression of what happens when a cold edge of lithosphere, of variable thickness, is juxtaposed against an accreting plate boundary (full spreading rate can vary from 2 to 18 cm/yr). The model that we propose (Figs. 7, 8, 9, 10) is speculative and must be tested against the acquisition of high resolution data that can be obtained by carefully designed experiments that involve multi-narrow beam echo sounders, deep-towed geophysical and photographic packages, submersibles and geophysical equipment (e.g. ocean bottom seismometers, multi-channel seismic systems). It is critical that maps of the principal transform displacement zones of both fast-slipping and slowly-slipping transforms be made so that we can obtain a better description of how these contrasting tectonic environments behave temporally and spatially. More information is needed on structural relationships developed at ridge-transform intersections as well as a better definition of the change in properties of the oceanic lithosphere that occur proximal to ridge–transform–ridge plate boundaries.

ACKNOWLEDGEMENTS

The ideas and model presented in this paper are the outgrowth of field programs to the Mid-Cayman Rise, the Tamayo, Oceanographer and Vema transforms, and a multi-narrow beam investigation of the axis of the East Pacific Rise between 8°N to 17°N. We thank the many investigators who worked with us on these projects for their help. Over the last several years that we have worked on our model a large number of colleagues has contributed to our model by asking questions, providing criticism and offering support. In particular, we would like to thank J. Cann, S. DeLong, R. Detrick, J. Dewey, D. Forsyth, J. Francheteau, J. Karson, W.F.S. Kidd, K. Macdonald, R.H. Moody, D. Needham, A. Nicolas, D. Rowley and J. Stroup. X. LePichon and S. Uyeda offered constructive criticisms during the formal review process. Support for the field programs came from NSF (Cayman Trough Project

OCE-76-21882; Tamayo Transform OCE-79-13144) and ONR (Oceanographer N00014-81-C-0820; East Pacific Rise investigation N00014-81-C-0062). We are particularly grateful to ONR for support that allowed us to synthesize and integrate our data from various field programs into a larger framework (ONR N00014-81-C-0062).

REFERENCES

ARCYANA, 1975. Transform fault and rift valley from bathyscaphe and diving saucer. Science, 190: 108–116.

Aumento, F. and Loubat, M., 1971. The Mid-Atlantic Ridge near 45°N, XVI Serpentinized ultramafic inclusions. Can. J. Earth Sci., 8: 631–663.

Aumento, F., Melson, W.G., et al., 1977. Initial Reports of the Deep Sea Drilling Project. U.S. Government Printing Office, Washington, D.C., 37: 998 pp.

Barazangi, M. and Dorman, J., 1969. World seismicity maps compiled from ESSA Coast and Geodectic Survey epicenter data, 1961–1967. Bull. Seismol. Soc. Am., 59: 369–380.

Batiza, R., Rosendahl, B.R. and Fisher, R.L., 1977. Evolution of oceanic crust. 3. Petrology and chemistry of basalts from the East Pacific Rise and Siqueiros Transform fault. J. Geophys. Res., 82: 265–276.

Bender, J.F., Langmuir, C.H. and Hanson, G.N., 1984. Petrogenesis of basalt glasses from the Tamayo region, East Pacific Rise: correlation of glass chemistry with distance from a transform fault. J. Petrol., in press.

Bideau, D., Hebert, R., and Hekinian, R., 1983. Metagabbro and metaperidotite from the Garret Transform Fault (East Pacific Rise near 13°S). Earth Planet. Sci. Lett., 65: 107–125.

Bonatti, E., 1976. Serpentinite protrusions in the oceanic crust. Earth Planet. Sci. Lett., 32: 107–113.

Bonatti, E., 1978. Vertical tectonism in oceanic fracture zones. Earth Planet. Sci. Lett., 37: 369–379.

Bonatti, E. and Čhermák, A., 1981. Formerly emerging crustal blocks in the equatorial Atlantic. Tectonophysics, 72: 165–180.

Bonatti, E. and Hamlyn, P.R., 1978. Mantle uplifted block in the western Indian Ocean. Science, 201: 249–251.

Bonatti, E. and Honnorez, J., 1976. Sections of the earth's crust in the equatorial Atlantic. J. Geophys. Res., 81: 4104–4116.

Bonatti, E., Honnorez, J. and Ferrara, G., 1970. Equatorial Mid-Atlantic Ridge: Petrologic and Sr isotopic evidence for alpine-type rock assemblage, Earth and Planet. Sci. Lett., 9: 247–256.

Bottinga, Y. and Allègre, C.J., 1978. Partial melting under spreading ridges. Philos. Trans. R. Soc. London, Ser. A, 288: 501–525.

Castillo, D.A., Miller, S.P., Macdonald, K.C., Kastens, K. and Fox, P.J., 1982. The tectonic character of a slow-slipping principal transform displacement zone. EOS, Trans. Am. Geophys. Union, 63: 1101.

CAYTROUGH, 1979. Geological and geophysical investigation of the mid-Cayman Rise spreading center: initial results and observations. In: M. Talwani, C.G. Harrison and D.E. Hays (Editors), Deep Drilling Results in the Atlantic Ocean: Ocean Crust. Am. Geophys. Union, Maurice Ewing Ser., 2: 66–93.

Choukroune, P., Francheteau J. and LePichon, X., 1978. Structural observation in an oceanic transform fault from manned submersibles: Transform fault "A" in the FAMOUS area. Geol. Soc. Am. Bull., 89: 1013–1029.

Cochran, J.R., 1973. Gravity and magnetic investigations of the Guiana Basin, Western equatorial Atlantic. Bull. Geol. Soc. Am., 84: 3249–3268.

Collette, B.J., Schouten, J.M., Rutten, K. and Slootweg, A.P., 1974. Structure of the Mid-Atlantic Ridge Province between 12° and 18°N. Marine Geophys. Res., 2: 143–179.

Cormier, M.H., Detrick, R.S. and Purdy, G.M., 1983. New evidence for anomalously thin oceanic crust along the Kane fracture zone. EOS, Trans. Am. Geophys. Union, 64: 314.

Courtillot, V., Tapponnier, P. and Varet, J., 1974. Surface features associated with transform faults: a comparison between observed examples and an experimental model. Tectonophysics, 24: 317–329.

Crane, K., 1976. The intersection of the Siqueiros transform fault and the east Pacific Rise. Mar. Geol., 21: 25–46.

Cyamex Scientific Team, and Pastoret, L., 1981. Submersible structural study of Tamayo Transform Fault, East Pacific Rise, 23°N (Project RITA). Mar. Geophys. Res., 4: 381–402.

DeLong, S.E., Dewey, J.F. and Fox, P.J., 1977. Displacement history of oceanic fracture zones. Geology, 5: 199–202.

DeLong, S.E., Dewey, J.F. and Fox, P.J., 1979. Topographic and geologic evolution of fracture zones, J. Geol. Soc. London, 136: 303–310.

Detrick, R.S. and Purdy, G.M., 1980. The crustal structure of the Kane fracture zone from seismic refraction studies. J. Geophys. Res., 85: 3759–3777.

Detrick, R.S., Mudie, J.D., Luyendyk, B.P. and Macdonald, K.C., 1973. Near bottom observations of an active transform fault (Mid-Atlantic Ridge at 37°N). Nature (London), Phys. Sci., 246: 59–61.

Detrick, R.S., Cormier, M.H., Prince, R. and Forsyth, D.W., 1982. Seismic constraints on the crustal structure within the Vema Fracture Zone. J. Geophys. Res., 87: 10,599–10,612.

Dewey, J.F., 1975. Finite plate implications: some implications for the evolution of rock masses at plate margins. Am. J. Sci., 275-A: 260–284.

Eittreim, S. and Ewing, J., 1975. Vema Fracture Zone Transform Fault. Geology, 3: 555–559.

Embley, R.W., Malahoff, A., and Fornari, D.J., 1984. Tectonics of the eastern Galapagos Rift–Inca Transform. J. Geophys. Res., in press.

Fornari, D.J., Perfit, M.R., Malahoff A. and Embley, R., 1983. Geochemical studies of abyssal lavas recovered by DSRV ALVIN from the Eastern Galapagos Rift–Inca Transform–Ecuador Rift: I. Major element variations in natural glasses and spatial distribution of lavas. J. Geophys. Res., 88: 10,519–10,529.

Fox, P.J., 1972. The geology of some Atlantic fracture zones, Caribbean escarpments and the nature of the oceanic basement and crust. Ph.D. Thesis, Columbia University, New York, pp. 357.

Fox, P.J., 1978. The effect of transform faults on the character of the oceanic crust. Geol. Soc. Am., Abstr. Progr., 7: 403.

Fox, P.J. and Gallo, D.G., 1982. A mantle weld at ridge–transform intersections: implications for the development of oblique structures. EOS, Trans. Am. Geophys. Union, 63: 446.

Fox, P.J., Lowrie, A. and Heezen, B.C., 1969. Oceanographer fracture zone. Deep-Sea Res., 16: 55–66.

Fox, P.J., Schreiber, E., Rowlett, H. and McCamy, K., 1976. The geology of the Oceanographer Fracture Zone: A model for fracture zones. J. Geophys. Res., 81: 4117–4128.

Fox, P.J., Detrick, R.S. and Purdy, G.M., 1980. Evidence for crustal thinning near fracture zones: implications for ophiolites. In: A. Panayiotou (Editor), Proceedings of the International Ophiolite Symp. Ministry of Agriculture and Natural Resources, Cyprus Geological Survey Dept., pp. 161–168.

Fox, P.J. Gallo, D.G. and Sloan, H.S., 1981. Ridge-transform intersections: a general model for the bathymetry of fracture zones. EOS, Trans. Am. Geophys. Union, 62: 1049.

Fox, P.J., Schroeder, F., Moody, R. and Pitman, W.C., III, 1984. The morphotectonic character of the Oceanographer Fracture Zone. Mar. Geophys. Res., in press.

Francheteau, J., Choukroune, P., Hekinian, R., LePichon, X. and Needham, D., 1976. Oceanic fracture zones do not provide deep sections into the crust. Can. J. Earth Sci., 13: 1223–1235.

Francis, T.J.G., 1981. Serpentinization faults and their role in the tectonics of slow spreading ridges, J. Geophys. Res., 86: 11,616–11,622.

Gallo, D.G. and Fox, P.J., 1979. The influence of transform faults on the generation of oceanic lithosphere. EOS, Trans. Am. Geophys. Union, 60: 376.

Gallo, D.G. and Fox, P.J., 1981. Fragmentation of oceanic plates and pivoting subduction: implications for tectonic behavior of ridge–transform systems and the propagation of oceanic ridges. EOS, Trans. Am. Geophys. Union, 62: 1035.

Gallo, D.G., Rosencrantz, E.R. and Rowley, D.B., 1980. Oblique structures at ridge–transform intersections: implications for ridge dynamics and pole determinations, EOS, Trans. Am. Geophys. Union, 61: 358.

General Bathymetric Chart of the Oceans, North Atlantic Chart, 1982. Canadian Hydrographic Service, Ottawa, Ont.

General Bathymetric Chart of the Oceans, South Atlantic Chart, 1978. Canadian Hydrographic Service, Ottawa, Ont.

Heezen, B.C. and Tharp, M., 1965. Tectonic fabric of the Atlantic and Indian Oceans and continental drift, R. Soc. Philos. Trans., 258: 90–106.

Heezen, B.C. and Tharp, M., 1977. World Ocean Floor. Office of Naval Research, U.S. Navy.

Heezen, B.C., Bunce E.T. and Tharp, M., 1964. Chain and Romanche fracture zones. Deep-Sea Res., 11: 11–18.

Jackson, N.R., Reid I. and Falconer, R.K.N., 1982. Crustal structure near the Arctic Mid-Ocean Ridge, J. Geophys. Res., 87: 1773.

Johnson, G.L. and Vogt, P.R., 1973. Mid-Atlantic Ridge from 47° to 51°N. Geol. Soc. Am. Bull., 84: 3443–3462.

Karson, J.A., 1982. Reconstructed seismic velocity structure of the Lewis Hills massif and implications for oceanic fracture zones, J. Geophys. Res., 87: 961–978.

Karson, J.A., 1983. Variations in structure and petrology in the coastal complex, Newfoundland: the anatomy of an oceanic fracture zone. J. Geol. Soc. London, in press.

Karson, J.A. and Dewey, J.F., 1978. Coastal complex, western Newfoundland: an early Ordovician oceanic fracture zone. Geol. Soc. Am. Bull., 89: 1037–1049.

Karson, J.A. and Dick, H., 1983. Tectonics of ridge-transform intersections at the Kane fracture zone, Mar. Geophys. Res., 6: 51–98.

Kastens, K.A., Macdonald, K.C., Becker, K. and Crane, K., 1979. The Tamayo Transform Fault in the mouth of the Gulf of California. Mar. Geophys. Res., 4: 129–152.

Klitgord, K.D. and Mammerickx, J., 1982. Northern East Pacific Rise: magnetic anomaly and bathymetric framework. J. Geophys. Res., 87: 6725–6750.

Kureth, C.L., Jr. and Rea, D.K., 1981. Large-scale oblique features in an active transform fault, the Wilkes fracture zone near 9°S on the East Pacific Rise. Mar. Geophys. Res., 5: 119–137.

Kusznir, N.J. and Bott, M.H.P., 1976. A thermal study of the formation of oceanic crust. Geophys. J.R. Astron. Soc., 47: 83–95.

Langmuir, C.M. and Bender, J.F., 1984. Chemical variations around transform faults: observations and implications. Earth Planet. Sci. Lett., submitted.

Leg 82 Scientific Party, 1982. Elements traced in Atlantic. Geotimes, 27: 21–23.

Lonsdale, P., 1978. Near-bottom reconnaissance of a fast-slipping transform fault zone at the Pacific–Nazca plate boundary. J. Geol., 86: 451–472.

Louden, K.E. and Forsyth, D.W., 1982. Crustal structure and isostatic compensation near the Kane fracture zone from topography and gravity measurements. I. Spectral analysis approach. Geophys. J.R. Astron. Soc., 68: 725–750.

Macdonald, K.C. and Fox, P.J., 1983. Overlapping spreading centers: a new kind of accretion geometry on the East Pacific Rise. Nature, 301: 55–58.

Macdonald, K.C. and Luyendyk, B.P., 1977. Deep-tow studies of the structure of the Mid-Atlantic Ridge crest near 37°N (FAMOUS). Geol. Soc. Amer. Bull., 88: 621–636.

Macdonald, K.D., Kastens, K., Miller, S. and Spiess, F.N., 1979. Deep-tow studies of the Tamayo transform fault. Mar. Geophys. Res., 4: 37–70.

Mammerickx, J. and Klitgord, K.D., 1982. Northern East Pacific Rise: evolution from 25 m.y. B.P. to the present. J. Geophys. Res., 87: 6751–6759.

Mammerickx, J. and Smith, S.M., 1978. Maps, Charts Ser. Mc 26. Geol. Soc. Am., Boulder, Colo.

McClain, J.S. and Lewis, B.T.R., 1980. A seismic experiment at the axis of the East Pacific Rise. Mar. Geol., 35: 147–170.

Melson, W.G. and Rabinowitz, P.D. et al., 1978. Initial Reports of the Deep Sea Drilling Project, U.S. Government Printing Office, Washington, D.C., 45: 717 pp.

Melson, W.G. and Thompson, G., 1971. Petrology of a transform fault zone and adjacent ridge segments. R. Soc. Philos. Trans., 268: 423–441.

Menard, H.W. and Atwater, T., 1968. Changes in direction of sea floor spreading. Nature, 219: 463–467.

Menard, H.W., and Atwater, T., 1969. Origin of fracture zone topography. Nature, 222: 1037–1040.

Menard, H.W. and Chase, T.E., 1970. Fracture zones. In: A.E. Maxwell (Editor), The Sea. Wiley-Interscience, New York, 4: 321–443.

Miyashiro, A., Shido, F. and Ewing, M., 1969. Composition and origin of serpentinites from the Mid-Atlantic Ridge, 24° and 30°N. Contrib. Mineral. Petrol., 32: 38–52.

Needham, H.D. and Francheteau, J., 1974. Some characteristics of the rift valley in the Atlantic Ocean near 36°48′N. Earth Planet. Sci. Lett., 22: 29–43.

Nishimori, R.K. and Anderson, R.N., 1973. Gabbro, serpentinite and mafic breccia from fracture zones in the east Pacific. Geol. Soc. Am., Abstr. Progr., Cordilleran Section, 86.

OTTER Scientific Team, 1980. The Oceanographer transform: morphotectonic character of a ridge–transform intersection. EOS, Trans. Am. Geophys. Union, 61: 46, 1105.

OTTER Scientific Team, 1981. High resolution investigations of the Mid-Cayman Rise and the Oceanographer transform: evidence for profound changes in the thickness of oceanic crust proximal to slowly-slipping ridge–transform–ridge intersections. A.G.U. Chapman Conf.—The Generation of Oceanic Lithosphere, 15.

OTTER Scientific Team, 1983. The geology of the Oceanographer transform: the ridge–transform intersection. Mar. Geophys. Res., in press.

OTTER Scientific Team, 1984. The geology of the Oceanographer transform: The Transform Domain. Mar. Geophys. Res., in press.

Ouchi, T., Ibrahim, A.B.K. and Latham, G., 1982. Seismicity and crustal structure in the Orozco Fracture zone: Project Rose Phase II. J. Geophys. Res., 87: 8501–8509.

Parker, R.L. and Oldenburg, D.W., 1973. Thermal model of ocean ridges. Nature (London) Phys. Sci., 242: 137–139.

Phillips, J.D. and Fleming, H.S., 1978. Multi-beam sonar study of the mid-Atlantic rift valley 36°–37°N: FAMOUS. Geol. Soc. Am., MC-19.

Prinzhofer, A. and Nicolas, A., 1980. The Bogota peninsula, New Caledonia: a possible oceanic transform fault. J. Geol., 88: 387–398.

Prothero, W.A. and Reid, I.D., 1982. Microearthquakes on the East Pacific Rise at 21°N and the Rivera fracture zone. J. Geophys. Res., 87: 8509–8519.

Purdy, G.M., Rabinowitz P.D. and Velterop, J.J.A., 1979. The Kane fracture zone in the central Atlantic Ocean, Earth Planet. Sci. Lett., 45: 429–434.

Ramberg, I.B. and Van Andel, T., 1977. Morphology and tectonic evolution of the rift valley at latitude 36°30′N, Mid-Atlantic Ridge. Geol. Soc. Amer. Bull., 88: 577–586.

Ramberg, I.B., Gray, D.F. and Reynolds, R.G.H., 1977. Tectonic evolution of the FAMOUS area of the Mid-Atlantic Ridge, latitude 35°50′ to 37°20′N. Geol. Soc. Am. Bull., 88: 609–620.

Rea, D.K., 1981. Tectonics of the Nazca–Pacific divergent plate boundary. In: L.D. Kulm, J. Dymond, E.J. Dash and D.M. Hussong (Editors), Nazca Plate: Crustal Formation and Andean Convergence. Geol. Soc. Am., Mem., 154: 27–62.

Reid, I.D., 1976. The Rivera Plate: a study in seismology and plate tectonics. Ph.D. Thesis, University of California, San Diego, Calif., 288 pp.

Reid, I.D. and Jackson, H.R., 1981. Oceanic spreading rate and crustal thickness. Mar. Geophys. Res., 5: 165–172.

Renard, V., Schrumpf, B., Sibuet, J.C. and Carré, D., 1975. Bathymetrie Détaillée d'une partie de vallée du rift et de faille transformante, près de 36°50'N dans l'Océan Atlantique. Centre National pour l'Exploration des Océans,Paris.

Robb, J.M. and Kane, M.F., 1975. Structure of the VEMA fracture zone from gravity and magnetic intensity profiles. J. Geophys. Res., 80: 4441–4445.

Ryan, W.B.F. and Hsu, K.J. et al., 1973. Initial Reports of the Deep Sea drilling Project. U.S. Government Printing Office, Washington, D.C., 13: 1447 pp.

Schouten, H. and Klitgord, K.D., 1982. The memory of the accreting plate boundary and the continuity of fracture zones. Earth Planet. Sci. Lett., 59: 255–266.

Schouten, H. and White, R.S., 1980. Zero-offset fracture zones. Geology, 8: 175–179.

Schouten, H., Karson, J. and Dick, H., 1980. Geometry of transform zones. Nature, 288: 470–473.

Schroeder, F.W., 1977. A geophysical investigation of the Oceanographer fracture zone and the Mid-Atlantic ridge in the vicinity of 35°N. Ph.D. Thesis, Columbia University, 458 pp.

Searle, R.C., 1979. Side-scan sonar studies of North Atlantic fracture zones. J. Geol. Soc. London, 136: 283–293.

Searle, R.C., 1981. The active part of the Charlie-Gibbs fracture zone: a study using sonar and other geophysical techniques. J. Geophys. Res., 86: 243–262.

Searle, R., 1983. Multiple, closely spaced transform faults in fast-slipping fracture zones. Geology, 11: 607–610.

Searle, R.C. and Francis, T.J.G., 1982. Multiple, closely-spaced transform faults in fast-slipping fracture zones and stresses in young oceanic lithosphere. EOS, Trans. Am. Geophys. Union, 63: 1100.

Searle, R.C. and Laughton, A.S., 1977. Sonar studies of the mid-Atlantic ridge and Kurchatov Fracture zone. J. Geophys. Res., 82: 5313–5328.

Sibuet, J.-C., and Veyrat-Peiney, B., 1980. Gravimetric model of the Atlantic Equatorial fracture zones. J. Geophys. Res., 85: 943–954.

Sinha, M.C., 1981. The seismic structure of aseismic ridges and fracture zones. Ph.D. Thesis, University of Cambridge, 150 pp.

Sinha, M.C. and Louden, K.E., 1981. Crustal structure, gravity and topography across the Oceanographer fracture zone, EOS, Trans. Am. Geophys. Union, 62: 406 pp.

Sinha, M.C. and Louden, K.E., 1983. The Oceanographer fracture zone. 1. Crustal structure from seismic refraction studies. J.R. Astron. Soc. London, 75: 713–736.

Sleep, N.H., 1975. Formation of ocean crust: some thermal constraints. J. Geophys. Res., 80: 4037–4042.

Sleep, N.H. and Biehler, S., 1970. Topography and tectonics at the intersections of fracture zones and central rifts. J. Geophys. Res., 75: 2748–2752.

Stroup, J.B. and Fox, P.J., 1981. Geologic investigations in the Cayman Trough: evidence for thin crust along the mid-Cayman Rise. J. Geol., 89: 395–420.

Supko, P.R., Perch-Nielsen, K. et al., 1977. Initial Reports of the Deep Sea Drilling Project. U.S. Government Printing Office, Washington, D.C., 39: 1139 pp.

Sykes, L.R., 1967. Mechanism of earthquakes and nature of faulting on the Mid-Atlantic Ridge. J. Geophys. Res., 72: 2131–2153.

Tamayo Tectonic Team, 1983. Tectonics at the East Pacific Rise/Tamayo Transform Fault intersection. Mar, Geophys. Res., in press.

Tchalenko, J.S., 1970. Similarities between shear zones of different magnitudes. Geol. Soc. Am. Bull., 81: 1625–1640.

Tchalenko, J.S. and Ambrasseys, N.N., 1972. Structural analysis of the DashT-E-Bayaz (Iran) earthquake fractures. Geol. Soc. Am. Bull., 81: 41–60.

Trehu, A.M., 1982. Seismicity and structure of the Orozco transform fault from ocean bottom seismic

observations. Ph.D. Thesis Woods Hole Oceanographic Institution–Massachusetts Institute Technology, 370 pp.

Van Andel, T.H., Corliss, J.B. and Bowen, V.T., 1967. The intersection between the Mid-Atlantic Ridge and the Vema Fracture Zone in the North Atlantic. J. Mar. Res., 25: 343–351.

Van Andel, T.H., Von Herzen, R.P. and Phillips, J.D., 1971. The Vema Fracture Zone and the tectonics of transverse shear zones in oceanic crustal plates. Mar. Geophys. Res., 1: 261–283.

White, R.S., 1983. Atlantic oceanic crust: seismic structure of a slow spreading ridge. Geol. Soc. London, in press.

White, R.S. and Matthews, D.H., 1980. Variations in oceanic crustal structure in a small area of the northeastern Atlantic. Geophys. J. R. Astron. Soc., 61: 401–436.

Whitmarsh, R.B. and Laughton, A.S., 1975. The fault pattern of a slow-spreading ridge near a fracture zone. Nature, 258: 509–510.

Whitmarsh, R.B. and Laughton, A.S., 1976. A long-range sonar study of the mid-Atlantic ridge crest near 37°N (FAMOUS area) and its tectonic implications. Deep-Sea Res., 23: 1005–1023.

Wilcox, R., Harding, T. and Sealy, D.R., 1973. Basic wrench tectonics. Amer. Assoc. Pet. Geol. Bull., 57: 74–96.

Wilson, J.T., 1965. A new class of faults and their bearing on continental drift. Nature, 207: 343–347.